Norwegian University of Life Sciences

Master's Thesis 2019 60 ECTS
Faculty of Chemistry, Biotechnology and Food Science

Production of potential immune modulating proteins from *Methylococcus capsulatus* Bath and characterization of their putative roles in inflammation

Kristin Hovden Aaen
Master of Science, Biotechnology

Production of potential immune modulating proteins from *Methylococcus capsulatus* Bath and characterization of their putative roles in inflammation

Kristin Hovden Aaen

Faculty of Biotechnology, Chemistry and Food Science

Norwegian University of Life Sciences

Ås, 2019

ACKNOWLEDGEMENTS

The research presented in this thesis was carried out at the Laboratory of Molecular Cell Biology and The Protein Engineering and Proteomics (PEP) Group at the Faculty of Chemistry, Biotechnology and Food Science at the Norwegian University of Life Sciences (NMBU, Ås), under supervision by Dr. Geir Mathiesen, Dr. Yke Jildouw Arnoldussen and Professor Tor Lea. The study was part of a larger project funded by The Norwegian Research Council.

Geir Mathiesen, thank you for always having your office door open to welcome me whenever I had questions. Tor Lea, thank you for including me in your research project and introducing me to the incredible field of immunology. Yke Jildouw Arnoldussen, you have been an invaluable support to me at the cell lab. Thank you for always believing in me and inspiring me to pursue a career within research.

Thank you to all the members of the Laboratory of Molecular Cell Biology and PEP group for welcoming me to your groups. You have always been there to answer my questions and help me. Fatemeh Askarian, thank you for inspiring me, and taking time from your busy schedule to discuss experiment designs and results with me.

Fellow students and friends, thank you for all the laughs, coffee breaks and conversations. I wish you all the best in your academic and personal futures.

Kristin Hovden Aaen

May 15th 2019

Ås

ABSTRACT

Commensal microbes have for a long time been considered important for the function and development of the human immune system. Later studies also highlight the beneficial potential of non-commensals to human health. The non-commensal, gram-negative bacterium *Methylococcus capsulatus* Bath, mainly found in soil and water, has shown to reduce soybean meal-induced enteritis in Atlantic salmon (*Salmo salar*) and dextran sulfate sodium (DSS) induced colitis in mice. However, the immunomodulatory mechanism behind the anti-inflammatory effects has not been identified. This study is a part of a larger project aiming to characterize the mechanism through which *M. capsulatus* Bath elicit its anti-inflammatory functions. The main aim of the present study is to investigate whether proteins from *M. capsulatus* Bath may contribute to its immunomodulatory effects.

Four *M. capsulatus* Bath proteins, namely the TIR-like protein, MIF, SIMPL-like protein, and MAM, with sequence or structure homology to proteins with known immunomodulatory properties, were produced by recombination and purified. The proteins were used *in vitro* to explore the proteins' putative abilities to regulate expression of the pro-inflammatory cytokine interleukin-8 (IL-8) in human intestinal cells and their effect on the nuclear factor-kappa B (NF-κB) signaling pathway. Results from the current study show that all the tested proteins from *M. capsulatus* Bath can influence IL-8 expression either positively or negatively, and therefore may contribute to the bacterium's immunomodulatory effects. However, the results indicate that the NF-κB pathway not necessarily is involved. Additional experiments are required to characterize the exact mechanisms to which the proteins modulate a host immune response, both *in vitro* and *in vivo*. In conclusion, the results from this study provide important steps towards identifying the mechanism behind the anti-inflammatory effects of *M. capsulatus* Bath.

SAMMENDRAG

Kommensale mikroorganismer har i lang tid vært vurdert som viktige for det humane immunsystemet. Nyere forskning åpner også opp for at ikke-kommensale mikroorganismer kan bidra til forbedret human helse. Den ikke-kommensale, gram-negative bakterien *Methylococcus capsulatus* Bath har evne til å redusere soyabønneprotein-indusert enteritt i atlanterhavslaks (*Salmo salar*) og dextran sulfate sodium (DSS) indusert kolitt i musemodeller. Mekanismen bak den immunmodulerende effekten av *M. capsulatus* Bath er hittil ikke kartlagt. Denne studien er en del av et større prosjekt med mål om å kartlegge mekanismen bak de anti-inflammatoriske effektene til *M. capsulatus* Bath. Hovedmålet med denne studien er å undersøke nærmere om proteiner fra *M. capsulatus* Bath kan stå for, eller bidra til, de immunmodulerende effektene til bakterien.

Fire proteiner fra *M. capsulatus* Bath, kjent som TIR-like protein, MIF, SIMPL-like protein, og MAM, med sekvens- eller strukturhomologi til proteiner med kjent evne til å modulere immunresponser i en vert, ble produsert og isolert. Proteinene ble videre testet med to tilnærminger for å evaluere deres effekt på humane immunresponser. Disse tilnærmingene undersøker proteinenes evne til å påvirke produksjon av det pro-inflammatoriske cytokinet IL-8 og aktiviteten til den viktige nuclear factor-kappa B (NF-κB) signalveien. Resultatene i denne studien viser at alle proteinene kunne modulere IL-8 produksjon, men at NF-κB signalveien ikke nødvendigvis var involvert i den prosessen. Påfølgende forsøk er nødvendige for å kartlegge mekanismene bak proteinenes effekter, både *in vitro* og *in vivo*. *M. capsulatus* Bath har et stort terapeutisk potensial, og resultatene fra denne studien er et viktig steg i riktig retning for å identifisere mekanismen bak *M. capsulatus* Baths anti-inflammatoriske effekter.

ABBREVIATIONS

aa	amino acid
bp	base pair
Caco-2 cells	Cancer colon 2 cells
CIKS	Connection to IκB-kinase and SAPK
CV	Column volume
DC	Dendritic cell
dsDNA	Double-stranded DNA
GIT	Gastrointestinal tract
GMP	Guanosine monophosphate
GTP	Guanosine triphosphate
His	Histidine
IL	Interleukin
kDa	Kilo-Dalton
MALDI-TOF MS	Matrix-Assisted Laser Desorption Time of Flight Mass Spectrometry
MAM	Microbial anti-inflammatory molecule
MHC	Major histocompatibility complex
MIF	Macrophage inhibitory factor
MyD88	Myeloid Differentiation factor 88
NF-κB	Nuclear factor kappa-light-chain-enhancer of activated B cells
nm	Nano meters
PCR	Polymerase chain reaction
SARM	Sterile α- and Armadillo-Motif-containing protein
SEC	Size exclusion chromatography
SEM	Standard error of the mean
SIMPL	Signaling molecule that associates with the mouse pelle-like kinase
TIR	Toll/Interleukin-1 receptor
TNF	Tumor necrosis factor

CONTENTS

1. INTRODUCTION

It has been estimated that the ratio between amounts of human cells versus microbial cells are 1:1, partly due to the high density of microbes in the human gut (Sender et al., 2016). The gut microbiota is known to have a beneficial effect on the gut immune system, however, dysbiosis of the gut microbiota is correlated with various inflammatory diseases and is an increasing problem in western countries. One disorder related to gut dysbiosis and chronic inflammation is inflammatory bowel disease (IBD), which encompasses the chronic relapsing disorders ulcerous colitis and Crohn's disease. In Norway, the prevalence of Crohn's disease is 100-200 incidents per 100,000 inhabitants, and of ulcerative colitis 2-3 per 1000 inhabitants (Norsk Helseinformatikk, 2017a; Norsk Helseinformatikk, 2017b). Many therapeutic approaches to treat IBD are in use, however associated with several side-effects and failure of response in certain patients. Therefore, there is a need to investigate and develop better therapy for IBD.

The non-commensal soil bacterium *Methylococcus capsulatus* Bath has shown anti-inflammatory effects in animal models of intestinal inflammation (Kleiveland et al., 2013; Romarheim et al., 2010). Further studies are needed in order to identify the underlying mechanisms of these effects. This thesis describes studies of potential immunomodulatory proteins from *M. capsulatus* Bath, with the overall aim to characterize the protein's putative anti-inflammatory properties *in vitro* using human cell lines. The possible immunomodulatory potential of the selected *M. capsulatus* Bath derived proteins may later be exploited to improve livestock gut health and/or treatment in obesity and lifestyle associated inflammatory disorders in humans.

1.1 *Methylococcus capsulatus*

Methylococcus capsulatus is a non-commensal, gram-negative bacterium mainly found in soil and water. This bacterium is methanotrophic, meaning it utilizes methane as a carbon and energy source. *M. capsulatus* belongs to the class of Gammaproteabacteria, the order Methylococcales, the family Methylococcacea, and the genus Methylococcus (Bowman, 2006). Two strains of *M. capsulatus*, Bath and Texas, have been sequenced. Interestingly, the strains do not share the same cytokine profiles, and hence immunoregulatory effects, when exposed to human cells (Christoffersen et al., 2015). As to be further described, *M. capsulatus* Bath has shown to be a very interesting species for commercial use in animal feed and potentially as an anti-inflammatory, therapeutic agent for live-stock and human colitis.

M. capsulatus Bath has shown to be an ideal for animal feed because of the quality of proteins, its amino acid and fatty acid composition, and digestibility (Risso et al., 2018; Øverland et al., 2010). The commercial use of *M. capsulatus* Bath started with the aim of producing single-cell protein for animal feed by fermentation using methane gas. BioFerm, a company consisting of Dansk BioProtein, Nycomed and Statoil, first attempted the commercial-scale gas fermentation. In 1995, the *M. capsulatus* Bath containing feed was approved by the European Union under the name BioProtein® (Risso et al., 2018). BioProtein® consists of 88% *M. capsulatus* Bath, and minor parts of *Ralstonia* sp., *Brevibacillus agri*, and *Aneurinibacillus* sp. (Romarheim et al., 2010). BioFerm chose *M. capsulatus* Bath based on its inexpensive media requirement and that it thrives at 45°C, which is a desired temperature in large-scale fermentation as it minimizes contamination risk. The production of BioProtein® was stopped in 2017, but today, Calysta Inc. produces a feed based on the research done in Norway, under the name FeedKind (Risso et al., 2018).

The effects of BioProtein® on soybean-meal (SBM)-induced gastroenteritis in Atlantic salmon (*Salmo salar*) were studied previously by Romarheim et al. (2010). SBM is a commonly used feed for farmed salmonids, due to its digestibility and amino acid composition, but it often causes enteritis in the distal part of the salmonid's intestine. SBM-induced enteritis shares clinical similarities to IBD in mammals, such as disruption of the intestinal barrier leading to exposure of mucosal layer contents (e.g. antigens). Results of this study showed that the bacterial meal could counteract or neutralize SBM-induced gastroenteritis in Atlantic salmon (Romarheim et al., 2010). In the study, BioProtein® inclusion in the salmon feed resulted in an increased cell proliferation and improved intestinal barrier function in comparison to the SBM-induced enteritis salmon fed SBM without BioProtein® supplement (Romarheim et al., 2010).

To further investigate the effect of BioProtein® feed in mammalian models of IBD, Kleiveland and colleagues tested the effect of BioProtein® in mice models with dextran-sulfate-sodium (DSS)-induced colitis, a well-established model of mammalian enteritis (Kleiveland et al., 2013). A potential abrogation of disease development by BioProtein® in murine models of DSS-induced colitis would hold potential to human IBD therapy development. BioProtein® fed mice had remarkably fewer symptoms of DSS-induced colitis than those fed with conventional feed (Kleiveland et al., 2013). The symptoms of colitis such as reduced body weight, colon shortening, and epithelial damage were improved by inclusion of BioProtein® in the mice feed. The colonic barrier was also improved by increased epithelial cell proliferation and enhanced

Mucin 2 transcription, hence reducing the infiltration of neutrophils. To investigate whether the observed effects of BioProtein® were due to the *M. capsulatus* Bath component of the feed, mice were given a feed with 20% inclusion of *M. capsulatus* Bath. The results found with BioProtein® were nearly similar as to those found with only *M. capsulatus* Bath as the bacterial constituent of the feed. Hence, holds *M. capsulatus* Bath supplemented mice feed great potential to ameliorate DSS-induced colitis by enhancing the colonic barrier function (Kleiveland et al., 2013).

The underlying mechanisms for the effect of *M. capsulatus* Bath on mice and salmon were however unknown. A later study showed that *M. capsulatus* Bath interacts with human dendritic cells (DCs) and induces DC maturation and T-cell activation, proliferation and differentiation (Indrelid et al., 2017). Furthermore, it was shown that that large molecules and water insoluble components of the *M. capsulatus* Bath cell wall contributed to protection against SBM-induced enteritis in Atlantic salmon (Romarheim et al., 2013). An *in silico* analysis and subsequent proteomic analysis of the *M. capsulatus* Bath genome showed proteins with structural or functional similarities to proteins with known anti-inflammatory or immune modulatory effects (Indrelid et al.; Indrelid, 2017). Therefore, proteins may be of relevance for *M. capsulatus* Bath's putative roles in ameliorating IBD symptoms and forms the background for the present study.

1.2 The gastrointestinal immune system

All living organisms have evolved mechanisms to counteract pathogenic infections. In mammals, these mechanisms can be divided into the innate and the adaptive immune systems. The innate immune system is recognized as the non-specific, immediate response, while the adaptive immunity is highly specific (Palm & Medzhitov, 2009). The innate and adaptive immune systems are fundamentally different as the innate immune system uses germ-line encoded receptors that recognize conserved patterns on pathogenic microorganisms, while the adaptive immune system uses highly specific receptors developed with seemingly limitless specificity. Cells of the adaptive immune system (e.g. lymphocytes) conquer infections specifically, by developing antibodies in response to recognition of a pathogenic microbe's antigen. These antibodies have the same antigen binding specificity as the antigen-binding receptors and can therefore contribute to a faster response at a subsequent infection (Cooper & Alder, 2006).

The gastrointestinal immune system can be viewed as the body's most important immune organ. The gut contains the majority of lymphoid cells of the human body and includes most of the commensal bacteria (Kim & Pritts, 2017). The mucosal immune system of the gastrointestinal tract (GIT) is connected to the body's other mucosal membranes, such as the oral, nasal and vaginal membranes (Tlaskalová-Hogenová et al., 2004). Thus, a disturbance of its barrier function can potentially affect multiple regions of the body.

The gastrointestinal immune system is comprised of a layer of epithelial cells with villi on the apical side, connected through tight-junctions (Figure 1.2). There are several types of epithelial cell lines in the gut intestine; absorptive enterocytes, Paneth cells and goblet cells. The absorptive enterocytes are the most abundant cell type, which have microvilli structures on their apical site, contributing to an increased ability of ion, water, peptide, etc. uptake from the lumen content (Gunawardene et al., 2011). Paneth cells are found in the crypt and usually reside in the small intestine (Yen & Wright, 2006). These cells contribute to the innate immune system by sensing antigens and bacteria, and consequently discharging antimicrobial peptides (Ayabe et al., 2000). Goblet cells among others produce glycoproteins that constitute the mucosal lining of the intestines and secrete immunoglobulins to enter the mucosal layer (Pelaseyed et al., 2014).

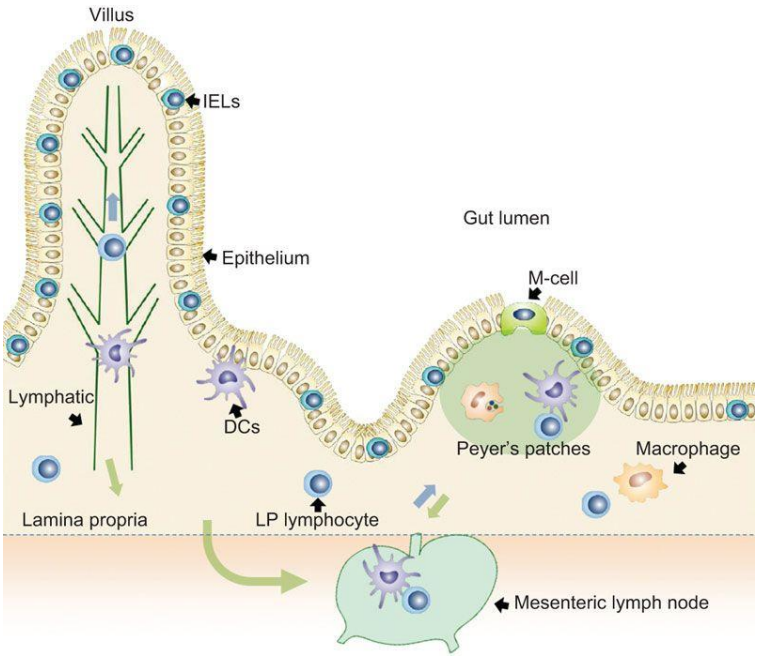

Figure 1.2. The gastrointestinal mucosal immune system. The immune lymphocytes of the gastrointestinal tract reside as intraepithelial (intraepithelial lymphocytes; IELs) or within the sub-epithelial lamina propria (LP). The LP also contains DCs, macrophages, and other lymphocytes. The epithelial lining is covered by an apical mucus layer (not shown), an essential defense mechanism for the gastrointestinal immune system. Microfold cells (M-cells) at the Peyer's patches and DCs are important for antigen sampling and to connect the innate and adaptive immune systems of the gastrointestinal tract. The lymphatic system is connected to the gastrointestinal immune system. Figure taken from Wu et al. (2014).

The GIT mucosa is a crucial component of the gastrointestinal immune system, as it is the first defense mechanism to stop pathogenic bacteria from entering mucosal tissue by crossing the epithelial cell layer. The mucosal immune system is recognized as a part of the innate immune response (Kim & Pritts, 2017). As the mucosal layer is not anchored to the epithelial cells, it moves with peristaltic movements in a distal direction. To compensate, the goblet cells constantly produce fresh mucosa. The mucosa of the gastrointestinal tract contains both cellular and non-cellular contents (Mayer, 2003). The non-cellular components of the mucosa are mostly molecules secreted by the various intestinal cells. Mucus from the goblet cells will be in contact with molecules (e.g. anti-microbial peptides) secreted from the Paneth cells and enterocytes. Consequently, the intestinal cells make an anti-microbial gradient to avoid commensals and pathogenic microorganisms to make contact with the epithelial lining of the gut (Pelaseyed et al., 2014).

There are various regions of the gastrointestinal immune system with specific functions (Figure 1.2). The lamina propria is the sub-epithelial area. Regions called Peyer's patches are

recognized as dome-like structures under a thinner mucosal layer than the rest of the epithelial lining. The Peyer's patches are a part of the gut associated lymphoid tissue (GALT), as they connect the lymphoid tissue to the gut. Peyer's patches are comprised of goblet cells, Microfold cells (M-cells) and enterocyte-like cells, with a layer of mucus from adjacent goblet cells. M-cells transcytose various antigen types, such as bacteria, viruses, fungi and immune complexes, and deliver them to antigen-presenting cells (APCs) within the Peyer's patches. One important APC within the Peyer's patch are the dendritic cells (DCs), which themselves can sample antigens from the gut lumen. DCs sample antigens by extending a dendrite through the tight junction of the epithelial cells, and process and present the antigens to lymphocytes via major histocompatibility complex (MHC) Class I Molecules (Neutra et al., 2001; Reboldi & Cyster, 2016). As lymphocytes are presented to various antigens, they can differentiate to cell types corresponding to the correct response. $CD4^+$ T-cells can differentiate to T-regulator (T_{reg}) or T-helper (T_H) -cells, which are involved with anti-inflammatory responses. The immediate innate immune system is hence connected to the more advanced and specific adaptive immune system of the gut (Yuan & Walker, 2004).

Although the innate immune system is known to be unspecific, it does have discriminatory properties. To ensure the ability of cells to separate self from non-self in the gastrointestinal immune system and hence reduce risk of auto-immunity, the cells must recognize motifs on pathogens specific to pathogens (Takeuchi & Akira, 2010). Macrophages, DCs and nonprofessional immune cells (e.g. epithelial cells) can recognize microbial motifs by using their pathogen recognition receptors (PRRs), which sense microorganisms by the recognition of pathogen-associated molecular patterns (PAMPs) on microbes (Gordon, 2002). PAMPs can be components of bacterial cell walls (e.g. lipopolysaccharides), cytosolic DNA and RNA, proteins, and peptidoglycans (Palm & Medzhitov, 2009). There are four major classes of PRRs; Toll-like receptors (TLRs), Nod-like receptors (NLRs), C-type lectin receptors (CLRs) and intracellular retinoic acid-inducible gene (RIG)-I-like receptors (RLRs). The recognition of PAMPs by PRRs, except for some NLRs, leads to an intracellular signal cascade that activates the Nuclear Factor Kappa B (NF-κB) signaling pathway resulting in transcription of genes that encodes molecules involved in inflammatory responses with the aim of eliminating pathogens and infected cells. These genes include pro-inflammatory cytokines, type I interferons (IFNs), chemokines and antimicrobial proteins (Takeuchi & Akira, 2010).

1.2.1 The NF-kB signaling pathway

The NF-κB transcription factor is an important regulator of the immune system, and part of a signaling pathway expressed in nearly all cell types. After an appropriate extracellular signal (e.g. pro-inflammatory cytokines) that activates a precursor of the NF-κB signaling pathway, the NF-κB proteins are activated and respond accordingly. The NF-κB pathway regulates gene expression of many proteins involved in inflammation, such as cytokines, chemokines, MHC molecules and proteins important in antigen presentation (Hoesel & Schmid, 2013).

There are five families of the NF-κB transcription factors that bind to the enhancer element of the immunoglobulin kappa light-chain of B-cells. The NF-κB family consists of NF-κB1 (p50), NF-κB2 (p52) and the Rel proteins RelA (p65), RelB and c-Rel, which all share high sequence homology (Yu et al., 2004). All proteins of the NF-κB protein family form homo- or heterodimers that normally are bound to the Inhibitor of κB (IκB). The IκBs inhibit NF-κB activity by binding to the regions of the NF-κB protein which normally would bind DNA upon gene transcription (Hoesel & Schmid, 2013). The IκB also secures that NF-κB is kept in the cytoplasm and does not translocate to the nucleus without appropriate signaling (Hoffmann et al., 2002). Gene expression induced by NF-κB is strictly regulated, and depends on type of PRR activated, cell type and stimuli (Wang et al., 2009). The canonical NF-κB pathway activation starts with ligand binding (e.g. PAMP) to a PRR, activating the binding of the Inhibitor of κB kinase (IκBK) onto the NF-κB complex (Figure 1.2.1) (Hoffmann et al., 2002; Wang et al., 2009). The active IκBK phosphorylates the IκB, which promotes ubiquitination and rapid proteasomal degradation of the IκB of the NF-κB complex. Degradation of IκB releases NF-κB, enabling it to transport into the cell nucleus where it binds the enhancer element to induce gene expression (Wang et al., 2009).

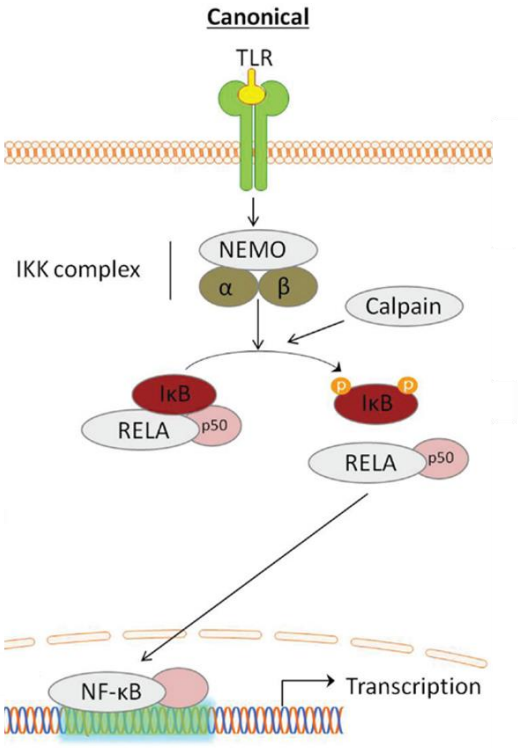

Figure 1.2.1. The canonical NF-κB pathway activation. Upon ligand binding to a PRR (e.g. TLR) the IκBK complex is activated, which in turn facilitates activation of the NF-κB complex. The activation results in phosphorylation and release of IκB from the complex. NF-κB (e.g. RelA and p50) can then transport to the nucleus to induce gene transcription of molecules involved in inflammation. Figure taken from Godwin et al. (2013), with modifications.

The extracellular signal directs NF-κB pathway regulation, as the signals often directly or indirectly activate IκBK via the PRR, enabling it to activate the NF-κB complex. Activation of NF-κB signaling may result in cross-talk between various signaling pathways and is important for the cell's capacity to cope with various stress exposures (Hoesel & Schmid, 2013).

The NF-κB pathway is important in host defense against pathogens, as seen through the activation of the PRR TLR4 by lipopolysaccharides (LPSs) (Figure 1.2.2). LPS, a virulence factor of gram-negative bacteria's outer membrane known to cause septic shock, is important for the host cell to recognize as a PAMP in order to activate mechanisms against a potential bacterial invasion (Takeuchi & Akira, 2010). The TLR4 is located on the plasma membrane of the vertebrate cell with both extra- and intra-cellular regions. Upon ligand (e.g. LPS) binding, the cytosolic tail of the TLR4 changes its conformation. This enables adaptor proteins with Toll/Interleukin-1 (TIR) domains (e.g. MyD88) to bind to the TIR domain of the TLR's tail, resulting in a signaling cascade. For example, MyD88 is involved in a signaling cascade that activates IκBK, which therefore connects TLR4 signaling with NF-κB pathway regulation

(Hoesel & Schmid, 2013; Takeda & Akira, 2004). Various TLRs control adaptive immune responses at several levels, such as regulation of cytokine production, antigen uptake and DC maturation (Palm & Medzhitov, 2009).

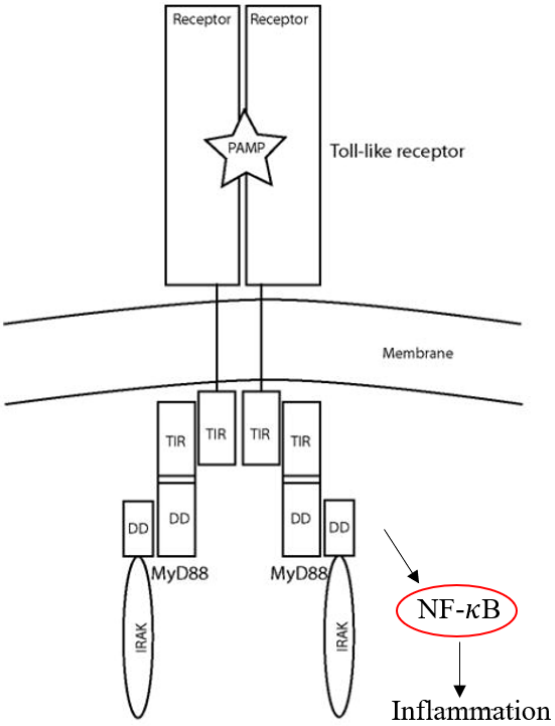

Figure 1.2.2. Activation of the NF-κB pathway by PAMP recognition. PAMPs bind to and activate PRRs (e.g. TLRs), which enables TIR-domain containing proteins such as MyD88 binding to the cytosolic tail of the TLR. The active Myd88 is next involved in a signaling cascade promoting activation of the NF-κB pathway. Figure taken from Low et al. (2007), with modifications.

1.2.2 Cytokines

Cytokines are a family of secretory proteins with effects on communication and interaction between cells. The function of a cytokine can depend on conditions such as cell type, type of signal and persistence of the signal. The cytokine protein family consists of chemokines, interleukins, lymphokines and monokines (Zhang & An, 2007). Secreted cytokines can affect the cell that secreted them (autocrine), a nearby cell (paracrine action) or distant cells (endocrine). This initiates a signaling cascade in the recipient cell to produce additional cytokines.

There are two major classifications of cytokines; pro- and anti-inflammatory. Pro-inflammatory cytokines are produced primarily to mediate the innate immune response against a pathogen by initiating an inflammation (Zhang & An, 2007). Interleukin-1 (IL-1) is a family of pro-inflammatory cytokines produced by monocytes, macrophages, and certain non-immune cells

(e.g. endothelial cells) in response to cell injury, infection, invasion and inflammation (Zhang & An, 2007). IL-1 cytokines are unusual, compared to other cytokines, because they affect nearly all cell types. IL-1 production often occurs as an interplay with another pro-inflammatory cytokine, the tumor necrosis factor (TNF) (Dinarello, 1997). IL-1 cytokines are grouped into IL-α and -β. IL-1β binds specifically to the transmembrane Interleukin-1 receptor (IL-1R) on the plasma membrane. The cytoplasmic regions of IL1-R and TLRs share great similarities, because these receptors both have Toll/Interleukin-1 Receptor (TIR) domains on the cytosolic tails (Section 1.2.1). Because IL-1Rs contain the TIR domain, the IL1-Rs can interact with adaptor proteins (e.g. MyD88) similarly to the mechanism for TLRs (Section 1.2.1; Figure 1.2.2). Subsequently after adaptor protein binding to IL-1R are IL-1 associated kinases (IRAKs) activated by the intracellular adaptor proteins (Figure 1.2.2). IRAKs are serine/threonine kinases with death domains, which interact with the adaptor protein, and a central kinase domain. The IRAK mediates activation of NF-κB and mitogen-activated protein kinase (MAPK) pathways that promote transcription of pro-inflammatory cytokines (Takeda & Akira, 2004).

The IL-1 receptor antagonist (IL1-Ra), a specific IL-1R antagonist, binds competitively to the same receptor as IL-1β. The IL-Ra binding does not induce signals, and thus solely blocks IL-1β activity (Zhang & An, 2007).

Another cytokine, Interleukin-8 (IL-8), is a pro-inflammatory cytokine produced by macrophages and somatic cells (e.g. epithelial cells) primarily functioning as a chemoattractant for neutrophils and T-cells (Zhang & An, 2007). In healthy tissues IL-8 is hardly detectable, but as a response to other pro-inflammatory cytokines (e.g. IL-1β, TNF) it is rapidly induced. IL-8 production in infected or injured tissue can attract immune cells from the blood (e.g. neutrophils) with therapeutic functions (Hoffmann et al., 2002). Neutrophils can migrate through the epithelium to the inflamed tissue, where the neutrophils employ anti-microbial properties, such as degranulation and formation of reactive oxygen species (ROS) through oxidative burst (Headland & Norling, 2015).

1.2.3 Inflammation: an immediate defense mechanism with potentially detrimental consequences

Acute inflammation is a protective response to restore tissue homeostasis after a detrimental stimulus, such as an infection or tissue damage. Inflammation is typically indicated by five symptoms; redness, swelling, heat, pain, and loss of tissue function (Takeuchi & Akira, 2010). Although an acute inflammation serves beneficial functions, it can be detrimental if it persists over time and develops to a chronic inflammation. An uncontrolled inflammation can result in a variety of chronic inflammatory diseases, such as colitis, diabetes, sepsis and arthritis (Dinarello & Thompson, 1991). Recently, a connection between conditions previously not considered having an inflammation component and unresolved inflammation has been drawn. Examples of such conditions are Alzheimer's disease, cardiovascular disease, cancer and atherosclerosis (Sugimoto et al., 2016).

Resolution of acute inflammation is crucial to restore tissue homeostasis and to avoid chronic inflammation of the tissue (Sugimoto et al., 2016). The resolution-stage is initiated shortly after the inflammatory response has begun (Headland & Norling, 2015; Sugimoto et al., 2016). However, a complete understanding of the mechanism behind resolution of acute inflammation is not established yet. Interestingly, components of the initiation of inflammation can be involved in resolution of the acute inflammation where for example down-regulation of pro-inflammatory cytokines can occur through negative-feedback loops (Sugimoto et al., 2016).

IBD is related to chronic inflammation of the gut and is caused by genetic, microbial, environmental and immunological factors (Pithadia & Jain, 2011). Symptoms of IBD include diarrhea, abdominal pain, bleeding, anemia and weight loss. Furthermore, IBD is associated with several other conditions at other locations than the GIT, such as septic shock, arthritis, colitis and diabetes (Pithadia & Jain, 2011). The goal of therapy for IBD and other diseases caused by chronic inflammation is to induce and remain remission (Pithadia & Jain, 2011). Conditions as IBD have shown to be partly mediated by IL-1 and TNF-α (Section 1.2.2). In fact, anti-cytokine-therapies directed towards blocking IL-1 and TNF-α are used widely today with success. Three IL-1 blockers have been approved, in which one of them is IL-1Ra (Dinarello & van der Meer, 2013). Also, probiotics, live microorganisms that give beneficial health effects to the host when given orally, might be helpful to reduce symptoms of IBD for many patients. Probiotics can contribute to controlling the number of harmful bacteria, reduce inflammation and improve the mucus layer of the GIT (Herias et al., 2005). Conditions such as

IBD are complicated, and there does not seem to be one universal solution working for all patients. In fact, 25-30% of Crohn's disease patients fail to respond to current drugs and, due to side-effects, 20% of the patients will discontinue the therapy (Zaylaa et al., 2018). There is a need to investigate better treatments for IBD. Investigating the potential effects of *M. capsulatus* Bath on intestinal inflammation may therefore serve an important contribution to the field of IBD treatment.

1.3 Microbial contributions to health

The gut microbiota is defined as the collection of microorganisms colonizing the human gut, which involves bacteria, viruses, fungi and parasites, and is a result of a symbiosis between microbes and humans through millions of years (Cho & Blaser, 2012; Kamada et al., 2013). Bacteria inhabiting the human gut are commonly referred to as the "commensal" bacteria. Despite its major contribution in human health, the gut microbiota is incompletely characterized and there is a lack in defining its diversity (Hooper & Gordon, 2001). The bacteria found in the gut mostly belong to the phyla; *Bacteroidetes, Firmicutes* and *Actinobacteria*. The gut microbiota composition is greatly influenced by the ratio between *Firmicutes* and *Bacteroidetes* (Mariat et al., 2009). The importance of the microbiota has been shown in several studies, and the microbiota's contributions to health are, among others, to digest and ferment carbohydrates, promote GALT development (Peyer's- and crypt-patches, isolated lymphoid follicles), and contribute to gut-specific immune responses and in protection against pathogens (Kamada et al., 2013).

Studies show that germ-free (GF) mice have smaller Peyer's patches and reduced numbers of $CD4^+$ T-cells and Immunoglobulin-A (Ig-A) producing plasma cells compared to non-GF mice (Belkaid & Hand, 2014; Kamada et al., 2013). Mice deficient in PRRs (e.g. TLR4), which are stimulated by microbial molecular patterns, have insufficient maturation of lymphoid follicles (Section 1.2) (Bouskra et al., 2008; Kamada et al., 2013). The microbiota also contributes to the defense against pathogens by several other mechanisms; nutrient competition, promotion of mucosal barrier function, enhancing innate immunity (e.g. promoting IL-1β production) and adaptive immunity (e.g. T-cell generation) (Kamada et al., 2013). The microbiota's contribution to development of a gastrointestinal immune system is therefore important for gut immune responses, such as inflammation.

A dysbiosis of the gut microbiota has in many studies shown to be associated with development of IBD. Dysbiosis of the gut microbiota is considered as transient or permanent deviations from

the normal gut microbiota (Casen et al., 2015). In patients with ulcerous colitis and Crohn's disease, a decrease in specific *Firmicutes* strains followed by an increase in *Bacteroidetes* and *Enterobacteriaceae* have been found (Carding et al., 2015). However, whether the dysbiosis is the cause of development of IBD or merely a consequence of a disturbance in the GIT by the disorder must be further investigated (Carding et al., 2015).

Probiotics have been developed as a result of an increased understanding of the beneficial contributions of the gut microbiota. Probiotics can be administrated orally as a single bacterium or a mixture of several strains (Zaylaa et al., 2018). Most probiotics are composed of commensal bacteria (e.g. lactobacilli), but non-commensals are also a target for development of probiotics.

1.4 Proteins of interest from *Methylococcus capsulatus* Bath

The proteins investigated in this study have been chosen based on an *in silico* analysis of the *M. capsulatus* Bath genome performed by Dr. Stine Anita Indrelid, revealing genes encoding proteins with sequence and/or structure homologues with known immunomodulatory properties (Indrelid et al., 2014; Ward et al., 2004). Each of the chosen proteins will be discussed in the following sections.

1.4.1 Toll/interleukin-1 receptor (TIR) like protein

The *M. capsulatus* Bath gene MCA_RS14775 encodes the 314 aa protein Toll/Interleukin-1 receptor (TIR) like protein (MCA3012) (Ward et al., 2004). The TIR-like protein contains a SEF/IL-17 receptor (SEFIR) domain, with similarity to the TIR domains on the cytosolic face of TLRs and the corresponding adaptor proteins (Section 1.2.1) (Wu et al., 2012).

In mammals, an intracellular signaling cascade is initiated when TIR domains of the TLRs and cytosolic adaptor proteins such as MyD88 interact (Takeda & Akira, 2004). The SEFIR domain is structurally and functionally similar to the TIR domain, as it shares secondary structure, sequence similarity and is involved with interactions similarly to those described for TLRs and adaptor proteins (Novatchkova et al., 2003; Wu et al., 2012). The SEFIR domain in humans are found in IL-17 receptors (IL-17R) and the corresponding adaptor proteins "connection to IκB-kinase and SAPK" CIKS, which are involved in an important signaling cascade for innate immunity (Onishi et al., 2010).

Bacterial and human SEFIR domains share similarity. It is hypothesized that bacterial SEFIR domains do not have an intrinsic role within bacteria, but that it might interact with eukaryotic signaling pathways (Wu et al., 2012). This is supported by the fact that most SEFIR domain-

containing prokaryotic proteins only have a single copy of the domain, disabling it to form protein-protein interactions with other SEFIR domains. The prokaryotic SEFIR domain may be able to form protein-protein interactions with SEFIR domains of eukaryotic proteins (e.g. IL-17R) (Wu et al., 2012). As illustrated in Figure 1.4.1, bacterial TIR-like proteins (TLPs) are suggested to inhibit activation of the NF-κB pathway by preventing an interaction between a TLR and its corresponding adaptor protein (Low et al., 2007). An interaction between the TIR domains of the TLR and the bacterial TIR-like protein could physically restrain the adaptor protein to interact.

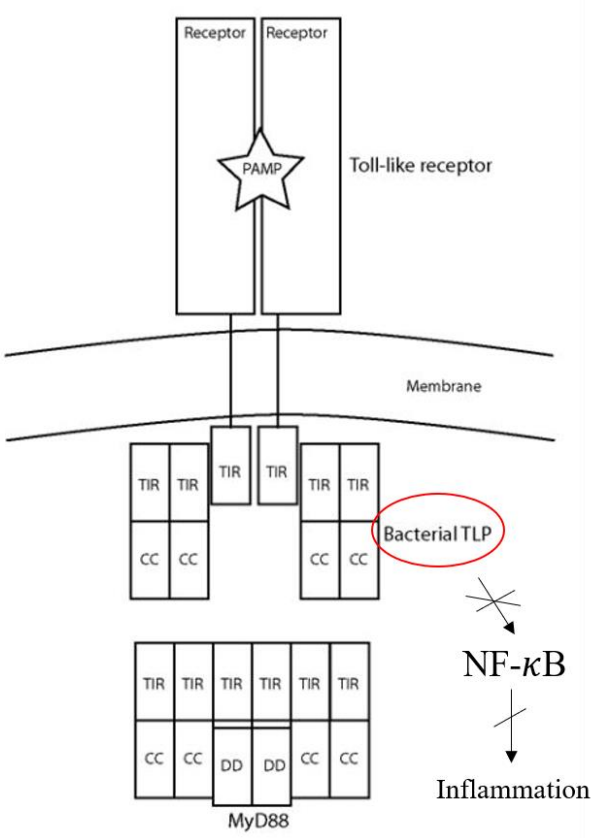

Figure 1.4.1. Proposed mechanism of bacterial TIR-like proteins in host cells. Host cells with a Toll-like receptor (TLR) can bind to PAMPs (e.g. LPS), which changes the conformation of the receptor's cytosolic tail. The tail exposes TIR domains, enabling adaptor proteins with TIR-domains (e.g. MyD88) to bind and further activate the NF-κB pathway. Bacterial TIR-like proteins (TLPs), such as the *M. capsulatus* Bath TIR-like protein, are suggested to bind in similar manner as the MyD88, hence inhibiting the signaling cascade to be initiated. Bacterial TLPs could hence reduce inflammation by inhibiting the signaling cascade induced upon ligand binding to a TLR. Figure taken from Low et al. (2007) with modifications.

Because of the importance of SEFIR and TIR domains in crucial eukaryotic signaling pathways and the fact that prokaryotic SEFIR domain-containing proteins do not have any known interaction partners within bacteria, the TIR-like protein from *M. capsulatus* Bath was chosen for this study to investigate its potential immune modulatory properties.

1.4.2 Macrophage inhibitory factor (MIF) domain

The *M. capsulatus* Bath gene MCA_RS13685 encodes the 114 amino acids (aa) hypothetical protein with Macrophage inhibitory factor (MIF) domain (MCA2795) (Ward et al., 2004).

Mammalian MIF and its paralog D-dopachrome tautomerase (D-DT) have enzymatic tautomerase activity and are constitutively expressed in a variety of tissues and cell types, including the epithelial cells of the GIT, leukocytes and several tissues of the endocrine system (Fingerle-Rowson et al., 2003). Mammalian MIF is secreted by immune cells as a cytokine in response to microbial molecules and pro-inflammatory cytokines (e.g. TNF-α) (Augustijn et al., 2007). Bozza et al. (1999) showed that MIF knock-out (-/-) mice survived lethal doses of LPS, and that the macrophages from MIF -/- mice had lowered TNF-α production, but a normal IL-6 and IL-12 expression. MIF is thus a crucial regulator of host immune cells' antimicrobial defense against endotoxin-containing particles or pathogens, by upregulating TLR4 expression in macrophages (Roger et al., 2003). Levels of serum and epithelial MIF in patients of gastric cancer and inflammation is significantly higher than of healthy patients, indicating that MIF levels may serve as an early bio-marker of gastric cancer (He et al., 2006). In addition to MIF's role as a cytokine, MIF can act as a hormone by performing glucocorticoid-antagonist function. Glucocorticoids are anti-inflammatory steroids produced in adrenal glands in response to stress or injury. By suppressing glucocorticoids' immunosuppressive functions, MIF regulates inflammatory and immune responses (Fingerle-Rowson et al., 2003; Nobre et al., 2017).

As MIF is an evolutionary ancient molecule, it is not surprising that genes encoding proteins related to the mammalian MIF superfamily members (MIF, and its paralog D-DT) have been found in different prokaryotes (Sparkes et al., 2017). Homologues to mammalian MIF are found in a range of species, including bacteria, nematodes, protozoan parasitic species, fish, amphibians and birds, several of which pathogenic to mammalian hosts. Augustijn et al. (2007) found that *Plasmodium* MIF (*p*MIF) is expressed by the parasite upon infection to modulate the host immune response. *p*MIF can reduce monocyte TLR4 surface expression (Cordery et al., 2007). Noteworthy, this means that endogenous MIF can reduce TLR4 expression in human immune cells, while the human MIF contributes to the opposite. The MIF homologue in the

cyanobacterium *Prochlorococcus marinus* is the only bacterial MIF homologue crystalized and functionally characterized (Sparkes et al., 2017; Wasiel et al., 2010). The *P. marinus* MIF homologue was found to have tautomerase activity. Further experiments are required to characterize the functions of bacterial MIF homologues in a host immune response.

1.4.3 Signaling molecule that associates with the mouse pelle-like kinase

The *M. capsulatus* Bath gene MCA_RS01535 encodes the 232 aa protein "signaling molecule that associates with the mouse pelle-like kinase" (SIMPL)-like protein (MCA0312) (Ward et al., 2004). The functions of bacterial SIMPL-like proteins have to our knowledge not been studied.

In mammals, SIMPL is a coactivator of TNF-α mediated NF-κB pathway activation. Benson et al. (2010) showed that SIMPL is required for full induction of TNF-α type I receptor (TNF-α R1)-dependent expression of NF-κB controlled cytokines in endothelial cells (Figure 1.4.3). SIMPL is first activated via TNF-α R1 bound to TNF-α. Active, cytosolic SIMPL and IκBK promote dissociation of the NF-κB complex, freeing NF-κB to enter the nucleus and bind the enhancer element. SIMPL also translocates to the nucleus, where it binds to and activates the p65 region of NF-κB, resulting in gene transcription of cytokines (Milanovic et al., 2014).

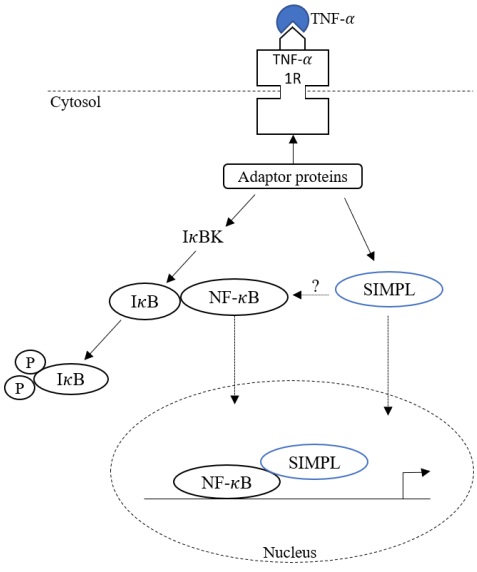

Figure 1.4.3. Activation of the TNF-α mediated NF-κB pathway by mammalian SIMPL. Upon binding of TNF-α to the TNF-α Type I Receptor (TNF-α 1R), cytosolic adaptor proteins can bind to the receptor. Thus, a signaling cascade involving activation of the IκBK is initiated. IκBK activates the NF-κB complex and releases IκB to be degraded. Free NF-κB can then transport to the nucleus and bind to the enhancer element. Simultaneously, cytosolic SIMPL is activated and transported to the nucleus, where it binds to the p65 unit of NF-κB. Gene transcription is thus initiated. Bacterial SIMPL-like proteins may have a similar role in host cells.

Because mammalian SIMPL coactivates the NF-κB pathway that in turn transcribes genes involved in acute and chronic inflammatory responses, it is interesting to investigate if similar functions can be observed in bacterial SIMPL homologues, such as the *M. capsulatus* Bath SIMPL-like proteins.

1.4.4 Microbial anti-inflammatory molecule (MAM) protein

The *M. capsulatus* Bath gene MCA_RS01660 encodes the 588 aa protein MAM (Ward et al., 2004). The *M. capsulatus* Bath MAM is a putative diguanylate phosphodiesterase containing GGDEF and EAL domains, named after their conserved residues. The GGDEF and EAL domains are conserved domains in bacteria with many residues that may contribute to the phosphodiesterase active site, however, the function of most bacterial GGDEF/EAL-containing proteins is not characterized (Galperin et al., 2001). The two domains may together be involved in regulating cell surface adhesiveness to bacteria.

Bacterial GGDEF domains can possess cyclic-di-GMP synthase activity that produce cyclic-di-GMP (Mankan et al., 2016). Cyclic-di-GMP is an intracellular signaling molecule involved in biofilm formation and motility, which can be recognized by a host as a microbial associated microbial pattern (MAMP). Recognition of cyclic-di-GMP as a MAMP by a host cell induces gene expression of various pro-inflammatory molecules of the innate immune system and subsequent activation of the adaptive immune system (Mankan et al., 2016). However, the novel mechanism of bacterial cyclic-di-GMP stimulation of the mammalian immune system seems to have great similarity to the mechanism of cytosolic DNA detection (McWhirter et al., 2009). Cytosolic DNA, and most likely cyclic-di-GMP, induces host anti-microbial defense via stimulation of the adaptor protein Stimulator of IFN genes (STING) resulting in expression of Type I interferons (IFNs) (Cui et al., 2019; McWhirter et al., 2009).

The *M. capsulatus* Bath MAM has structural homology to *Faecalibacterium prausnitzii* microbial anti-inflammatory molecule (MAM) (Quévrain et al., 2016b). *F. prausnitzii,* a common bacterium of the gut microbiota, has anti-inflammatory properties *in vitro* and *in vivo (Zhang et al., 2014).* Patients of Crohn's disease often have a decrease of *F. prausnitzii* in their gut flora. The presence of this bacterium is an indicator of Crohn's disease relapse after surgery or after immunotherapy treatment against Crohn's disease (Quévrain et al., 2016b). A BLAST-search of the *F. prausnitzii* MAM showed hits with proteins containing a putative GGDEF domain (Quévrain et al., 2016b). This domain is associated with a diguanylate cyclase activity,

but the *F. prausnitzii* MAM GGDEF domain lacks the residues critical for this catalytical activity. Quévrain et al. (2016b) showed that *F. prausnitzii* MAM and its derived peptides reduced IL-8 production in human intestinal cells (Caco-2 cells) and reduced activation of the NF-κB pathway. The anti-inflammatory properties of *F. prausnitzii* MAM were confirmed in *in vivo* mice models of colitis (Breyner et al., 2017; Quévrain et al., 2016b). *F. prausnitzii* derived MAM proteins in human stool samples have been identified, confirming *in vivo* expression of bacterial MAM proteins in the human GIT. This was an important step towards explaining the putative immunomodulatory roles of bacterial MAM in the human gut, but further experiments are required to gain additional knowledge (Quévrain et al., 2016a).

1.5 Aims of study

The overall aim of the work described in this thesis is to investigate the putative immunomodulatory effects of the TIR-like protein, MIF, SIMPL-like protein and MAM from *M. capsulatus* Bath on human cell lines *in vitro*. An increased understanding of the selected proteins' interaction with mammalian cells may potentially be utilized in treatment of human patients suffering from IBD or other inflammatory conditions of the gut.

To produce the proteins of interest, the gene sequences with a histidine-tag are to be cloned into appropriate vectors. Thereafter, the proteins will be produced in an *E. coli* BL21 system and purified with immobilized metal affinity chromatography (IMAC). After verification of the purification process, the proteins will be tested in two *in vitro* cell-based inflammation assays. An assay using human epithelial cells resembling the enterocytes of the gastrointestinal tract (Caco-2 cells) was designed to mimic an inflammation of the gastrointestinal system by exposing the cells to IL-1β. Here, the proteins' putative immunomodulatory effects are to be measured as the Caco-2 cell's IL-8 response to the exposure of both IL-1β and the protein in question. In addition, the proteins' potential ability to regulate the NF-κB pathway by using an assay with transformed HEK-293TLR4 cells is used.

2. MATERIALS

2.1 Laboratory equipment

Overview of laboratory equipment used in the study is listed in Table 2.1.

Table 2.1. List of laboratory equipment used in this study.

CATEGORY	ITEM	SUPPLIER
INSTRUMENTS	Certoclav® Labor Autoclav 18L	VWR
	Countess™ II Automated Cell Counter	Invitrogen
	LEX-48 Bioreactor	Epiphyte Three Inc.
	Magnet stirrer	Bio-Rad
	Mastercycler gradient	Eppendorf
	Milli-Q® Direct Water Purification System, Direct 16	Merck Millipore
	pH-meter, 827 pH Lab	Metrohm Nordic AS
	Qubit® fluorometer	Invitrogen
	Teflon Stirring Bar (magnet)	SP Scienceware
	VacuSafe aspiration system	Integra Biosciences
	Vibra-Cell™ VCX 500 Ultrasonic Processor	Sonics & Materials, Inc.
	Äkta Pure Protein Purification System	GE Healthcare Life Sciences
CENTRIFUGES	5418R Centrifuge	Eppendorf
	Allegra X-30R Centrifuge	Beckman Coulter, Inc.
	Avanti™ J-25 Centrifuge	Beckman Coulter, Inc.
	Heraeus General Purpose Megafuge 1.0	VWR
	MiniStar Silverline Microcentrifuge, table top centrifuge	VWR
	MS2 Minishaker	IKA
SPECTROPHOTO-METERS & RELATED EQUIPMENT	Disposable cuvettes	Eppendorf
	Disposable UVettes	Eppendorf
	Eppendorf BioPhotometer® D30	Eppendorf
	Power Wave HT Microplate Spectrophotometer	BioTek Instruments, Inc.
	SpectraMax M2 Spectrophotometer	Nerliens Meszansky
INCUBATORS	New Brunswick Scientific™ Innova® 44 Incubator	Eppendorf
	Steri-Cycle™ CO2 Incubator, HEPA Class 100	Thermo Electron Corporation
HOODS AND CABINETS	Golden Line Class II biological safety cabinet	Kojair
	Safe 2020 Class II Biological Safety Cabinet	Thermo Scientific

FILTRATION SYSTEMS & COLUMNS	Filtropur S 0,45 µm PES Membrane syringe filter unit	Sarstedt
	IMAC Column, HisTrap™ High-Performance (HP) column, 5 mL	GE Healthcare Life Sciences
	Membrane dry vacuum pump/compressor, VCP 80	VWR
	Vacuum Filtration Systems, 0.2 µm PES Membrane	VWR
	Vivaspin 20, 10,000 MWCO PES	Satorius
GEL EQUIPMENT	Benchtop UV Transilluminator	UVP
	GelDoc™ EZ Imager	Bio-Rad
	Mini-PROTEAN® Tetra Cell, vertical electrophoresis system	Bio-Rad
	Mini-PROTEAN® TGX Precast Gels	Bio-Rad
	Mini-Sub® Cell GT Systems, horizontal electrophoresis system	Bio-Rad
	Mini-Sub® Cell, horizontal gel casting tray	Bio-Rad
	PowerPac™ Basic Power Supply	Bio-Rad
	PowerPac™ Power Supply 300	Bio-Rad
	Stain-Free Sample Tray	Bio-Rad
	UV tray	Bio-Rad
	Well combs	Bio-Rad
APPLIANCES	**TUBES**	
	Cellstar® Tubes (15, 50 mL), conical bottom, sterile	Greiner Bio-One
	CryoPure Tubes, white, 1.6 mL	Sarstedt
	Eppendorf tubes, 1.5 mL	Axygen
	Glass tubes, 13 mL	Sarstedt
	Nalgene™ Oak Ridge Centrifugation bottles with caps, 25 mL	Sigma-Aldrich
	Nalgene™ Ultracentrifugation bottles with caps (250, 500 mL)	Sigma-Aldrich
	PCR tubes with flat caps, 0.2 mL	Axygen
	Screw cap tube, polypropylene, sterile, 13 mL	Sarstedt
	SCALES	
	Laboratory Digital Scale, LC621P	Sartorius
	Entris® Precision Balances	Sartorius
	Nitrile gloves	VWR
	Nunc™ Sealing Tape	Thermo-Scientific
	Parafilm M® All-purpose Laboratory Film	Pechiney, WI (US)
	Scalpel, surgical blade, stainless steel, no 10	Swann-Morton
	Toothpicks	Playbox
	Automated pipettes	Thermo-Fisher
	Costar® 96 Well EIA/RIA Plate, Flat Bottom, no lid, polystyrene	Corning Inc.
	Countess™ Cell Counter Chamber Slides	Invitrogen
	Falcon® Tissue Culture Flasks, vented caps, (T25, T75, T225)	Corning Inc.

	Falcon® Tissue Culture Plates, Multiwell (12, 96 wells)	Corning Inc.
	Glass ware	Duran, VWR
	JA 25-50 Rotor for Ultracentrifugation	Beckman
	JA-10 Rotor for Ultracentrifugation	Beckman
	Petridish, 90 mm	Heger
	PipetBoy 2.0	Integra
	Plastic Concentric Luer-Lock Syringe, 1-50 mL	BD Plastipak™
	Refill pipette tips	VWR
	Serological pipette (5, 10, 25 mL)	Sarstedt

2.2 Chemicals

Overview of chemicals used in the study is listed in Table 2.2.

Table 2.2. List of chemicals used in this study.

CHEMICAL	SUPPLIER
10x Fastdigest® Green Buffer	Thermo Scientific
2x Quick Ligation Buffer	New England Biolabs® Inc.
5x Q5 Reaction Buffer	New England Biolabs® Inc.
ABTS Liquid Substrate	Sigma-Aldrich
Agar Powder	VWR
Ampicillin, $C_{16}H_{19}N_3O_4S$	Sigma-Aldrich
Antifoam 204	Sigma-Aldrich
Bacto™ Tryptone	Becton, Dickinson and Co
Bacto™ Yeast Extract	Becton, Dickinson and Co
Brain-Heart-Infusion (BHI)	Oxoid
Dimethyl Sulfoxide (DMSO	MP Biomedicals
Dipotassium Phosphate (K_2HPO_4)	Merck
Distilled water (Endotoxin Screened)	Gibco®
DNA Gel Loading Dye, 6x	New England Biolabs® Inc.
Dulbecco's Phosphate Buffered Saline (PBS), 1x	BioWest
Ethanol, C_2H_5OH	VWR
Glycerol, $C_3H_8O_3$	Merck
Hek-Blue™ Endotoxin Standard (E. Coli 055:B5 LPS), Cat#Rep-Hbes-10	InvivoGen
Hek-Blue™ Selection	InvivoGen
Hydrochloric Acid (HCl)	Merck
Imidazole, $C_3H_4N_2$	Sigma-Aldrich
Isopropyl Alcohol	VWR
Isopropyl B-D-1-Thiogalactopyranoside (IPTG), 1M	Sigma-Aldrich
Kanamycin, $C_{18}H_{36}N_4O_{11}$	Sigma-Aldrich
Monopotassium Phosphate, KH_2PO_4	Merck
Non-Essential Amino Acids (NEAA) 100x	Biowest
Normocin™, 1x	InvivoGen

NuPAGE® Lds Sample Buffer	Invitrogen
NuPAGE® Sample Reducing Agent	Invitrogen
Penicillin-Streptomycin, 100x	Biowest
PeqGreen DNA/RNA Dye	VWR Peqlab
Phenylmethylsulfonyl Fluoride (PMSF)	Sigma-Aldrich
QUANTI-Blue™ Detection Medium Powder	InvivoGen
Seakem® LE Agarose	Lonza
Super Optimal broth with Catabolite repression (S.O.C) medium	Invitrogen
Sodium Chloride (NaCl)	VWR
Sodium Hydroxide (NaOH)	VWR
Tris Base, $C_4H_{11}NO_3$	Sigma-Aldrich
Tris-Acetat-EDTA (TAE) Buffer, 50x	Thermo Scientific
Tris-Glycine-SDS(TGS) Buffer, 10x	Bio-Rad
Trypan Blue 0.4%	Invitrogen
Tween-20	Sigma-Aldrich

2.3 Proteins, enzymes and DNA

An overview proteins and enzymes used in the study with the relevant supplier is found in Table 2.3.1.

Table 2.3.1. Proteins. The table shows the proteins and enzymes used in this study with the relevant supplier.

PROTEIN	**SUPPLIER**
5x In-Fusion HD Enzyme Premix	Clontech Laboratories Inc.
Benchmark™ Protein Ladder, 10-220 kDa	Invitrogen
Bovine Serum Albumin (BSA)	Biowest
Fastdigest® BamHI	ThermoFisher
Fastdigest® NdeI	ThermoFisher
Fetal Bovine Serum (FBS)	Biowest
Il-1β Human, Recombinant, Expressed in *E. coli*	Sigma-Aldrich
Interleukin-1 Receptor Antagonist (IL-Ra), Human	Sigma-Aldrich
Q5 High-Fidelity DNA Polymerase Master mix	New England Biolabs® Inc.
Quick T4 DNA Ligase	New England Biolabs® Inc.
Red-Taq DNA Polymerase Master Mix	VWR
Trypsin-EDTA 1x In Solution W/O Calcium W/O Magnesium W/ Phenol Red	Biowest

DNA was used in this study as a ladder in agarose gel electrophoresis and in PCR reactions (Table 2.3.1).

Table 2.3.1. DNA. DNA and nucleotides with the relevant supplier used in this study.

DNA	SUPPLIER
Quick-Load® Purple, 1 kb plus DNA ladder	New England Biolabs® Inc.
10 mM dNTPs	New England Biolabs® Inc.

2.4 Primers

Primers used in this study are presented in Table 2.4.

Table 2.4. **Primers used in the study.**

PRIMER	SUPPLIER	SEQUENCE (5'-3')	RESTRICTION SITES
pMAL_TIR-R	Eurofins Genomics	CAGGGAATTCGGATCCTCAATGGT GGTGATGATGGT	BamHI
pMAL_TIR-F	Eurofins Genomics	GAAGGATTTCACATATGACTGCAC CAAAAGTTTTTGT	NdeI
SeqTIR_F	Eurofins Genomics	CAG GTC CAG CTC CAT	

2.5 Bacterial strains, plasmids and cell lines

Table 2.5.1 presents the plasmids used in the study. pNIC-CH plasmids were used in the current study for overexpression of a target gene with a C-terminal Histidine tag. The pNIC-CH derived vectors include sites for LIC cloning, and a fragment with the *SacB* gene that allows for negative selection on 5% sucrose. The pMAL_C5X plasmid was used to make a construct of *Tir*, to enable protein expression when induced in an *E. coli* BL21 system.

Table 2.5.1. **Plasmids used in the study.**

PLASMID	SOURCE	ANTIBIOTIC RESISTANCE
pMAL_C5X	New England Biolabs, Inc.	Ampicillin
pNIC-CH	Opher Gileadi	Kanamycin
pNIC-CH_MIF	Sveen (2016)	Ampicillin
pNIC-CH_SIMPL	Sveen (2016)	Ampicillin
pMAL-c5X_MAM	Stine A. Indrelid (unpublished)	Ampicillin
pMAL-c5X_MAM-GGDEF	Stine A. Indrelid (unpublished)	Ampicillin
pMAL-c5X_MAM-EAL	Stine A. Indrelid (unpublished)	Ampicillin
pNIC-CH_TIR	Sveen (2016)	Kanamycin
pMAL_C5X-TIR	The current study	Kanamycin

An overview of the bacterial strains used in the study are found in Table 2.5.2.

Table 2.5.2. **Bacterial strains used in the study.**

BACTERIAL STRAINS	SUPPLIER
BL21® Star™ (DEM3) Chemically Competent E. coli	Thermo Fisher Scientific
OneShot® TOP10 Chemically Competent E. coli (C44100)	Invitrogen by Thermo Scientific

The human cell lines used in the study and a short description of their properties are presented in Table 2.5.3.

Table 2.5.3. **Human cell lines used in the study**.

CELL LINE	SUPPLIER	CAT NO/ CODE	DESCRIPTION
Caco-2	European Collection of Authenticated Cell Cultures (ECACC)	ECACC 86010202	Human epithelial colon cells, adherent
HEK-Blue™ hTLR4 cells	InvivoGen	hkb-htlr4	Kidney cells, genetically modified to over-express TLR4, adherent
HEK-Blue™ Null1 cells	InvivoGen	hkb-null1	Kidney cells, adherent

2.6 Kits

A list of kits used in the study and an overview of the respective contents are presented in Table 2.6.

Table 2.6. **Kits used in the study.**

KIT	SUPPLIER
Nucleospin® Plasmid	Macherey-Nagel
Nucleospin® Plasmid column and Collection Tube (2 ml) Resuspension Buffer A1 Lysis Buffer A2 Neutralization Buffer A3 Wash Buffer AW Wash Buffer A4 Elution Buffer AE	
Qubit® dsDNA BR Kit	Invitrogen
Qubit® dsDNA BR Standard #1 Qubit® dsDNA BR Standard #2 Qubit® dsDNA BR Buffer Qubit® dsDNA BR Reagent	
Nucleospin® Gel and PCR Clean-Up Kit	Macherey-Nagel
Nucleospin® Extract II Column and Collection Tube (2 mL) Binding Buffer NTI Wash Buffer NT3 Elution Buffer NE	

Human IL-8 (CXCL8) STANDARD ABTS ELISA Development Kit (CAT#900-K18, LOT0515018)	Peprotech®
Rabbit Anti-Human IL-8 (CXCL8), "Capture Antibody" Biotinylated Rabbit Anti-Human IL-8 (CXCL8), "Detection Antibody" Recombinant Human Il-8 (CXCL8), "Standard IL-8" Avidin-HRP Conjugate	
ToxinSensor™ Chromogenic LAL Endotoxin Assay Kit (Cat# L00350)	GenScript
LAL Reagent Water Limulus Amebocyte Lysate (LAL) *E. coli* Endotoxin Standard Chromogenic Substrate Buffer S for Color Stabilizer #1 Color-Stabilizer #1 Color-Stabilizer #2 Color-Stabilizer #3 Endotoxin-Free Tubes Endotoxin-Free Tips, 200 µl Endotoxin-Free Tips, 1000 µl Incubation Rack	

2.7 Agars and media

An overview of the agars and media used in the study and a protocol of preparing the media that were not pre-mixed by the supplier is given in Table 2.7.

Table 2.7. Agars and media. An overview of the media, with the respective protocols, used in the study.

AGARS AND MEDIA
Brain-Heart-Infusion (BHI) medium
Medium: 37 g BHI to 1 L dH2O. Mixed, autoclaved at 115°C 15 min. Antibiotics added when appropriate. Agar: 16 g agar (1.5% w/v) was added to the solution above before autoclaving. Antibiotics added when temperature reached below 60°C. Plated to petri dishes immediately. Stored at 4°C, wo/light.
LB medium
Medium: 10 g Bacto™ Tryptone, 5 g Bacto™ Yeast Extract, 10 g NaCl, ddH_2O to 1 L. Mixed, adjusted pH to 7 and autoclaved at 115°C 15 min. Agar: See BHI agar protocol above. Stored at room temperature.
Super Optimal broth with catabolite repression (S.O.C) medium
Pre-mixed from the supplier. Stored at -20°C.
TB medium
Medium: 6 g Bacto™ Tryptone, 12 g Bacto™ Yeast Extract, 2.34 mL 85% glycerol, ddH2O to 450 mL. Mixed and autoclaved at 115°C 15 min. Stored at room temperature.
Dulbecco's Modified Eagle's Medium (DMEM) w/Sodium Pyruvate w/L-Glutamine
Pre-mixed from supplier. Supplemented with FBS, Pen-Strep and/or Normocin™ and NEAA as described in Sections 3.14-16. Stored at 4°C.

2.8 Buffers and solutions

Overview of buffers and solutions used in the study is given in Table 2.8.

Table 2.8. Buffers and solutions used in the study.

BUFFER/SOLUTION	PROTOCOL
Phosphate buffer	0.17 M H_2KPO_4, 0.72 M K_2HPO_4, dH_2O to 1 L. Autoclaved at 115°C for 15 min. Stored at room temperature.
1M Tris-HCl pH 8.0 buffer	121.1 g Tris base was dissolved in 800 mL dH2O. pH adjusted to 8,0 with HCl. Stored at room temperature.
Buffer A (binding buffer)	5 mM imidazole, 50 mM Tris-HCl pH 8.0, 500 mM NaCl dissolved in dH_2O. Sterile filtrated with a 0.2 µm PES membrane vacuum filtration system. Stored at room temperature.
Buffer B (elution buffer)	250 mM imidazole, 50 mM Tris-HCl pH 8.0, 250 mM NaCl dissolved in dH_2O. Sterile filtrated with a 0.2 µm PES membrane vacuum filtration system. Stored at room temperature.
Agarose (1.2% w/v)	6 g SeaKem® LE Agarose to 500 mL 1x TAE Buffer. Autoclaved at 115°C 15 min. Stored at 60°C.

2.9 Software and online resources

Table 2.9 gives an overview of the software and web resources utilized in the present study.

Table 2.9. Software and web resources used in the study.

SOFTWARE/ ONLINE RESOURCE	SUPPLIER
CLC Main Workbench	Qiagen Bioinformatics
Image Lab™ Software	Bio-Rad
GraphPad® Prism	GraphPad Software, San Diego, CA
Gen5 Software	BioTek Instruments, Inc.
SoftMax Pro 6	Molecular Devices
pDRAW 32	AcaClone Software
In-Fusion Cloning Calculator	Takara Bio, Inc. Accessed at: https://www.takarabio.com/learning-centers/cloning/in-fusion-cloning-tools/in-fusion-molar-ratio-calculator.
ELISA Analysis Tool	Elisakit.com Pty Ltd Accessed at: https://elisaanalysis.com/.
Unicorn 6.4	GE Healthcare Life Sciences

2.10 Statistical analysis

All statistics and graphics have been performed with GraphPad Prism (GraphPad Software, San Diego, CA). Results are represented as means ± SEM. Statistical significance was determined by the Student t-test and shown as follows: *P < 0.05, **P < 0.01, ***P < 0.001, **** P < 0.0001.

3. METHODS

3.1 Cultivation of *Escherichia coli* and long-term storage of bacteria

E. coli strains were grown in glass tubes for liquid overnight cultures, with 10 mL BHI medium containing appropriate antibiotics for the plasmids' selection genes (Table 3.1). The cultures were incubated at 37°C with shaking. To prepare a liquid culture from *E. coli* grown on agar plates, one colony was selected using a sterile toothpick. The toothpick was thereafter dropped into liquid medium supplemented with antibiotics in a glass tube and incubated overnight with shaking at 37°C. Glycerol stocks were made by transferring 1 mL of the overnight cultures a cryotube containing 300 µL sterile 85% glycerol. The content was thoroughly mixed and stored at -80°C.

Table 3.1. Overview of the appropriate antibiotics for the different plasmids used in the study.

SPECIES	PLASMID	ANTIBIOTIC	ANTIBIOTICS IN LIQUID MEDIA	ANTIBIOTICS IN AGAR
E. coli	pMAL-c5X derivates	Ampicillin	200 µg/mL	100 µg/mL
E. coli	pNIC-CH derivates	Kanamycin	100 µg/mL	50 µg/mL

3.2 Plasmid isolation from Escherichia coli

Plasmids were isolated from overnight cultures of transformed *E. coli* containing the desired plasmid. The overnight culture was centrifuged and the Nucleospin® Plasmid kit (Table 2.6) was used according to the manufacturers' recommendations on the pellet. The volume of the elution volume varied (30-50 µL).

3.3 Measuring dsDNA concentration using Qubit®

Measurement of concentration of double-stranded DNA was performed using Qubit® dsDNA BR Assay Kit (Table 2.6).

Materials

Qubit® assay tubes

Qubit® dsDNA BR Assay Kit
Qubit® fluorometer

Procedure

1. Qubit® Working Solution was prepared as a solution of Qubit® dsDNA BR Reagent and Qubit® dsDNA BR Buffer in a 1:200 ratio in an Eppendorf tube.
2. Sample solutions were prepared by mixing 2 µL sample and 198 µL Qubit® Working Solution.
3. The standards and sample solutions were vortexed and centrifuged shortly, followed by 2 minutes of incubation in room temperature.
4. The DNA concentrations of the samples were measured using the Qubit® fluorometer, and at ng DNA per mL.

3.4 DNA digestion by restriction enzymes

Restriction enzymes are enzymes with highly specific binding sites, designed to digest DNA at the desired site of a DNA sequence. Digestion of DNA using two restriction enzymes is commonly used to prepare DNA sequences for ligation, as it results in compatible ends on the sequences to be ligated. In the present study were the plasmids digested using NdeI and BamHI.

Materials
DNA
Nuclease free water
10X FastDigest® Green Buffer
FastDigest® NdeI
FastDigest® BamHI

Procedure

The protocol for Fast Digestion of Different DNA of Different DNA (Thermo Fisher Scientific) was used as a guide for the following reaction solution given in Table 3.4.

Table 3.4. Composition of reaction solution for digestion of DNA.

COMPONENT	VOLUME (TOTAL: 50 µL)
Water, nuclease free	Adjust to total volume of 50 µL
10X Fast Digest Green Buffer	5 µL
DNA	0.2-1 µg
FastDigest Enzyme	5 µL (maximum 10% of total volume)

The volume of DNA to be added was calculated based on the concentration measured in Section 3.3.

1. The components in Table 3.5 were gently mixed in an Eppendorf tube at room temperature and spun down briefly, before incubating it in a water bath at 37°C for 30-60 minutes.
2. After incubation, the mixture was loaded onto an agarose gel for size analysis by gel electrophoresis (Section 3.5). Fragments of the digested DNA could be excised from the gel and used for further work, if desired (Section 3.6).

3.5 Agarose gel electrophoresis and isolation of DNA from an agarose gel

Gel electrophoresis validates of the results from DNA digestion (Section 3.4) or PCR reactions (Section 3.7), in addition to providing a purified DNA strand that can be isolated from the gel for further analysis. An agarose gel separates DNA fragments in size by a voltage dependent manner, where the negatively charged DNA molecules move towards the anode. Due to the charge and the fact that the agarose gel is porous, shorter strands moves faster through the gel than longer strands, leading to a size separation. By using a DNA ladder, one can determine the fragment sizes in numbers of kilobases (kb).

Materials

Quick-Load® Purple, 1 kb plus DNA ladder Loading dye
DNA samples to be analyzed
1x TAE Buffer
SeaKem® LE Agarose
peqGreen DNA dye
Mini-Sub® Cell GT Systems
Mini-Sub® Horizontal Gel casting tray
Well comb (15 or 10 wells)

GelDoc EZ Imager

UV-Tray

Benchtop UV Transilluminator

NucleoSpin® Gel and PCR Clean-up Kit (Table 2.6)

Procedure

1. An 1.2% (w/v) agarose solution was prepared by mixing 6.0 g SeaKem® LE Agarose with 500 mL 1x TAE buffer and autoclaved at 115°C for 15 minutes. The 1.2% Agarose can be stored at 60°C.
2. 2.5 µL peqGreen DNA dye was added to 60 mL of 1.2% agarose solution. After gentle stirring, the solution was poured onto a Mini-Sub® Cell casting tray with well combs. The solution was left to solidify for at least 30 minutes. The well combs were then removed.
3. The solidified gel was placed onto a Mini-Sub® Cell GT System and 1x TAE buffer was poured until covering the gel.
4. The wells were loaded with the samples and 1 kb DNA ladder to a final concentration of 10% (v/v). The sample volume loaded onto the gels depended on the well size; the 10 and 15 well gels' maximum loading volume was 30 µL and 15 µL, respectively.
5. The gel was run at 90V for 15-45 minutes.
6. An image of the gel was made by using the GelDoc EZ Imager and an UV-tray, and the sample DNA sizes were determined using the DNA ladder.
7. To isolate the desired DNA or PCR fragments were the respective bands excised from the gel and isolated in accordance to the manufacturer's recommendation with the NucleoSpin® Gel and PCR Clean-up Kit (Table 2.6).

3.6 Cloning of DNA

3.6.1 In-Fusion Cloning

In-Fusion cloning is a fast, directional cloning technique to fuse a PCR amplified DNA fragment (insert) and a linearized vector. The insert was amplified by PCR using specific primers to create ends with a 15 bp overhang. These ends correspond to the ends of the vector linearized using specific restriction enzymes, hence enabling the In-Fusion enzyme to fuse the corresponding ends together.

Materials

Linearized vector

Purified PCR product

In-Fusion® HD Cloning kit (Table 2.6)

Procedure

In-Fusion cloning was performed according to the manufacturers' In-Fusion® HD Cloning Kit (Table 2.6). The In-Fusion Cloning Calculator (Table 2.9) was used to calculate the amount of PCR product and linearized vector to use. The weight ratio of PCR fragment to linearized vector is recommended to 2:1 when performing In-Fusion cloning. See Table 3.6.1 for the In-Fusion cloning reaction mixture. Transformation of OneShot® TOP10 Chemically Competent *E. coli* was performed immediately after cloning (Section 3.9.2).

Table 3.6.1. In-Fusion Cloning reaction.

REAGENT	VOLUME
5X In-Fusion® HD Enzyme Premix	2 µL
PCR fragment	10-200 ng*
Linearized vector	50-200 ng**
dH_2O	Adjust to total 10 µL
Total volume	10 µL

*<0.5 kb: 10-50 ng, 0.5-10 kb: 50-100 ng, >10 kb: 50-200 ng

**<10 kb: 50-100 ng, >10 kb: 50-200 ng

3.6.2 Cloning using quick ligation

Using the T4 DNA ligase enables ligation of an insert and a vector within minutes. In contrast to In-Fusion Cloning, are not 15 bp overhang on the ends of the vector and insert necessary. Therefore, was the PCR amplified insert treated with restriction enzymes before proceeding to the quick ligation step. To match the ends with those of the linearized vector, was the insert treated with the same restriction enzymes at the vector had been treated with. Ligation of the insert DNA and plasmid vector was performed in accordance to the New England® BioLabs Inc. protocol "Quick Ligation™ Kit" with no modifications.

3.7 Polymerase chain reaction

A Polymerase Chain Reaction (PCR) is a widely applied technology for amplification of specific DNA molecules. PCR requires a thermostable polymerase, deoxynucleoside triphosphates (dNTPs), forward and reverse primers and template DNA. To amplify the template DNA, the reaction goes through several steps. In the first step called the denaturation step, the temperature is high in order to denature the double-stranded DNA molecule, resulting in single-stranded molecules. Next, the temperature is lowered to enable the primers to anneal to the template strands at sequences they are complimentary to. This step is called the annealing step. Thereafter, the temperature is increased to a level at which the polymerase can bind to the primers and add nucleotides (dNTPs) to the DNA strand. Finally, the result is a doubling in number of DNA molecules per cycle.

3.7.1 PCR using Q5® High-Fidelity DNA Polymerase

To amplify gene fragments, the New England Biolabs® Inc. Q5® High-Fidelity DNA Polymerase (M0491) protocol was used. The choice of annealing temperature relies on the lowest melting temperature (T_m) for the two primers, whereas the annealing temperature is set to approximately 3°C lower than the T_m. No loading dye is added to the samples during this procedure, hence must loading dye be added later when running agarose gel electrophoresis.

Materials

Template DNA

Forward and reverse primers (Table 2.4)

5X Q5 Reaction Buffer

Q5 High-Fidelity DNA polymerase

dNTPs

Procedure

The New England Biolabs™ Inc. protocol for PCR using Q5® High-Fidelity DNA Polymerase (M0491) was used with adjustments. The reaction components in Table 3.7.1.1 were mixed in a 0.2 mL PCR tube, and subsequently was the PCR reaction run as indicated in Table 3.7.1.2.

Table 3.7.1.1. Reaction setup for PCR using Q5® High-Fidelity DNA Polymerase

COMPONENT	REACTION (50 µL)	FINAL CONCENTRATION
5X Q5® Reaction Buffer	10 µL	1X
10 mM dNTPs	1 µL	200 µM
10 µM Forward primer	2.5 µL	0.5 µM
10 µM Reverse primer	2.5 µL	0.5 µM
Template DNA	1 µL	<1000 ng
Q5® High-Fidelity DNA Polymerase	0.5 µLs	0.02 U/µL
Nuclease-free water	32.5 µL (to total of 50 µL)	

Table 3.7.1.2. Thermocycler program for PCR using Q5® High-Fidelity DNA Polymerase.

STEPS	TEMPERATURE	DURATION/ NUMBER OF CYCLES
Initial denaturation	98°C	30 seconds / 1
Denaturation	98°C	10 seconds / 25-35
Annealing	50-72°C*	20 seconds / 25-35
Elongation	72°C	20 seconds / 25-35
Hold	4-10°C	2 minutes / 1

*Annealing temperature was based on melting temperature (T_m) of the primer with the lowest T_m, usually set to 3°C below T_m for the primer.

3.7.2 Colony-PCR using VWR Red Taq DNA Polymerase Master Mix

Colony-PCR was used to verify that a DNA insert was correctly inserted into a plasmid. With this method, a small part of a single *E. coli* colony is transferred to a PCR tube and used as a template for the PCR reaction.

Materials

Red Taq DNA Polymerase Master Mix (2X Master Mix w/1.5 mM $MgCl_2$).

Forward and reverse primers (Table 2.4)

Procedure

1. All components listed in Table 3.7.2.1 were thawed on ice.
2. A sterile toothpick was used to transfer material from one colony to a 0.2 mL PCR tube. Subsequently, the toothpick was then transferred to a tube containing liquid media with appropriate antibiotics and incubated overnight.

Table 3.7.2.1. Reaction components in colony-PCR.

COMPONENT	REACTION (50 µL)	FINAL CONCENTRATION
Taq 2X Master Mix (w/ 1.5 mM $MgCl_2$)	25 µL	1X
Forward primer (10 µM)	1 µL	0.2 µM
Reverse primer (10 µM)	1 µL	0.2 µM
Template DNA	From colony	
PCR-grade H_20	Add to total 50 µL	

3. The PCR reaction was placed in a thermocycler, and the program presented in Table 3.7.2.2 was run.

Table 3.7.2.2. Thermocycler program for colony-PCR.

STEP	TEMPERATURE	DURATION/CYCLES
Initial denaturing	95°C	2 minutes
Denaturing	95°C	20-30 seconds
Annealing	50-65°C*	20-40 seconds
Elongation	72°C	1 minute
Final elongation	72°C	5 minutes

*Annealing temperature was based on melting temperature (T_m) of the primer with the lowest T_m, usually set to 3°C below T_m for the primer.

4. The PCR products were run on an agarose gel for size analysis and/or PCR product isolation from gel (Sections 3.5).

3.8 Sequencing DNA

All PCR generated sequences were sequenced to verify that the PCR reaction amplified the DNA correctly, without errors such as mutations.

Procedure

The amount of DNA recommended for sequencing of plasmid and linear DNA is 400-500 ng and 100-400 ng, respectively. To prepare the samples for sequencing, were the components presented in Table 3.8 transferred to a 1.5 mL Eppendorf tube. The tubes were labelled with a barcode provided from the sequencing supplier (Eurofins Genomics) and kept refrigerated (+4°C) until sent for sequencing analysis to Eurofins Genomics. Sequencing results were later analyzed by CLC Main Workbench.

Table 3.8. Reaction mixture DNA sequencing.

COMPONENT	AMOUNT
PCR product	400-500 ng (plasmid), 100-400 ng (linear DNA)
10 pmol/µL primer (forward or reverse)	2.5 µL
dH_2O	Add to total volume of 11 µL
Total volume	11 µL

3.9 Transformation of *Escherichia coli* strains

3.9.1 Transformation of Chemically Competent *E. coli* TOP10

Materials

OneShot® TOP10 Chemically Competent *E. coli*

Sarstedt 13 mL tubes

Ligation reaction

Super Optimal broth with Catabolite Repression (S.O.C) medium

LB agar plates, supplemented with appropriate antibiotics (Table 2.1 and 2.7)

Procedure

The Invitrogen protocol (MAN0000633) "Transform Chemically Competent Cells" in the "One Shot® TOP10 Competent Cells" user guide provided by Thermo Fisher Scientific was followed for transformation of competent *E. coli,* with minor modifications.

1. A vial containing the competent cells was thawed on ice and briefly centrifuged to collect the cells before transferring 50 µL of the cells to a pre-chilled Sarstedt 13 mL tube placed in ice.
2. To the cells, was 4 µL of the ligation mixture added and mixed gently.
3. The solution was incubated on ice for 30 minutes, followed by heat-shocking the cells for exactly 30 seconds in a 42°C water bath.
4. The tube was returned to the ice and 250 µL room-temperature S.O.C-medium was added. The tube was then incubated at 37°C with shaking for approximately 1 hour.
5. After incubation, was 100 µL of the cells spread on pre-warmed LB-plates with appropriate antibiotics under sterile conditions and incubated overnight at 37°C.

3.9.2 Transformation of Chemically Competent *E. coli* BL21

Following verification of a successful cloning with sequencing, was the constructs transformed into chemically competent *E. coli* BL21 Star™ (DE3). This strain used as a production strain of the target protein, because it expresses the T7 RNA polymerase. The T7 RNA polymerase is necessary for induction of the T7 promotor upstream of the target gene, which induces protein expression via a *lac* operator system.

Materials

See Section 3.9.1

OneShot® BL21 Star™ (DE3) Chemically Competent *E. coli*

Methods

Transformation of *E. coli* BL21 was performed as described for transformation of *E. coli* TOP10 (Section 3.9.1). The amounts of cells and plasmid used were 25 µL and 1 µL, respectively. The same amount of S.O.C. medium was added, and 100 µL of the cell suspension was plated on LB agar plates with antibiotics overnight at 37°C.

3.10 Protein production in *Escherichia coli* BL21

3.10.1 Cultivation of *Escherichia coli* BL21 using Harbinger-system

To ensure a constant oxygen flow and a high biomass production, was the BioLex-48 BioReactor utilized for overexpression of the target protein in *E. coli* BL21 (DE3). The reactor

system used ensures constant mixture of the cells by the air flow and that the temperature is kept constant. The protein production is induced by adding IPTG to the culture, which triggers transcription of the *lac operon*.

Materials

BioLex-48 reactor

Caps (hose- and air diffuser–equipped)

TB-medium with appropriate antibiotics

Phosphate buffer (Table 2.8)

Antifoam 204

1M Isopropyl β-D-1-thiogalactopyranoside (IPTG)

Procedure

1. 450 ml TB-medium with appropriate antibiotic (Table 2.1) was prepared in a 1 000 mL flask and autoclaved (Table 2.7). The medium was supplemented with 50 mL sterile phosphate buffer and 150 µL sterile Antifoam 204.
2. An overnight culture of *E. coli* BL21 habouring the expression plasmid was prepared and the next day was 3 mL of bacteria culture inoculated to the medium flask.
3. The flask was closed with a hose- and air diffuser-equipped cap under sterile conditions.
4. The flask was connected to the BioLex-48 BioReactor system following the manufacturer recommendations.
5. Oxygen flow was turned on and adjusted to an air level in which the culture was mixed without creating high pressure inside the flask and incubated at 23°C overnight.
6. The following day, approximately 24h after start of incubation, was 100 µL IPTG added to the bottle to induce protein expression. The culture was then further incubated at 23°C overnight with continuous aeration.
7. Approximately 24h after IPTG addition, were the cells harvested as described in Section 3.10.2.

3.10.2 *Escherichia coli* BL21 harvesting, cell lysis and protein extraction

The cells cultured as described in Section 3.10.1 were harvested for protein extraction by centrifugation. Sonication of the cells disrupts the cell walls, which results in accessibility of the over-expressed proteins. The solution was centrifuged to extract the proteins, and the supernatant fraction was expected to contain the protein of interest.

Materials

50 mM Phenylmethylsulfonyl fluoride (PMSF), diluted in isopropyl alcohol

Buffer A (Table 2.8)

TB medium (Table 2.7)

Overnight culture of transformed *E. coli* BL21

Filtropur S 0,45 µm PES Membrane syringe filter

Procedure

Cell harvesting

1. The overnight culture of transformed *E. coli* BL21 from Section 3.10.1 was transferred to a 500 mL centrifugation tube and pelleted by centrifugation at 5000xg for 15 minutes at 4°C The pellet was washed once by resuspending in 50 mL TB-medium and centrifuged at the same conditions as previously. Step 2 was executed the same day as protein purification. If purification was performed another day, the pellet was kept at -80°C until the day of purification.

Cell lysis

2. For cell sonication, the pellet was transferred to a 50 mL tube and resuspended in 30 mL pre-chilled Buffer A. The cells were sonicated using the Sonics Vibra-Cell™ VCX 500 Ultrasonic Processor at 30% amplitude for 3 minutes with 5 seconds on/off cycles.

Protein extraction

3. After sonication, 60 µL pre-chilled PMSF (protease inhibitor) was added to the sample and mixed. Subsequently, the sample was transferred to a 50 mL centrifugation tube and centrifuged at 20 000xg for 15 minutes at 4°C. The supernatant was used for further analysis and protein purification.

4. Lastly, the protein suspension was filtered into a 50 mL tube with a Filtropur S 0,45 µm PES Membrane syringe filter unit before protein purification.

3.11 Protein purification

3.11.1 Immobilized Metal Ion Affinity Chromatography (IMAC)

Immobilized Metal Ion Affinity Chromatography (IMAC) was used to purify the proteins of interest, as a N-terminal Histidine-tag was fused to the target proteins. The histidine residues have affinity for the immobilized Nickel in the HisTrap™ High-Performance (HP) column. When loading the protein suspension onto the column, the target protein will bind reversibly to the column due to this affinity, and the non-His-tagged proteins will run through without binding. To elute the target protein an elution buffer (buffer B) with high imidazole concentration will run through the column. The imidazole has greater affinity to the Nickel than the histidine-tag and will outcompete the target protein. In this way, the protein of interest will be collected under conditions disabling contaminant proteins in the solution to co-elute.

The proteins were purified using the ÄKTA pure chromatography system. This system monitors the absorbance (A_{280} nm) of the proteins running through the column, enabling visualization of the flow-through. The purification can be presented as a chromatogram in the software for ÄKTA pure chromatography system, Unicorn™ 6.4.1.

Materials

Buffer A (Table 2.8), binding buffer
Buffer B (Table 2.8), elution buffer
Milli-Q Water
Ethanol (20%)
HisTrap™ High-Performance (HP) nickel-charged IMAC column, 5 mL

Procedure

1. The HisTrap™ HP column was attached to the ÄKTA pure chromatography system by running water through, disabling air to flow into the system. The Unicorn™ 6.4.1 software was thereafter connected to the chromatography system.

2. Because the column storage buffer contained 20% Ethanol, water was run through the system first with a flow rate of 2,5 mL/minutes. This was maintained until the amount corresponding to 5 CVs (column volumes) had run through the column.
3. The hose for Buffer B was placed into the Buffer B flask, and the hoses for sample, water and Buffer B placed into the Buffer A flask. The system was pump washed for 5 CVs with the rate 1.5 mL/minutes. Next, the hose meant for the sample was transferred to the sample tube.
4. The sample was then loaded to the system and run at the same rate as in step 3. When monitoring the flow on the chromatogram in Unicorn™ 6.4.1, it immediately showed a peak for the proteins which immediately ran through the column without binding (flow-through). After sample loading, the system was washed with Buffer A, until the absorbance returned to zero again, indicating that all the proteins not containing a histidine-tag was washed from the column.
5. After the washing step, Buffer B was added gradually until 100% to elute the target protein.
6. To prepare the system for future purifications, pump washes with dH_2O and 20% ethanol were executed in the respective orders.
7. The protein fractions were run LDS-PAGE to analyze the purification (Section 3.11.2).

3.11.2 Lithium Dodecyl Sulfate-Polyacrylamide Gel Electrophoresis (LDS-PAGE)

An LDS-PAGE (analogous method to SDS-PAGE) analysis was run to analyze the purity of the fractions from IMAC, and to analyze the pellet and supernatant from the protein extraction steps (Section 3.10.2). LDS-PAGE allows for separation of proteins based on molecular weight (kDa).

The proteins need a net negative charge to move towards the positively charged anode. This is obtained by treating the proteins with LDS, which has a net negative charge that binds the protein, disrupting their tertiary structure. Because LDS binds throughout the entire protein, the amount of negative charge will correspond to the molecular weight of the protein. The NuPAGE® LDS Sample Buffer contains a loading dye, hence is no additional loading dye necessary.

Materials

Mini-PROTEAN® TGX Stain-Free™ Precast Gel

Mini-PROTEAN Tetra Cell

NuPAGE® LDS Sample Buffer (4X)

NuPAGE® Reducing Agent (10X)

Tris-Glycine-SDS (TGS) Buffer (1X)

BenchMark™ Protein Ladder

Protein fractions with target protein (Section 3.13.1)

Flow through from IMAC (Section 3.13.1)

Pellet and supernatant from protein extraction (Section 3.12.2)

Procedure

1. A 2X working solution with 500 µL 4X NuPAGE® LDS Sample Buffer, 200 µL 10X NuPAGE® Reducing Agent and 300 µL dH_20 was prepared. The remains of the working solution after the first LDS-PAGE run was stored at 4°C.
2. Ten µL sample was mixed with 10 µL working solution. To analyze a pellet, a small amount was transferred to an Eppendorf tube via a sterile toothpick. Ten µL of working solution was also added to the pellet sample.
3. The Eppendorf tubes with the protein samples were placed in a boiling water bath (100°C) for 10 minutes to denature the proteins.
4. The electrophoresis chamber with the gel was assembled. 1X TGS Buffer were poured into the inner and outer chamber.
5. The boiled protein samples were applied to the gel and the gel was run at 270V for 20-30 minutes.
6. To visualize the proteins and analyze the gel was the ImageLab™ software utilized.
7. Pure fractions from IMAC containing the protein of interest were pooled, and the solution buffer was changed from buffer B to PBS according to Section 3.11.3.

3.11.3 Buffer exchange

The elution buffer from IMAC with high concentration of imidazole and NaCl, in which the protein is solubilized, has to be exchanged before exposure to the *in vitro* cell lines used in the study, as it is harmful to the human cells. The Dulbecco's Phosphate Buffered Saline (PBS) is a more physiologically relevant buffer. The filters used during buffer exchange have a cut off molecular weight at 10 000 Da, which implies that all molecules in the solution with lower

molecular weights than the cut off will run through the column. Thus, the final product contains proteins >10,000 Da.

Materials

Dulbecco's Phosphate Buffered Saline (PBS)

Ultrafiltration Unit Vivaspin® 20, 10,000 MWCO PES

Protein fractions pooled after SDS-PAGE (Section 3.13.2)

Procedure

1. A maximum of 15 mL of the pooled protein fractions from Section 3.11.2 of were transferred to a Vivaspin® 20, 10,000 MWCO PES Ultrafiltration Unit. The sample was centrifuged at 4 500xg at 4°C until approximately 1 mL was left in the upper part of the tube (above the column). Potential excess sample was included by repeating this step until all had been used.
2. The flow-through was discarded, and 10-15 mL PBS was added to the filter unit.
3. Steps 2 and 3 were repeated until five times.
4. The protein solution was transferred to sterile 15 mL tubes and stored at 4°C until further use.

3.11.4 Measurement of protein concentration

The concentration of the proteins was measured at absorbance 280 nm. At this wavelength, aromatic amino acids (phenyl alanine, tyrosine and tryptophan) absorb light. After the absorbance of the protein was determined by the Eppendorf BioPhotometer® D30, Beer-Lamberts law was used to determine concentration (Box 1). The extinction coefficient, a constant for the amount of light per molar concentration the protein can absorb at a given wavelength, was determined by using ProtParam (Gasteiger et al., 2005). The extinction coefficient assumes all pairs of cysteine form cysteine bonds. Length of light travel is also included, which corresponds to the length of the cuvette (1 cm in the present study).

Box 1. Beer-Lamberts law.

Beer-Lamberts law

$$A = \varepsilon * b * C$$

A = Absorbance at 280 nm, ε = extinction coefficient, b = length of light travel, C = sample concentration

Materials

Eppendorf BioPhotometer® D30

Cuvettes

1X Dulbecco's Phosphate Buffered Saline (PBS)

Procedure

1. The instrument was set to blank using 70 µL Dulbecco's Phosphate Buffered Saline 1X (PBS).
2. The sample concentration was determined from the average of ten parallels. For this step, a total of 70 µL sample was added to the cuvette.
3. The exact protein concentration was then calculated using Beer-Lamberts law, as described above.

3.11.5 Sterile filtration of protein solution

The protein solutions were required to be sterile, as the *in vitro* cell lines were to be exposed to the protein solutions.

Materials

Filtropur S 0,45 µm PES Membrane syringe filter and syringe

Protein solution from Section 3.11.3

Procedure

The protein solution was drawn into the syringe by suction, and the Filtropur S 0,45 µm PES Membrane syringe filter was attached to the syringe. Filtration was performed by transferring the solution from the syringe to a sterile tube. The protein solution was stored at 4°C.

3.12 Human epithelial Colorectal Adenocarcinoma (Caco-2) cells

3.12.1 Maintaining Caco-2 cells in culture

Maintaining a human cell line requires several steps to ensure healthy cells that are at the same differential stage and morphological similar when used in assays. When confluent, cells are passaged and transferred to a new cell culture flask. The passage number was kept between 45 and 65 in the present study. To ensure sterility, all work with human cell lines was performed in the Kojair class II biological safety cabinet Golden Line laminar flow bench. In addition, nitrile gloves sprayed with 70% ethanol and an appropriate lab coat was used to minimize the risk of bacterial contamination.

Materials

Dulbecco's Modified Eagle's Medium (DMEM) High Glucose

Fetal Bovine Serum (FBS)

Penicillin-Streptomycin (Pen-Strep) (100X)

Non-Essential Amino Acids (NEAA) (100X)

Dulbecco's Phosphate Buffered Saline (PBS) (1X)

Trypsin-EDTA (1X)

Dimethyl sulfoxide (DMSO)

Caco-2 (ECACC 86010202)

Cell culture flask (25, 75, 125 cm^2)

Steri-Cycle™ CO_2 Incubator HEPA100 (5% CO2, 37°C)

Countess™ Cell Counting Chamber slides

Countess™ II Automated Cell Counter

Trypan Blue Stain (0,4%)

Procedure

Thawing Caco-2 cells

1. The Caco-2 cell growth medium was prepared by adding heat-inactivated FBS, NEAA and Pen-Strep to the DMEM with end concentrations 10%, 1% and 1% (v/v), respectively. Before use, the growth media was pre-warmed to 37°C.
2. To start a culture from a new cell vial, 5 mL growth medium was first transferred to a 15 mL tube. Thereafter, the cell vial with Caco-2 (ECACC 86010202) was thawed on the 37°C water bath. Immediately after, the cells were transferred to the tube. The cells were centrifuged at 1 000 rpm for 5 minutes, and the supernatant containing the DMSO was removed. This step is essential, as the DMSO is highly toxic to the cells.
3. The pellet was resuspended in 5 mL of the freshly prepared, pre-warmed growth medium. The cell suspension was thereafter transferred to a 25 cm^2 cell culture flask. The cells were incubated at 37°C and 5% CO_2. When the cells reached approximately 80% confluency, they were split as described below.

Splitting a Caco-2 culture

4. The medium was carefully removed, and the cells were washed once with ~3 mL PBS.

5. Trypsination in order to detach adherent cells from the flask was performed by adding 1.5 mL Trypsin-EDTA to the culture and incubating the flask 5-10 minutes in the incubator (37°C, 5% CO_2). Using a microscope with bright field, the cells were observed every 2 minutes. In addition, the flask was shaken to detach the cells. When the cells had released from the flask, 5 mL of medium was added. Simultaneously mixing the cells and medium using serological pipettes, the suspension was transferred to a sterile 50 mL tube. The tube was centrifuged at 1 000 rpm for 5 minutes.
6. The supernatant was removed, and the pellet resuspended in 5 mL growth medium.
7. The cells were counted to determine volume to transfer to the next culture. In short, 10 µL of suspension was mixed with 10 µL Trypan Blue 0,4%. Ten µL of the mixture was transferred to a Countess™ Cell Counting Chamber Slide which immediately was placed into the Countess™ II Automated Cell Counter.
8. Based on the cell count in step 7, were 1 million cells transferred to a 75 cm^2 cell culture flask containing 15 mL growth medium. The culture was incubated at 37°C with 5% CO_2.

Freezing Caco-2 cells

9. To prepare stocks of the cell line, cells from step 6 were frozen as follows; after an additional centrifugation step (1000 rpm, 5 min) were the cells resuspended in 5 mL freezing medium (20% FBS, 7% DMSO, 73% DMEM High Glucose, v/v). Due to DMSO having a high melting point, it was included in the freezing media to ensure fast freezing of the cells. One mL of cell suspension was distributed per cryo-tube, followed by immediately placing the vials at -80°C.

3.12.2 *In vitro* inflammation assay using Caco-2 cells

To investigate the potential immunomodulatory effects of the proteins in question in the present study, an *in vitro* assay mimicking intestinal inflammation using Caco-2 cells was performed. Here, an inflammatory reaction was induced by Interleukin-1β (IL-1β) and the levels of Interleukin-8 (IL-8) were investigated for a possible effect of the proteins that the cells were exposed to (see Results for details). Release of IL-8 was quantified by Enzyme-linked immunosorbent assay (ELISA), as described in Section 3.13.

Materials

Caco-2 (ECACC 86010202) cells (from Section 3.14.1)

Protein solutions from Section 3.13.5

Falcon® 12-well Clear Flat Bottom TC-Cell Culture Plate with Lid (sterile)

Dulbecco's Modified Eagle's Medium (DMEM) High Glucose

Non-Essential Amino Acids (NEAA) (100X)

Penicillin-Streptomycin (Pen-Strep) (100X)

IL-1β

IL-1β-antagonist (IL-1Ra)

Procedure

Day 1 – cells split to 12-well plates

1. From the cell suspension obtained in 3.12.1 step 6-7, 1.8 x10^5 cells/well were plated in Falcon® 12-well Clear Flat Bottom TC-Cell Culture Plates with Lid with 1.5 mL Caco-2 growth medium/well (for medium, see Section 3.12.1 step 1). Cells were incubated at 37°C with 5% CO_2 for 72 h.

Day 3 – cell-climatization

2. The growth media in the wells was aspirated, and fresh, pre-warmed growth media was added (1.5 mL media/well). Cells were incubated as in step 1 for an additional 48 h.

Day 5 – cell starvation

3. Serum-free growth medium was prepared (450 mL DMEM High Glucose, 1% (v/v) NEAA, 1% (v/v) Pen-Strep) and pre-warmed at 37°C.
4. The old media in the plates was replaced with the fresh serum-free growth medium. Cells were incubated for 24 hours in the same conditions as in step 1.

Day 6 – cells were stimulated

5. To 50 mL tubes, serum free growth medium was added in accordance to 1 mL media/well. IL-1β was added to the suspension with a final concentration of 15 ng/mL. The cell suspension further distributed to 50 mL tubes corresponding to each of the stimuli in the experiment.

6. Based on protein concentrations calculated in Section 3.11.4, the proteins were diluted according to the relevant concentrations for cell exposure in the corresponding tubes from step 5.
7. For the wells with negative control, serum-free growth media without IL-1β was added. The positive control consisted of serum-free media with IL-1β. In addition, a control containing 15 ng/mL of the IL-1 antagonist IL-1Ra was prepared in serum-free media with IL-1 β.
8. For the exposures with IL-1Ra, cells were first exposed to the antagonist control media wo/IL-1 β for 30-40 minutes, before changing to media containing both IL-1Ra and IL-1β. The cells were exposed to the controls and protein solutions by first removing the cell media from the wells and then adding 1 mL of the control and protein solutions in the respective wells. The cells were observed in the microscope, to ensure healthy cells with similar morphology, and incubated at 37°C with 5% CO_2 for 24 hours.

Day 7 – supernatant was harvested

9. 1 000 µL of the supernatant from each well was transferred to labelled 1.5 mL Eppendorf tubes 24 hours after stimuli and directly placed in a -20°C freezer until use.

3.13 Enzyme-Linked Immunosorbent Assay (ELISA)

ELISA was performed using the PeproTech Human IL-8 (CXCL8) Standard ABTS ELISA Development Kit (Table 2.6) to quantify the production of IL-8 in the Caco-2 cells exposed to various controls and proteins.

The ELISA technique called a “Sandwich ELISA” uses antibodies with non-overlapping epitopes on the antigen (Figure 3.13). Here, IL-8 will be referred to as the antigen. Plate wells are first coated with a capture antibody. The following day is a blocking buffer that blocks un-specific binding sites of the capture antibody used, and the subsequent addition of the antigen enables binding of the capture antibody and the antigen. Subsequently after removing un-bound molecules from the antigen-containing sample by a washing step, is a biotinylated detection antibody added. An enzyme-linked secondary antibody (the conjugated detection agent) is thereafter added, which binds to the detection antibody. Lastly, is a chromogenic substrate added to the wells, resulting in a measurable color development. The color is proportional with

the amount of antigen in the sample, thus can the concentration of a specific antigen in a sample be determined using a standard curve.

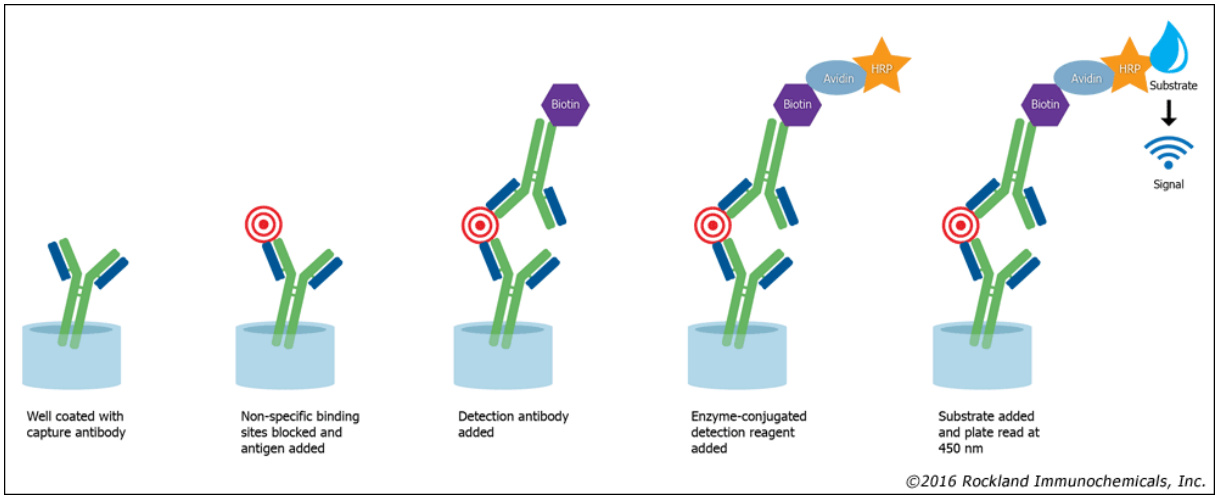

Figure 3.13. The steps of a sandwich ELISA. First wells are coated with capture antibody and incubated overnight. A blocking buffer is then added to block unspecific binding sites of the capture antibody. Antigen from the sample (red circle) in question is added and binds to the capture antibody. A biotinylated detection antibody can thereafter bind to the capture antibody, creating a sandwich between the antibodies and antigen. The enzyme-conjugated agent is then added, followed by substrate addition. The binding of substrate to the conjugate converts the enzyme to its detectable form. Figure taken from Rockland Immunochemicals Inc. (2016).

Materials

PeproTech Human IL-8 (CXCL8) Standard ABTS ELISA Development Kit (Table 2.6)

Sterile water

Costar® 96 Well EIA/RIA Plates

ABTS Liquid Substrate

Dulbecco's Phosphate Buffered Saline (PBS) 1X

Tween-20

Bovine Serum Albumin (BSA)

Procedure

1. Plates were coated with capture antibody (Rabbit Anti-Human IL-8) according to the manufacturers' protocol, and incubated overnight at 4°C. The antibodies were reconstituted in sterile water at the manufacturers' recommendation, and stored at -20°C.

2. The day after coating the ELISA plates, the supernatants collected in Section 3.12.2 step 9 were thawed at 4°C and centrifuged at 15 000 rpm for 10 minutes at 4°C.
3. ELISA Wash Buffer was prepared by adding 0,5% (v/v) Tween-20 to PBS. Diluent was made by adding 0,1% BSA and 0,05% Tween-20 (v/v) to 50 mL PBS.
4. ELISA was performed in accordance to the manufacturers' protocol. Absorbance was read at 405 and 620 nm using a BioTek Instruments Inc. Power Wave HT Spectrophotometer connected to the Gen5 Software, approximately 5 minutes after substrate addition.
5. To generate a 4-Parameter Logistic ELISA standard curve from the results, was www.ELISAanalysis.com utilized (Table 2.9). For statistical analysis, a Student's t-test was performed in GraphPad® Prism (San Diego, CA) (Table 2.9).

3.14 Human Hepatic Embryonic Kidney (HEK)-293 cells

3.14.1 Maintaining HEK-293 cells in culture

Cultivation of HEK-293 cells also includes thawing, splitting and freezing, as described for Caco-2 cells in Section 3.12.1. Both HEK-Blue™ hTLR4 cells transformed to overexpress TLR4 and HEK-Blue™ Null1 cells were used in the present study (InvivoGen, 2019a; InvivoGen, 2019b). To ensure fully efficient HEK-293 cells, the passage number did not exceed 30.

Materials

See materials list in section 3.12.1, the following materials are specific for HEK-293 cell maintenance;

HEK-Blue™ hTLR4 cells

HEK-Blue™ Null1 cells

HEK-Blue™ Selection (250X)

Normocin™ (1X)

Procedure:

See Section 3.12.1 for maintaining a Caco-2 cell culture. Listed are the deviations from that procedure;

1. Growth medium for HEK-293 derivative cells was prepared by adding 10% (v/v) FBS, 1% (v/v) Pen-Strep, 1% (v/v) Normocin™ to a flask of DMEM High Glucose. For the HEK-Blue™ hTLR4 cells, the growth medium was supplemented with 1X HEK-Blue™ Selection.
2. When splitting HEK-293 cells, one may use either Trypsin-EDTA (0,1%) or 1X PBS to release the cells from the flask. When using Trypsin-EDTA the cells detach within one minute, and when using PBS the cells were incubated 2-3 minutes at 37°C with 5% CO_2.
3. The cells were split at 60-80% confluency.
4. Approximately 2 million cells were cultured in 75 cm^2 tissue culture flasks.

3.14.2 NF-kB pathway regulation assay using HEK-BLUE™ hTLR4 cells

To investigate the proteins of interest's potential role in NF-κB-pathway regulation, an assay where TLR4 was activated by LPS to induce NF-κB-mediated transcription of the SEAP reporter gene was performed. The role of the proteins in question would be evaluated by the regulation of SEAP production, as this is a direct effect of NF-κB pathway activation. SEAP is secreted from the cells and its relative concentration can be determined in the supernatant. The HEK-Blue™ Nul1 cell line was used as an assay control, as this cell line does not over-express TLR4. The "HEK-Blue LPS Detection Kit 2" protocol from InvivoGen was used as a guide for the following assay (InvivoGen, 2019a).

Materials

HEK-Blue™ hTLR4 cells
HEK-Blue™ Null1 cells
Falcon® Tissue Culture Plates (96-wells)
HEK-Blue™ 293 cell growth medium (Section 3.16.1)
Protein solutions from Section 3.13.5
Distilled water (endotoxin free)
HEK-Blue™ Endotoxin Standard (O55:B5, *E. coli*)
QUANTI-Blue™ Detection medium powder

Procedure

Day 0

1. HEK-Blue™ hTLR4 and HEK-Blue™ Null1 cells were split to 96-well Falcon® Tissue Culture Plates with flat bottoms (test plates), using 20,000 cells per well and 160 µL growth medium/well. The cells were incubated at 37 °C for 24h.

Day 1

2. Growth medium was aspirated from the wells and 160 µL pre-warmed test media was added to each well.
3. Sample dilutions of the proteins were prepared in a Falcon® Tissue Culture Plate. Based on previous experience with HEK-Blue assays, the protein solution was first diluted to 1/2000 of the start concentration. Thereafter, this solution was diluted by three degrees for each well until well number 9. Well number 10 only contained water (blank).
4. 20 µL of the sample dilutions was transferred to the corresponding well in the test plate. The test plate was incubated for 1 h at 37 °C with 5% CO_2 (pre-treatment).
5. Spike solution (0.1 EU/mL endotoxin) was prepared by diluting 1.0 EU/mL HEK-Blue™ Endotoxin Standard stock solution. The endotoxin solutions were vortexed thoroughly, as LPS can bind to glass and plastic containers.
6. After incubation, 20 µL of endotoxin free water (unspiked solution) and spike solution was added to the wells in the test plate corresponding to the two exposures.
7. The plate was incubated 18-24 hours at 37°C, 5% CO_2.

Day 2

8. QUANTI-Blue™ solution was prepared by dissolving one pouch of powder in 100 mL endotoxin free water and warmed at 37 °C for 30 minutes before use. The solution was stored up to 2 weeks at 4°C.
9. 20 µL of the supernatant from each well of the test plate was transferred into corresponding wells of a new 96 well plate (detection plate).
10. To each well, 180 µL QUANTI-Blue™ solution was added. The plate was incubated 1-6 hours, until desired color development was reached, at 37°C.
11. Absorbance at 620 nm was measured using the SpectraMax M2 spectrophotometer with the SoftMax Pro 6 software.

3.15 ToxinSensor™ Chromogenic LAL Endotoxin Assay Kit

To investigate the potential content of endotoxins in the protein samples, a LAL endotoxin assay was performed.

Materials

ToxinSensor™ Chromogenic LAL Endotoxin Assay Kit (Table 2.6)

Protein solutions from Section 3.13.5

Procedure

The endotoxin detection assay was performed in accordance to the GenScript ToxinSensor™ Chromogenic LAL Endotoxin Assay Kit protocol. For these samples, the incubation time "T1" was set to 30 minutes. When measuring absorbance at 545 nm, 200 µL of each sample was transferred to a 96-well plate. The SpectraMax Pro M2 spectrophotometer with SoftMax Pro 6 was used to obtain the absorbance data and used to calculate the endotoxin concentration.

4. RESULTS

To investigate the putative immunomodulatory effects of a selection of *M. capsulatus* Bath-derived proteins, constructs of the proteins were first expressed with a His-tag in *E. coli* systems and purified using a nickel column. The purified proteins were incubated with different cell lines to unravel the potential immunomodulatory effects of the selected proteins. The chosen proteins were TIR, MIF, SIMPL, MAM and the two domains of the MAM protein, namely GGDEF and EAL. Two approaches were used to evaluate the putative effects of the proteins on an *in vitro* host immune response. Firstly, the proteins were evaluated in terms of their ability to affect expression of the pro-inflammatory cytokine IL-8 in an *in vitro* intestinal cell (Caco-2) model of IL-1β-induced inflammation. Secondly, the proteins' potential ability to regulate activation of the NF-κB pathway was investigated in a HEK-293 derived cell line overexpressing TLR4.

4.1 Plasmid construction using *E. coli* TOP10

Plasmids encoding the proteins TIR, MIF, SIMPL, MAM, and the two domains of MAM, were constructed previously (Sveen, 2016) (Indrelid, unpublished). The gene sequences of *Tir* and *Mif* were cloned into pNIC-CH plasmids, which translationally fuses the sequences to a His-tag. In addition to the full-length *Mam*, constructs for its two domains were also utilized. This was to enable investigation of the separate domains' potential to affect *in vitro* cell inflammation. The sequences for *Mam* and its two domains GGDEF and EAL were cloned into a pMAL-c5X plasmid, which fuses a maltose binding protein (MBP) to the protein (Indrelid, unpublished). Attachment of an MBP is a common strategy to keep a recombinant protein in solution. The attachment of MPB is acquired by cloning the gene of interest into the pMAL-c5X vector downstream of the *MalE* gene that encodes MBP (New England Biolabs Inc., 2019). *MalE* expression is controlled by the Ptac promoter and MBP translational signals. When protein expression is induced, the target protein sequence will be fused with a portion of MPB with a protease cleavage site in between. Due to the protease cleavage site the MBP can be detached from the target protein if desired.

After inducing protein expression in *E. coli* BL21 harboring the constructs, the cell content was harvested for protein purification by sonication and centrifugation. The supernatant from the latter step was purified with IMAC using a nickel-column. The nickel-column had affinity for the His-tag on the protein, hence enabling specific elution of only proteins containing the His-tag. The purification was thereafter evaluated on an LDS-PAGE in terms of purity and whether

the protein fractions contained the protein of interest. Relevant fractions were then pooled together, and the buffer was changed to a more relevant buffer to be used in cell-based inflammation assays. Lastly, the protein solutions were filtrated to ensure sterility before exposure to human cell lines.

Due to heavy precipitation of the TIR protein during buffer exchange when using the TIR construct from 2016 (Figure A-1) (Sveen, 2016), a new TIR construct was made in the present study. Here, the TIR sequence was attached to an MBP sequence in a pMAL-c5X plasmid as a strategy to keep the protein in solution (Figure 4.1.1).

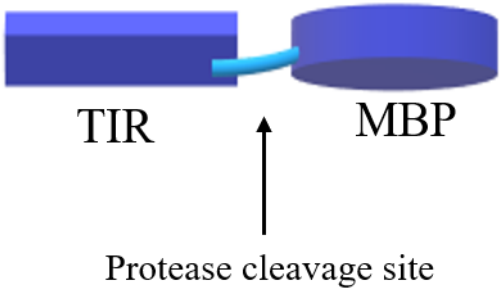

Figure 4.1.1. Illustration of the fusion protein consisting of TIR and MBP. To overcome precipitation challenges with TIR a fusion protein of TIR and MBP was made. The fusion protein of TIR and MBP is approximately 79 kDa. Between the two regions of the fusion protein is a protease cleavage site, enabling detachment of MBP from TIR if desired.

Two approaches were utilized in parallel to ensure successful construction of pMAL-c5X_TIR; quick ligation and In-Fusion cloning. These methods differ as In-Fusion cloning requires a 15 bp overhang on the vector and insert, while quick ligation does not require the overhang on the vector. The overhangs required for In-Fusion cloning were introduced to the insert during PCR with specific primers and to the vector by digestion with BamHI and NdeI. The insert used for quick ligation was therefore treated with BamHI and NdeI after PCR, to remove the overhang. Figure 4.1.2 shows a simplified illustration of the construction of pMAL-c5X_TIR.

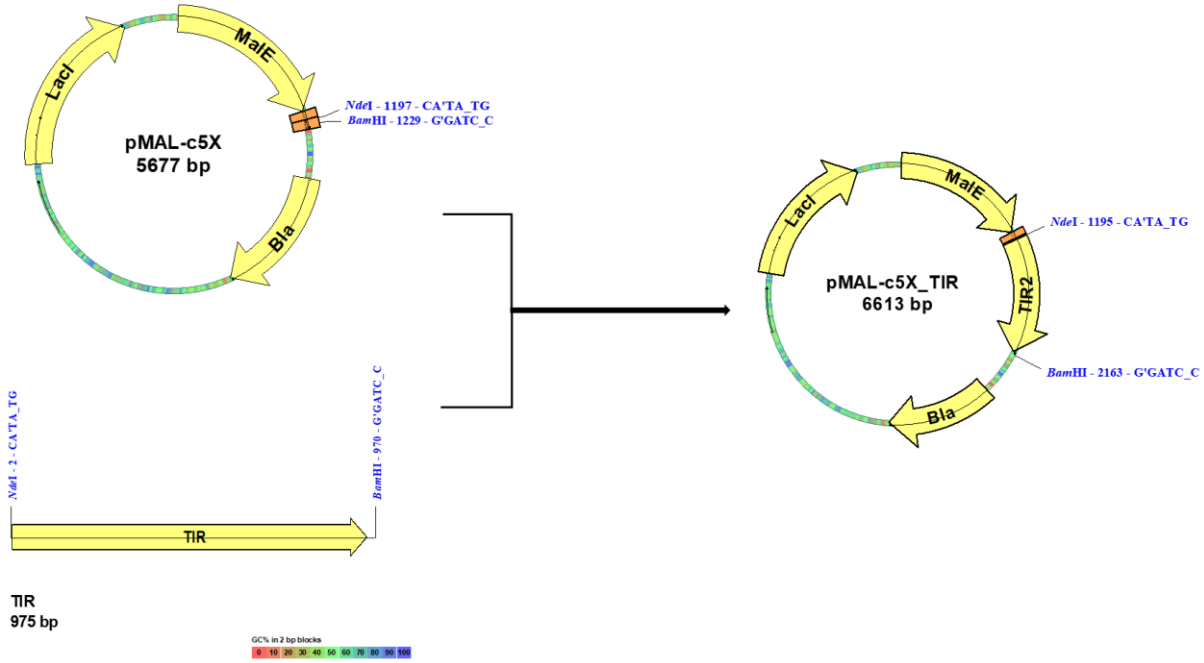

Figure 4.1.2. Strategy for construction of vector pMAL-c5X-TIR from pMAL-c5X and TIR. The TIR fragment was inserted into pMAL-c5X at the BamHI and NdeI restriction sites.

Figure 4.1.2 illustrates the simplified strategy for constructing the pMAL-c5X_TIR plasmid. pMAL-c5x was linearized with NdeI and BamHI, and the pNIC_TIR plasmid harboring the insert was amplified by PCR using the primer pairs pMAL_TIR-F and pMAL_TIR-R (Table 2.4). The products of these steps were verified by gel electrophoresis (Figure 4.1.3).

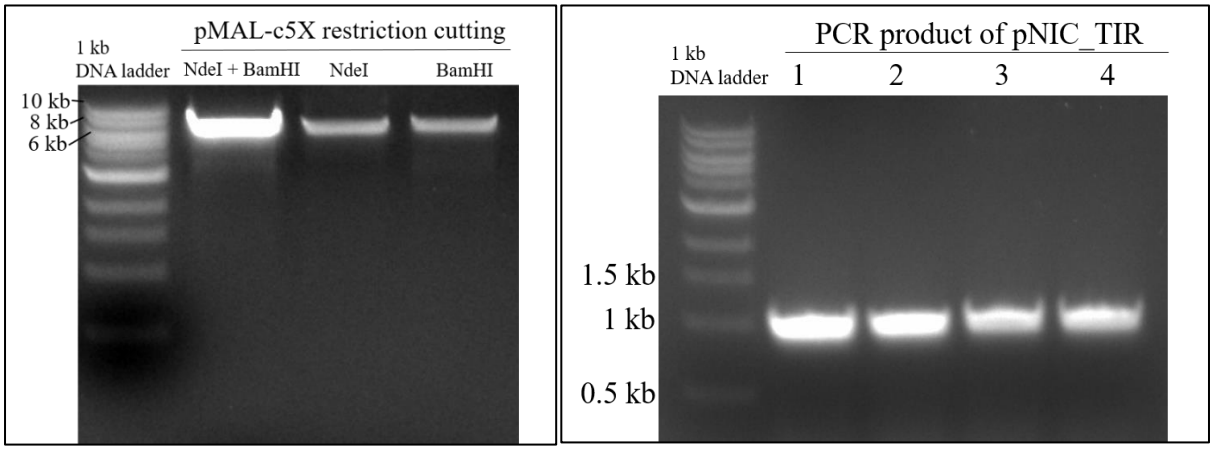

Figure 4.1.3. Agarose gel electrophoresis of the pMAL_c5X vector and the insert after PCR. Left: The pMAL_c5X vector (~7 kb) cut with NdeI + BamHI, NdeI only, and BamHI only. **Right:** Product of PCR run on pNIC_TIR at ~1 kb. PCR products from lanes 1 and 2 were used further for quick ligation and the products from lanes 3 and 4 were used further for In-Fusion ligation.

Fragments corresponding to both the pMAL-c5X vector and the insert (TIR), respectively at ~7 kb and 1 kb, were detected (Figure 4.1.3). There was a stronger signal in the well with vector cut with both restriction enzymes, compared to wells with plasmid cut with one enzyme, due to more vector used in the former reaction mixture. During the PCR reaction, 15 bp overhangs were created on the PCR product. The vector pMAL-c5X, linearized with both restriction enzymes NdeI and BamHI, and the insert were excised from the gel and purified, and the DNA concentrations were determined. The insert further used for quick ligation was treated with NdeI and BamHI, to remove the 15 bp overhangs introduced in the PCR before ligation. The linearized vector and the amplified insert were ligated, yielding the pMAL-c5X_TIR. Immediately after, the constructs (pMAL-c5X_TIR) were transformed into *E. coli* TOP10 and grown on plates. Colony PCR and gel electrophoresis were performed the following day to confirm successful cloning procedures (Figure 4.1.4). Respectively six and two colonies deriving from the quick ligation and In-Fusion cloning reactions were chosen, due to varying numbers of colonies on the plates.

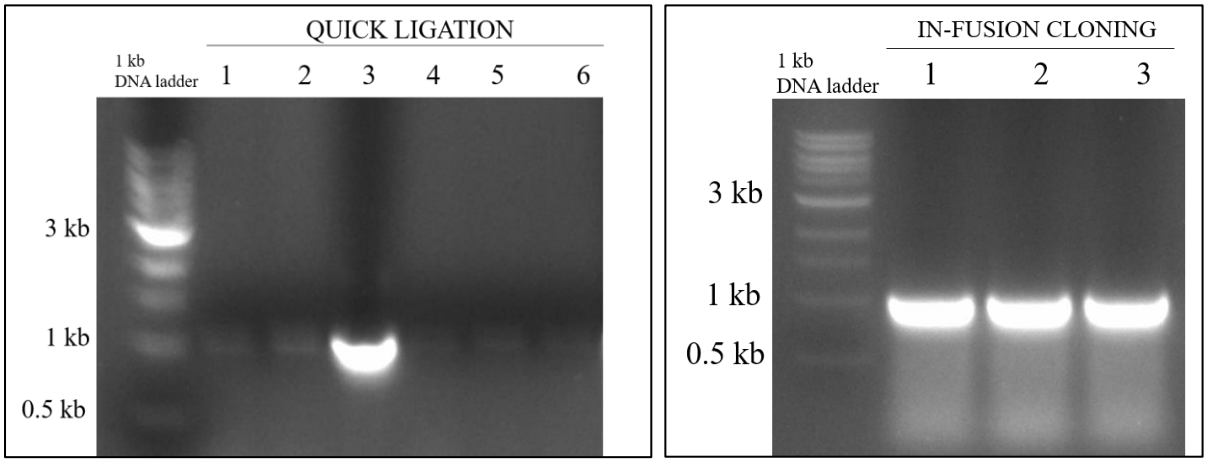

Figure 4.1.4. Result of colony PCR of transformed *E. coli* TOP10. Two techniques for ligating insert (TIR) and vector (pMAL-c5X) were used; quick ligation and In-Fusion cloning**. Left:** fragments of 1kb descending from plasmids prepared with quick ligation. Most successful in one out of six products. **Right:** Fragments of 1 kb from plasmids prepared with In-Fusion cloning. All three colonies were successful.

As Figure 4.1.4 shows, In-Fusion cloning gave the best results, hence the plasmids from this reaction were used further. The constructs were isolated from overnight cultures, followed by sequencing one of the isolated constructs and transforming it into *E. coli* BL21. Due to some irregularities, a second round of sequencing was performed to confirm that the insert was correctly incorporated into the vector.

4.2 Protein expression and purification using *E. coli* BL21

E. coli BL21 containing the constructs used in this study were cultivated at room temperature (23ºC) in the harbinger-system overnight, and the following day protein production was induced by IPTG. Approximately 24 hours later, the cells were harvested through centrifugation. The cells were lysed by sonication to make the cell content accessible in the supernatant, and this supernatant was purified by IMAC using the Äkta pure protein purification system with a HisTrap™ nickel-column. Because the proteins bind specifically to the nickel-column by their His-tag, the elution of the target protein can be controlled. The purification was analyzed by LDS-PAGE, and fractions containing the target protein were pooled. The buffer in the solution of pooled fractions were thereafter changed to a more physiologically relevant buffer, compared to the imidazole-containing buffer B, for the cell-based assays to be performed. The protein solutions were stored at 4ºC.

The protein purification was monitored through a chromatogram. Protein elution from the column was monitored by detecting A_{280} of the column flow through. The percentage of elution buffer (Buffer B) added to the system was monitored as well, and nearly all proteins eluted at approximately 30-60% Buffer B. TIR, however, eluted at much lower Buffer B concentrations. Figure 4.2.1 shows the chromatogram from the purification of TIR, whereas the first top represents the flow-through of non-His-tagged proteins and the second top represents elution of TIR. The purification of TIR resulted in a lower elution peak than compared to the other purifications, indicating a lower yield of this protein.

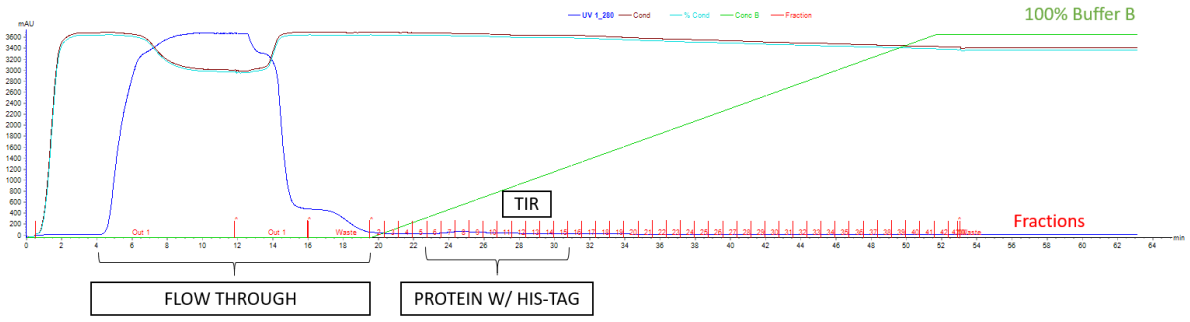

Figure 4.2.1. Chromatogram from IMAC purification of TIR. Protein elution from the column was monitored by detecting A_{280} (dark blue line) of the column flow through. The green line shows the imidazole gradient applied to the system via buffer B to elute the protein bound to the HisTrap™ column. The brown and light blue lines show the conductivity of the solutions in the column. Fraction numbers are shown in red along the x-axis. The first peak represents the non-bound protein (flow through) and the second peak represents the His-tagged protein (TIR). A small elution peak indicated low yield of the protein. Fractions 4-15 were analyzed further with LDS-PAGE. The chromatogram was generated using the UniCorn™ 64 Software.

The low second peak in Figure 4.2.1 indicated a low yield of TIR. To analyze if the purification resulted in pure fractions containing the protein of interest, fractions 4-15 from the purification of TIR were analyzed with LDS-PAGE (Figure 4.2.2). In addition to the fractions from the IMAC purification, the pellet and supernatant from the cell lysis step were included on the gel to investigate if TIR could be present in the pellet instead of the supernatant.

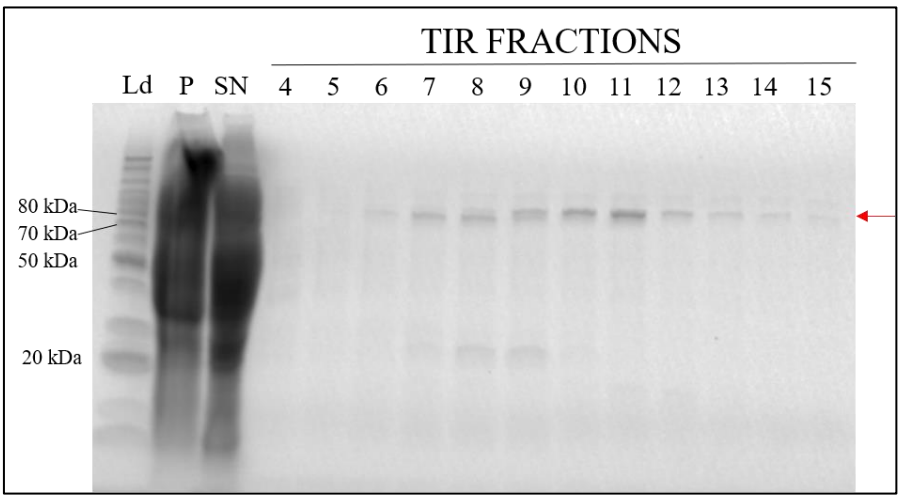

Figure 4.2.2. LDS-PAGE of fractions from the purification of TIR. The pellet (P) and supernatant (SN) from the protein extraction step showed proteins of various sizes. The SN showed indications of the band at ~80 kDa, as seen in the TIR fractions 5-15 (red arrow). Bands at ~20 kDa can be seen in fractions 7-9. The pellet contained proteins of various sizes, and the possibility of TIR content in the pellet could not be excluded. Fractions 8-12 were pooled.

Figure 4.2.2 shows that the fractions 5-15 contain a fragment corresponding to the ~80 kDa TIR protein with MBP. There is also an additional 20 kDa fragment in fractions 7-9. The pellet and supernatant contain proteins of various sizes, and the possibility of TIR content in the pellet cannot be excluded. Fractions 8-12 were pooled, and the buffer exchange procedure was conducted. All other proteins of this study were produced and purified by the same procedure as described for TIR. The chromatograms for the IMAC purifications of SIMPL, MAM and the two domains of MAM (GGDEF and EAL) are shown in the appendix (Figure A-2). An example of a production with higher yield than of TIR is that of MIF (Figure 4.2.3).

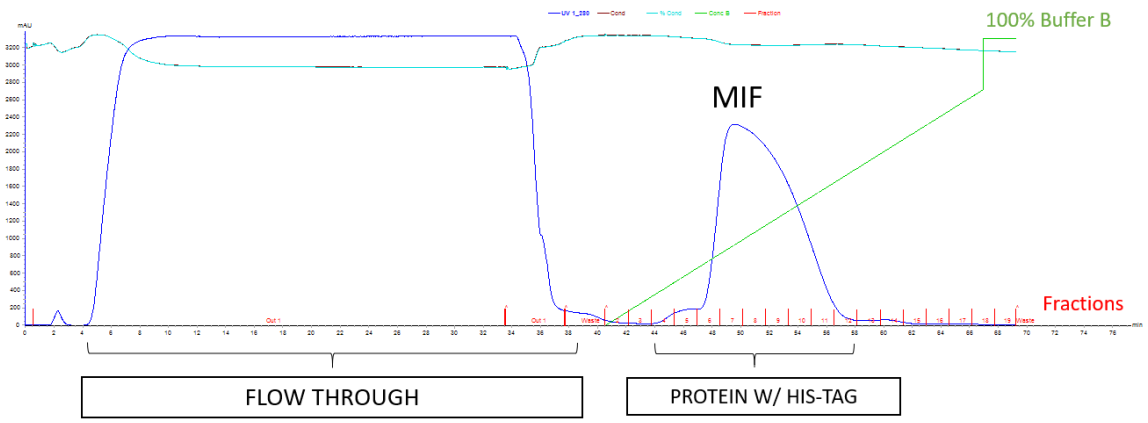

Figure 4.2.3. Chromatogram from IMAC purification of MIF. Protein elution from the column was monitored by detecting A_{280} (dark blue line) of the column flow through. The green line shows the imidazole gradient applied to the system via buffer B to elute the protein bound to the HisTrap™ column. The brown and light blue lines show the conductivity of the solutions in the column. Fraction numbers are shown in red along the x-axis. The first peak represents the non-bound protein (flow through) and the second peak represents the His-tagged protein (MIF). Fractions 6-14 were further analyzed. The chromatogram was generated using the UniCorn™ 64 Software.

The second peak, representing the His-tagged protein, is much higher for MIF (Figure 4.2.3) than of TIR, indicating that a higher yield of MIF than TIR was achieved. To validate that the target protein had been isolated, and to illustrate the purity of the protein fractions, an LDS-PAGE analysis of fractions 6-14 from the purification of MIF was performed (Figure 4.2.4).

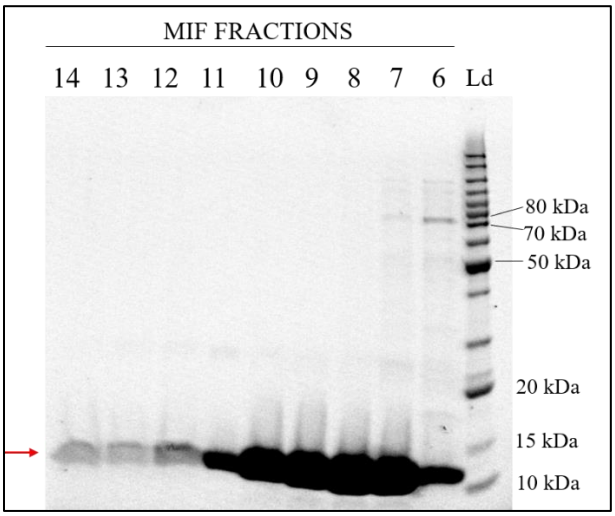

Figure 4.2.4. LDS-PAGE of fractions from the purification of MIF. Fractions 6-14 from the purification of MIF were analyzed. All fractions contained a ~13 kDa fragment corresponding to MIF (red arrow). Fractions 6-7 also contained a band at ~75 kDa. Fractions 7-9 were pooled and used for further analysis of MIF.

Figure 4.2.4 shows the presence of a fragment at ~13 kDa in the fractions from the purification of MIF, corresponding to the size of MIF (Table 4.2). Also, fractions 6-7 contain a ~75 kDa fragment. Strong signals in fractions 6-11 indicates high protein concentrations within these fractions. Fractions 7-9 were pooled, and buffer exchange was performed to prepare the solution for the *in vitro* cell-based inflammation assays.

The purifications of SIMPL, full-length MAM, and the two MAM domains GGDEF and EAL, were successful. The respective chromatograms can be seen in the appendix (Figures A-2). Figure 4.2.5 shows the LDS-PAGE analysis of these four proteins.

A

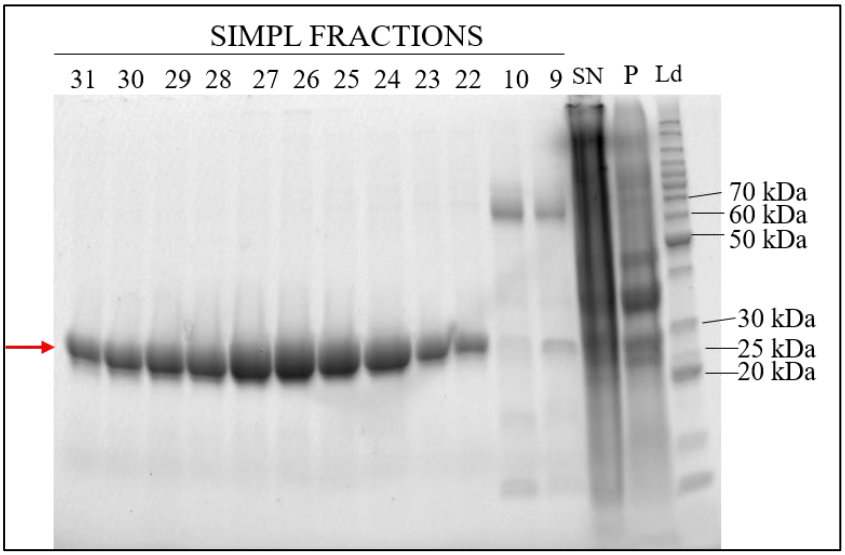

B

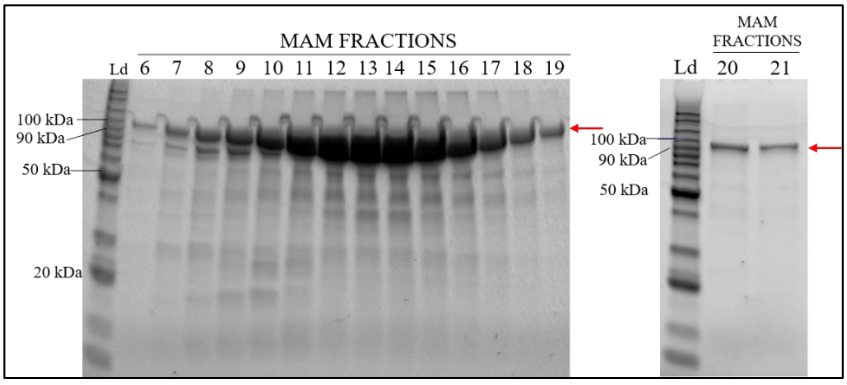

C

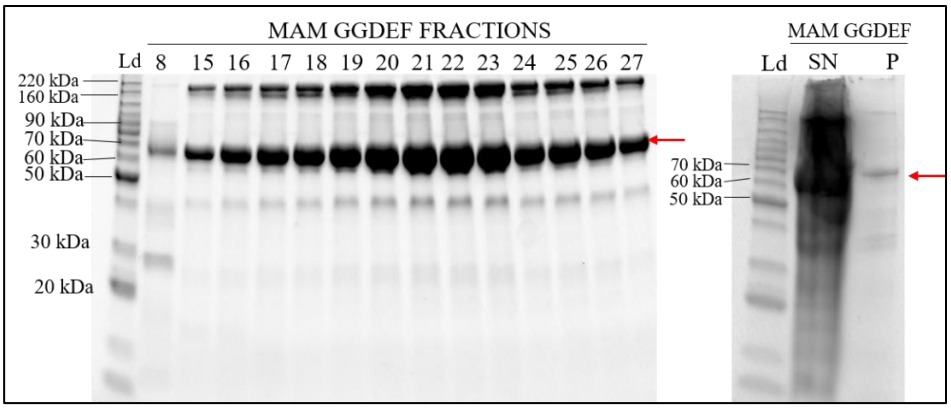

D

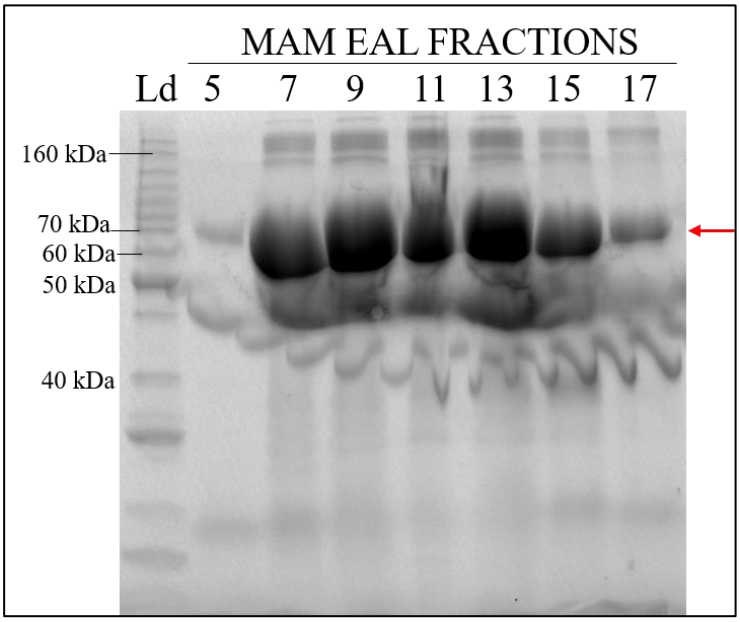

Figure 4.2.5. LDS-PAGE analysis of the purifications of SIMPL, full-length MAM, and the GGDEF and EAL domains of MAM. Red arrows indicate the expected band size of the purified protein. **A)** Fractions 9-10, 22-31 from the purification of SIMPL. Fractions 9-10 contain a 60 kDa fragment, in addition to that corresponding to SIMPL (24 kDa). Fractions 22-31 all contain a fragment corresponding to SIMPL at 24 kDa. **B)** Fractions 6-21 from the purification of MAM. Fractions 20-21 contain the 97 kDa bond corresponding to MAM, and the earlier fractions also contain other proteins. **C)** Fractions 8, 15-27 from the purification of the GGDEF domain of MAM, in addition to the supernatant and pellet from the cell lysis step. The GGDEF domain at 67 kDa was present in all fractions, in addition to contaminant proteins (e.g. at 160-200 kDa). **D)** Fractions 5-17 were kept after the purification of the EAL domain of MAM. The LDS-PAGE shows analysis of every other fraction, and an unusual pattern appeared on the gel. The EAL domain at 73 kDa was present, in addition to contaminant proteins at other sizes (e.g. at 160-200 kDa).

The protein concentrations were calculated after buffer exchange and determined using the Beer-Lambert law (Box 1) (Table 4.2). Thereafter, protein solutions were sterile filtrated and ready to use in the *in vitro* cell-based assays. A few of the protein solutions slightly precipitated over time, but this was resolved with additional filtration to remove the precipitate.

Table 4.2. Final protein concentrations of the proteins purified in this study. The concentrations were determined after change of buffer and sterile filtration. The protein concentrations were calculated using the Beer-Lambert law.

PROTEIN	SIZE (kDa)	EXTINCTION COEFFICIENT	CONCENTRATION
TIR (with MBP)	78.9	101300	2.1 µM
MIF	13.2	15470	2.3 mM
SIMPL	23.9	12950	159.5 µM
MAM (with MBP)	97.9	90675	11.2 µM
MAM GGDEF (with MBP)	67.6	70820	102.8 µM
MAM EAL (with MBP)	73.3	86205	219.2 µM

As indicated by the chromatograms from the IMACs and LDS-PAGE analyses the protein concentrations differed (Table 4.2). Therefore, different concentrations for each of the proteins had to be used in the cell-based assays (Sections 4.3 and 4.4).

4.3 IL-8 response in IL-1β exposed Caco-2 cells

A human intestinal cell line resembling the enterocytes of the gastrointestinal tract, Caco-2 cells, was used to investigate the putative immunomodulatory properties of the purified proteins.

For the assay, Caco-2 cells were grown for four days in 12-well plates before changing to serum-free media. Removal of serum was important to remove potential growth promoting factors, hormones and other molecules from the serum that potentially could affect the outcome of the inflammation assay. Approximately 24 hours after changing to serum-free medium, inflammation was induced by adding IL-1β which subsequently resulted in expression of the pro-inflammatory cytokine IL-8. Additional exposure of the proteins of interest could potentially reveal the proteins' ability to regulate IL-8 expression, and hence modulate a host cell immune response within the set conditions. ELISA, specific to human IL-8, was performed on the cell-medium supernatant 24 hours after stimulation. Cells were monitored by light microscopy to ensure healthy, morphologically similar cells in the assays (Figure A-3).

Various concentrations of the proteins were added due to available volumes and concentrations after buffer exchange (Table 4.2). The significance of the effects of the *M. capsulatus* Bath derived proteins on IL-8 expression was evaluated by the Student's t-test (Figure 4.3).

As the hypothesis is that the proteins possibly reduce IL-8 expression, IL-1Ra was included as a control in the assay. The IL-1Ra control could confirm the assays' credibility as to whether it was possible to reduce IL-8 expression in the cells after IL-1β exposure. As Figure 4.3 illustrates, IL-1Ra reduced IL-8 levels induced by IL-1β and was as expected.

A significant reduction in IL-8 levels was seen in exposures of all the proteins (Figure 4.3). TIR reduced IL-8 expression, despite the use of low protein concentrations. MIF increasingly reduced IL-8 levels when exposing the cells to 0.5-1 µM, but the effect decreased with higher concentrations. Different SIMPL exposures showed a significant reduction in IL-8 expression. Exposure with 0.25 µM SIMPL varied from the other SIMPL exposures. All exposures of MAM and its two separate domains, GGDEF and EAL, resulted in significant reduction of IL-8 expression. However, there was a difference in their respective fold reduction. At 1 µM protein full-length MAM reduced IL-8 from 302.2 pg/mL to 123.3 pg/mL (60% reduction), GGDEF from 321.5 pg/mL to 163.8 pg/mL (50%), and EAL from 299.5 pg/mL to 209.5 pg/mL (30% reduction).

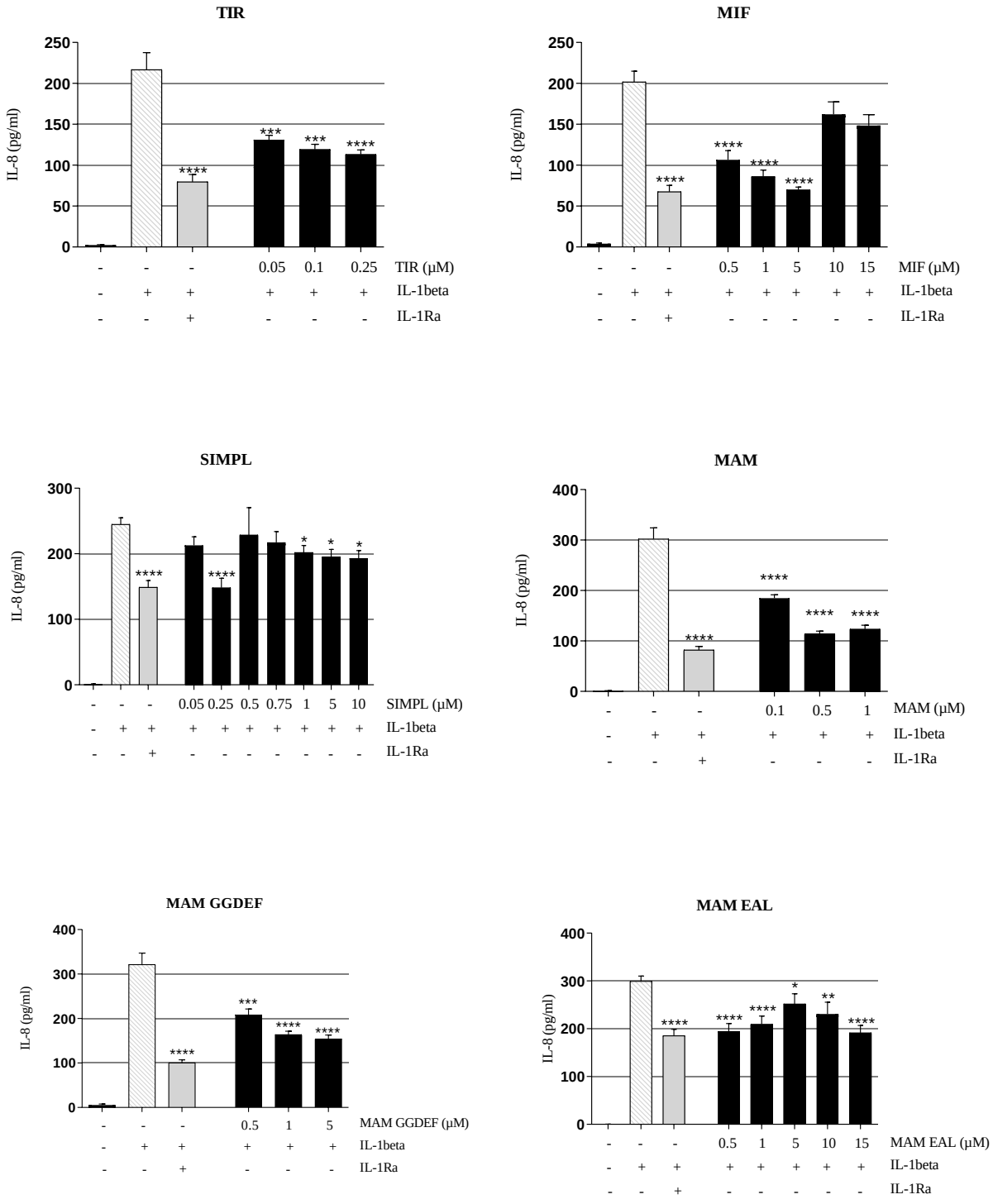

Figure 4.3. IL-8 expression in Caco-2 cells after exposure to IL-1β, the proteins of interest and IL-1Ra. Caco-2 cells were stimulated with IL-1β and the protein in question, 24 hours before measuring IL-8 concentration with ELISA. The values are expressed in means+SEM from three independent experiments in duplicate. *p ≤ 0.05. **p ≤ 0.01. ***p ≤ 0.001. ****p ≤ 0.0001 compared to IL-1β exposed control cells.

4.4 Effects on HEK-293 TLR4 cells

To investigate the potential effects of the proteins of interest on the NF-κB signaling pathway a HEK-293 cell line overexpressing TLR4 was utilized. The non-transfected cell line HEK-Null was included as a control. Monitoring the cells before, during and after the assay by light microscopy was performed to ensure healthy morphologically similar cells evenly distributed in the wells (Figure A-4). The assay was set up by plating HEK-TLR4 and HEK-Null cells in 96-well plates. The following day a protein gradient was added to wells 1-9, while the 10th was supplemented with endotoxin-free water (blank). After incubating 1 hour at 37^{o}C, the two first rows (wells 1-10) were supplemented with endotoxin-free water. The two last rows (wells 1-10) were spiked with LPS, hence activating TLR4 and the NF-κB signaling pathway resulting in subsequent expression of the reporter gene SEAP. To evaluate the potential inhibitory effect of the protein in question on the NF-κB pathway, the percentage difference in absorbance between unspiked and spiked wells with a protein exposure was compared to the blank measured ~3 hours after exposure. Following the manufacturers' recommendation, a difference lower than 75% was considered inhibitory on the NF-κB pathway. This means that the potential effect of a protein in question on the regulation of the NF-κB pathway must be by at least 25% to be considered inhibitory. See Section 3.14.2 for more details on the assay design, and Figure A-5 for an example of a plate setup.

For all the HEK-Null1 exposed cells, no SEAP expression was detected (data not shown). In comparison, HEK-TLR4 cells had induced SEAP expression and hence verified the specificity of the cells.

TIR did not inhibit the NF-κB pathway in the HEK cells, although the average result of 0.1 nM TIR is below the set threshold (Figure 4.4). As the error bar exceeds the set threshold, it cannot be considered inhibitory. It is noteworthy that the highest and lowest concentrations of TIR affected the NF-κB pathway more, compared to the concentrations in between. Interesting results were produced with MIF exposures and may indicate that MIF reduces activation of the NF-κB pathway, but nearly all errorbars exceed the threshold. False positives in the SIMPL exposure were removed before presenting the results. SIMPL did not show an inhibitory effect on the NF-κB pathway. MAM inhibited the NF-κB pathway with 5.6 nM, 1.8 nM and 0.6 nM exposures. The GGDEF domain of MAM might have inhibitory properties on the NF-κB pathway, as the 54.1 nM exposure was well below the threshold. The 17.1 nM GGDEF

exposure had a large errorbar exceeding the threshold, and the 5.7 nM exposure was right below the threshold. In contrast to the full-length MAM and the GGDEF domain, did not any exposures of the EAL domain inhibit the NF-κB pathway.

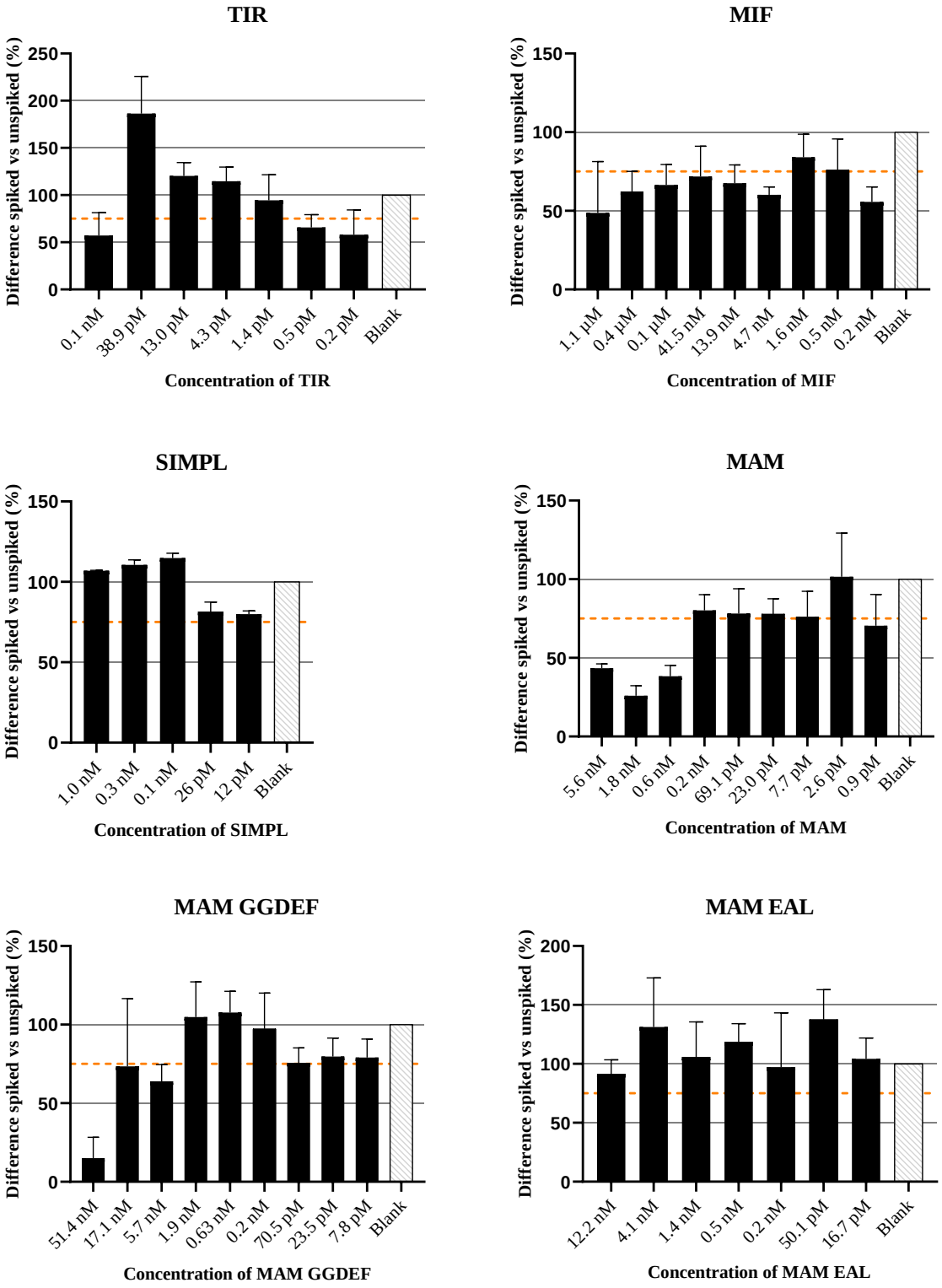

Figure 4.4. Effects of the proteins on the NF-kB pathway. The values are expressed in means+SEM from three independent experiments in duplicate (except for SIMPL where two experiments were performed). A percentage difference between spiked and unspiked cells for the protein exposure compared to the blank (no protein) exposure below 75% is considered as inhibitory of the NF-κB pathway.

4.5 LAL endotoxin sensor assay

When performing the NF-κB pathway assay with the HEK-cells presence of LPS was detected in the protein solutions due to a color change in the unspiked wells containing the protein and water (no LPS added), indicating expression of SEAP and hence activation of the NF-κB pathway by the protein solution (Figure A-5). To measure the potential LPS content in the protein solutions a LAL endotoxin detection assay was utilized. Table 4.5 lists the LPS concentrations found in the protein solutions.

Table 4.5. LPS concentration present in the protein solutions used in this study. The LAL endotoxin detection assay showed that LPS was present in all the protein stock solutions, at approximately 1.0 EU/mL.

PROTEIN	LPS CONCENTRATION (EU/mL) IN PROTEIN STOCK SOLUTION
TIR	1.18
MIF	1.20
SIMPL	1.28
MAM	1.13
MAM GGDEF	1.22
MAM EAL	1.00

The LAL endotoxin detection assay revealed a content of approximately ~1.0 EU/mL LPS in all protein stock solutions.

5. DISCUSSION

Research has demonstrated that *M. capsulatus* Bath elicits anti-inflammatory effects by reducing symptoms of SBM-induced enteritis in Atlantic salmon and DSS-induced inflammation in mice (Kleiveland et al., 2013; Romarheim et al., 2010). The underlying causes of the immunomodulatory mechanisms are not fully understood.

Selected proteins derived from *M. capsulatus* Bath with structure or sequence homology to proteins with well-known immunomodulatory effects were used for analysis in the present study. The proteins in question were the TIR-like protein, MIF, SIMPL-like protein, MAM and two domains of MAM; GGDEF and EAL. The potential immunomodulatory effect of each protein was evaluated in *in vitro* cell-based inflammation assays using the human cell lines Caco-2, HEK-TLR4 and HEK-Null1.

5.1 Protein expression and purification

To enable expression of the proteins, the sequences encoding the proteins were cloned into vectors. The constructs for the *M. capsulatus* Bath proteins TIR, MIF, SIMPL, MAM, MAM GGDEF domain and MAM EAL domain were constructed by Sveen (2016) and Indrelid (unpublished). All constructs contained a His-tag, enabling purification by IMAC using a nickel-column. The MAM proteins were in addition attached to a maltose binding protein (MBP), which contributes to increased solubility. As production of TIR by the construct from 2016 resulted in precipitation (Figure A-1), the TIR protein was attached to an MBP in the current study (Figure 4.1.1). The TIR sequence with His-tag and MBP was successfully cloned into the pMAL-c5X vector. The current study analyzed the hybrid proteins with the MBP, however MBP can be proteolytically cleaved if desired at a later stage. Especially if the current study reveals immunomodulatory effects of the hybrid proteins, it could be interesting to see if the effect persists after detaching the MBP.

The purification of the proteins was overall successful, although resulting in variable protein concentrations (Table 4.2). As indicated by the chromatogram and LDS-PAGE run for TIR (Figures 4.2.1, 4.2.2), a low concentration of TIR was obtained. One reason may be that the His-tag was non-optimally exposed on the protein surface, hence reducing its affinity to the nickel-column (Bolanos-Garcia & Davies, 2006). TIR has previously shown to be challenging to express and purify (Rana et al., 2013). The LDS-PAGE of the cell lysate from the TIR production showed a protein at ~80 kDa, corresponding to the size of TIR (Figure 4.2.2) which may indicate precipitated proteins as inclusion bodies. Inclusion bodies are aggregates of a

highly expressed protein often formed when using *E. coli* as a host for protein expression, which may occur as a result of an exhaustion of the protein quality control of the bacterium while expressing protein at a high translational rate (Singh et al., 2015). In addition, over-expression of recombinant protein in plasmid-encoded genes can trigger transcription of heat-shock proteins and other stress responses that results in aggregation of protein as inclusion bodies (Villaverde & Carrió, 2003).

On the contrary to TIR, as indicated by the chromatogram and LDS-PAGE (Figures 4.2.3, 4.2.4), a high concentration of MIF was acquired. Because of the various protein concentrations, not all proteins could be tested at the same concentrations in the cell-based assays (Table 4.2).

The LDS-PAGE gels indicated the purity of the protein fractions, which revealed contaminants in the purifications of all proteins (Figures 4.2.2, 4.2.4, 4.2.5). The contaminants from purification of full-length MAM could not affect the cell-based assays, as the pooled fractions were entirely pure (Figure 4.2.5B). The LDS-PAGE of the fractions from MAM EAL domain purification shows an unusual pattern (Figure 4.2.5D), due to unknown irregularities with possibly the buffer or other electrophoresis equipment. Testing various conditions during LDS-PAGE resulted in similar gel patterns.

The purification of MAM and the GGDEF and EAL domains resulted in fractions containing proteins of several sizes, in addition to the target proteins. The proteins at 160-200 kDa, found in the GGDEF and EAL domain fractions, are approximately three times the size of each of the domains (Figure 4.2.5). A possible explanation for the findings can be a combination of oligomerization and aggregation of the proteins, which are common challenges in purification of recombinant proteins (Bondos & Bicknell, 2003). Non-optimal conditions in the protein expression, purification or storage, potentially resulting in oligomerization of proteins, can in turn result in concomitant loss of function (Lu et al., 2001). If the potential oligomers are non-functional, they may not affect the *in vitro* cell-based inflammation assays of this study. Despite, the potential presence of such components and other unidentified proteins in the protein solutions will affect the measured protein concentrations, hence influencing the actual concentration of the protein of interest exposed to the cells.

There are several strategies to reverse an undesired protein precipitation during purification, such as adding a cosolvent that destabilizes, or by other means, prevents the intramolecular interactions (Bondos & Bicknell, 2003; Neagu et al., 2001). As it is currently not known how, if at all, the purified domains oligomerize in solution, it is challenging to decide what

component would be relevant to use. Also, this component is restricted to not influencing the following assays involving human cell lines. Moreover, the nickel-column used in this study was used for many purifications. It may be advantageous to re-load the column with nickel, to ensure a higher efficacy.

The additional proteins present in the solutions after purification have all eluted during the elution step for His-tagged proteins, thus is it possible that these contaminant proteins contain a histidine-rich region (Mateo et al., 2001). The elution buffer used in the IMAC contained 250 mM imidazole, and high imidazole concentrations during purification can be related to co-purification of contaminant proteins (Westra et al., 2001). There are several *E. coli* BL21 proteins with surfaced histidine clusters with affinity for divalent cations (e.g. nickel), that often cause challenges in purification of recombinant proteins, as they often are co-purified in IMAC (Bolanos-Garcia & Davies, 2006; Cai et al., 2004). Bolanos-Garcia and Davies (2006) identified a list of native *E. coli* proteins often co-purified during IMAC, with sizes ranging from 10.2-66.8 kDa. The sizes of the identified *E. coli* proteins do therefore not correspond to the potential oligomer found in purification of the GGDEF and EAL domains, but they might correlate to the smaller proteins present. This observation is relevant to several of the protein purifications in this study.

As purification of both GGDEF and EAL domains resulted in contaminant proteins at 160-200 kDa, it is not dismissible that these contaminant proteins at that size are the same in both solutions. Purification with IMAC using an empty vector may be advantageous to include in later studies, because it could possibly reveal the effect of the contaminants on the *in vitro* cell-based inflammation assays. Further analysis of the contaminants, by methods such as MALDI-TOF MS or SEC, is required to identify the proteins present in the solutions (Miernyk & Thelen, 2008). In addition, further optimization experiments (e.g. by varying pH, imidazole concentrations, etc.) should be performed to develop an optimal protocol for purification of the *M. capsulatus* Bath proteins.

5.2 *M. capsulatus* Bath TIR-like protein

Many pathogenic and non-pathogenic bacteria use molecular mimics of host proteins to establish a population *in vivo* (Askarian et al., 2014; Newman et al., 2006). Mimicry can involve bacterial TIR-containing proteins that interfere with host TLR signaling by blocking the binding of intracellular MyD88 to the TIR domain of the TLR. MyD88 binds TLR normally after TLR

has recognized a PAMP. Thus, hindrance of MyD88 binding by a bacterial TIR-like protein to TLR will suppress the subsequent innate immunity response of the host (Chan et al., 2009).

A TIR-like protein was identified by a genome analysis of *M. capsulatus* Bath (Indrelid et al., 2014). The present study overexpressed and purified the *M. capsulatus* Bath TIR-like protein in an *E. coli* system. Exposure of the *M. capsulatus* Bath TIR-like protein to Caco-2 cells with IL-1β induced inflammation showed a significant decrease in production of the pro-inflammatory cytokine IL-8 (Figure 4.3). The *in vitro* anti-inflammatory effect of the TIR-like protein as shown by a reduction in IL-8 expression, may be connected to *in vivo* gastrointestinal inflammation, hence are these findings of great interest to gain understanding of the anti-inflammatory properties of *M. capsulatus* Bath (Kleiveland et al., 2013; Quévrain et al., 2016b). The NF-κB pathway assay with HEK-293 cells did not show an inhibitory effect of the TIR-like protein, although concentrations at 0.1 nM, 0.5 pM and 0.2 pM of the TIR-like protein can be of interest but requires further investigation including these and possible other concentrations of the protein.

Although results indicate anti-inflammatory effects of *M. capsulatus* Bath TIR-like protein in the Caco-2 cell inflammation assay, the mechanism behind the effect is not identified. Based on knowledge on TIR-containing proteins from both eukaryotic and prokaryotic species, it may be that the *M. capsulatus* Bath TIR-like protein also interacts with the TIR domain of the host TLRs or MyD88 to interfere with the subsequent signaling cascade (Spear et al., 2012; Takeda & Akira, 2004). Studies show that an uropathogenic *E. coli* (UPEC), a strain causing urine tract infections, CTF073 TIR-containing protein negatively interferes with TLR4-MyD88-NF-κB signaling (Cirl et al., 2008; Yadav et al., 2010). Spear et al. (2012) showed that a specific proline residue of a TIR-domain protein from *Yersinia pestis* is crucial for its ability to downregulate IL-1β and LPS-dependent TLR-signaling. The specific proline residue enabled the *Y. pestis* protein's interaction with MyD88, hence preventing MyD88 to activate the NF-κB pathway. A similar approach as Spear and colleagues chose would be relevant to investigate if *M. capsulatus* Bath TIR-like protein interacts with MyD88.

TIR-like proteins could reduce IL-8 production independently from the NF-κB signaling pathway, as IL-8 expression may not explicitly be regulated through NF-κB. Studies show a cytokine-induced NF-κB-independent mechanism, possibly including mitogen-activated protein kinases (MAPKs), to mediate IL-8 expression in human airway epithelial cells (Cormet-Boyaka et al., 2011; Dauletbaev et al., 2011). Although epithelial cells from a different organ

than the GIT were used in the study, MAPK mediated IL-8 expression in intestinal epithelial cells could be of interest to investigate the effect of TIR-like protein. Such assays can be based on immunoblotting with anti-phospho antibody to detect MAPK activation (Shaul & Seger, 2006).

Host cell TIR-domains interact in the cytosol, hence must the TIR-like domain transport into the cytosol of the host to interact in a similar manner as its homologues. Several suggestions to how bacterial TIR proteins localize into the host cytosol have been proposed and studies indicate that there might be several mechanisms involved depending on the type of bacteria (Rana et al., 2013; Spear et al., 2012). For example, an UPEC TIR-containing protein is suggested to be taken up by macrophages in a cholesterol-dependent manner to interfere with TLR mediated TNF induction (Cirl et al., 2008). A fusion protein of MBP and a *Brucella melitensis* TIR-containing protein was detected inside macrophages in a dose dependent manner (Radhakrishnan & Splitter, 2010). There is a need to further investigate the potential uptake of TIR-containing proteins into human cells.

TIR-containing proteins are found in a wide range of human pathogenic and non-pathogenic bacteria (including soil-bacteria), in addition to fungi, archaea, viruses and eukaryotes (Cirl et al., 2008; Low et al., 2007; Spear et al., 2009). SARM is the only human TIR-containing adaptor protein that negatively regulates TLR signaling (O'Neill & Bowie, 2007). Interestingly, SARM is more closely related to bacterial TIR-containing proteins than animal TIR adaptor proteins, indicating a common origin for these types of TIR proteins (Rana et al., 2013; UniProt, 2019; Zhang et al., 2011). Although homologues of the TIR-like protein modulate host immune responses, the *M. capsulatus* Bath TIR-containing protein could have other functions within both the species and in host cells (Spear et al., 2009). For example, studies show that some bacterial TIR-containing proteins are fused to proteins involved in nucleic acid metabolism (Iyer et al., 2008). The potential immune modulatory effect on host cells by bacterial TIR-containing proteins are possibly a side-effect of the protein's main function.

5.3 *M. capsulatus* Bath MIF domain

MIF is an important component of the early pro-inflammatory innate immune system in mammals (Roger et al., 2012). *M. capsulatus* Bath encodes a MIF protein, which in the present study was expressed and purified from *E. coli*, and exposure of 0.5, 1 and 5 µM MIF to the Caco-2 cells significantly reduced expression of IL-8 (Figure 4.3). Higher concentrations (10 and 15 µM) did not reduce IL-8 significantly, possibly indicating that these concentrations are

too high and thereby masks the actual effect of the protein. The NF-κB pathway assay did not indicate an inhibitory role of *M. capsulatus* Bath MIF on NF-κB signaling (Figure 4.4). Thus, similarly to the results with the TIR-like protein, *M. capsulatus* Bath MIF reduced IL-8 in Caco-2 cells, while not inhibiting NF-κB signaling.

As mammalian MIF up-regulates TLR4 (the PRR for LPS) in macrophages, it contributes greatly to mammals' defense against gram-negative bacteria (Roger et al., 2003; Roger et al., 2012). Studies show that MIF-deficient macrophages are hypo-responsive to exposure of LPS and gram-negative bacteria, and have a down-regulation of TLR4 in such conditions, indicating an autocrine effect of MIF (Roger et al., 2003). Host MIF is also protective in parasitic infections, such as against the malaria-parasite *Plasmodium falciparum* (Awandare et al., 2006; Awandare et al., 2007). Interestingly, *P. falciparum* possess a MIF (*p*MIF) protein, structurally similar to the human MIF, that modulates the host immune response (Bozza et al., 2012; Cordery et al., 2007; Gardner et al., 2002). Neither the role of host MIF or *p*MIF in malaria development is completely understood. Cordery and colleagues found that *p*MIF did not significantly affect IL-8 expression in human monocytes, but that it moderately, but significantly, reduced the monocyte TLR4 surface expression (Cordery et al., 2007). Endogenous MIF can therefore reduce TLR4 expression in human immune cells, while the human MIF is required for TLR4 expression. Studies using pull-down assays also show that *p*MIF interacts with the mammalian MIF cell surface receptor "cluster of differentiation 74" (CD74), implying that the MIF homologue can interfere or modulate host MIF function by competitive binding to the MIF receptor (Dobson et al., 2009). In the current study, M. *capsulatus* Bath MIF is hypothesized to modulate a host cell response by influencing TLR4 expression or by outcompeting the host MIF receptor.

Further analysis of the *M. capsulatus* Bath MIF domain's effect on TLR4 expression (e.g. by western blotting or quantitative PCR) should be considered an important step towards explaining the observed reduction in IL-8 levels. If *M. capsulatus* Bath MIF can reduce TLR4 expression in human cells, as seen by *p*MIF in monocytes, it might contribute to explaining the mechanism behind the reduction in IL-8 expression in Caco-2 cells. However, this rational does not comply with the results seen in the NF-κB assay, as a potential downregulation of TLR4 would be inhibitory on the NF-κB pathway. However, as HEK-TLR4 cells are transformed to over-express TLR4, a potential reduction in expression of TLR4 induced by the protein may not be detectable. In addition, the HEK-Null1 cells did not show activation of NF-κB when

exposed to MIF, indicating that there was not an induction of TLR4 expression by MIF. Note that cells deriving from different organs may hold different expression patterns (Marcu et al., 2018), hence may TLR4 expression patterns in intestinal cells (Caco-2 cells) and kidney cells (HEK-TLR4 cells) not be comparable.

The host cell MIF-receptor CD74 is expressed in the mouse cell line CT26, with similarity to Caco-2 cells as it also is a human colon carcinoma epithelial cell line (Maharshak et al., 2010). Binding of human MIF or the pathogenic bacterium *Helicobacter pylori* to human CD74 activates the NF-κB and MAPK pathways (Beswick et al., 2005; Leng et al., 2003). The CD74 mediated NF-κB activation by *H. pylori* has shown to induce IL-8 expression (Beswick et al., 2005). *M. capsulatus* Bath MIF reduced IL-8 expression in human intestinal cells, while the NF-κB assay did not show an inhibitory effect of the protein. Further experiments are required to identify whether Caco-2 cells express CD74, and if *M. capsulatus* Bath MIF could interact with the receptor if present. The potential interaction may occur without inducing IL-8 expression, due to the complexity of NF-κB induced gene expression (Hoesel & Schmid, 2013). To further investigate, real-time PCR and western blot analysis of CD74 expression in Caco-2 cells is relevant (Wong & Medrano, 2005) to investigate a possible *M. capsulatus* Bath MIF-CD74 interaction (Jain et al., 2012).

MIF is expressed in the human GIT, and studies show significantly higher levels of MIF in the gastrointestinal epithelium and the serum of gastric cancer and - inflammation patients, compared to healthy individuals (He et al., 2006). Characterizing the potential effect of *M. capsulatus* Bath MIF on TLR4 expression and/or CD74 interaction in intestinal immune cells might give an indication as to how the bacterium can elicit immune modulatory effects (Kleiveland et al., 2013; Romarheim et al., 2010).

5.4 *M. capsulatus* Bath SIMPL-like protein

The functions of bacterial SIMPL-like proteins are yet to be identified. A SIMPL-like protein is encoded by *M. capsulatus* Bath, which in the current study was overexpressed and purified from *E. coli*. The potential immunomodulatory effects of the SIMPL-like protein were explored in relation to effect on IL-8 in Caco-2 cells and ability to regulate the NF-κB pathway in HEK-293 cells. The Caco-2 assay results showed a significant reduction in IL-8 by exposure of the SIMPL-like protein at 0.25, 1, 5 and 10 µM (Figure 4.3). The SIMPL-like protein did not inhibit the NF-κB pathway (Figure 4.4).

Mammalian SIMPL facilitates the TNF-α mediated NF-κB pathway, but not the IL-1 mediated NF-κB pathway (Vig et al., 2001). SIMPL is involved as a coactivator of the NF-κB pathway by both freeing NF-κB from its complex enabling it to translocate to the nucleus and by activating the p65 unit of the NF-κB in the nucleus (Figure 1.4.3) (Kwon et al., 2004; Milanovic et al., 2014). p65 can bind the transcription factor binding site on the IL-8 promoter and thus promote IL-8 expression (Kwon et al., 2004). Hence, if *M. capsulatus* Bath SIMPL share functionality with the mammalian SIMPL, increased IL-8 levels and NF-κB activation would be shown in the *in vitro* cell-based assays.

The *in vitro* cell-based assays showed a potential activation of NF-κB, however did 0.25, 1, 5 and 10 µM show a small, but significant reduction in IL-18 in Caco-2 cells. Therefore, the homologues SIMPL proteins could potentially have different functions on mammalian immune responses.

The fact that the *M. capsulatus* Bath SIMPL-like protein can reduce an *in vitro* inflammation induced via the IL-1 receptor in intestinal epithelial cells is interesting, as mammalian SIMPL is not known to share that ability (Kwon et al., 2004). However, Caco-2 cells grown in 3D to complete differentiation expresses the TNF-α type I receptor and has shown ability to produce IL-8 in response to TNF-α through the TNF-α type I receptor (Sonnier et al., 2010). If the Caco-2 cells grown in this study (not grown to complete differentiation) expresses TNF-α, the cells could increase IL-8 levels because of both the exposure of TNF-α and IL-1β (Hoffmann et al., 2002; Osawa et al., 2002; Rossem & Vos, 1998). This observation is relevant for all protein analyses in the current study. Measuring TNF-α levels at the same conditions as in this study would be of interest for future work (e.g. by multiplex or ELISA). TNF-α and IL-1 can increase IL-8 by more than 100-fold (Hoffmann et al., 2002). As the *M. capsulatus* Bath SIMPL-like protein reduced IL-8 expression in the Caco-2 assay, it is not probable that TNF-α was produced in the cells as a response to the protein or IL-1β.

Nuclear localization of mammalian SIMPL is required for its type I TNF-α receptor-induced NF-κB activity (Kwon et al., 2004). The mammalian SIMPL protein contains a lysine-rich nuclear localization signal (NLS) at the carboxyl terminus (**K**VFITFEVKGKE**KKKK**HL)[1], a motif common to nuclear proteins (Fontes et al., 2000; Kwon et al., 2004). The NLS motif in the *M. capsulatus* Bath SIMPL-like protein was not found to our knowledge, which may

[1] Bold letters indicate the basic residues of the monopartite and bipartite (Kwon et al., 2004).

indicate that this bacterial SIMPL-like protein cannot enter the host nucleus, and thus serves other functions than the mammalian SIMPL. Note that other mechanisms of nuclear localization of the *M. capsulatus* Bath SIMPL-like protein may be relevant (Nigg, 1997). The SIMPL-like protein of the soil bacterium *M. capsulatus* Bath may perhaps have had the NLS once, but later lost it due to lack of functionality in the species (Wu et al., 2012). Phylogenetic studies comparing SIMPL-proteins from a variety of species is required to increase an understanding of their respective roles.

5.5 *M. capsulatus* Bath MAM

M. capsulatus Bath MAM was selected because a previous study showed anti-inflammatory properties of the homologue *F. prausnitzii* MAM and five peptides deriving from the MAM protein (Quévrain et al., 2016b). The *F. prausnitzii* MAM and its peptides reduced IL-8 levels and inhibited the NF-κB pathway in *in vitro* human intestinal epithelial cells (Caco-2 cells), and ameliorated symptoms of colitis in *in vivo* mice models (Breyner et al., 2017; Quévrain et al., 2016b). The *M. capsulatus* Bath MAM protein consists of GGDEF and EAL domains, as the *F. prausnitzii* MAM also does, and both the full-length protein and the two individual domains were analyzed in this study. The mechanism behind the putative anti-inflammatory effects of MAM homologues is not known (Breyner et al., 2017).

Both MAM and the two domains, GGDEF and EAL, showed anti-inflammatory properties in terms of down-regulating IL-8 in Caco-2 cells in the current study (Figure 4.3). When comparing their respective fold IL-8 reduction, full-length MAM and the GGDEF domain reduced IL-8 expression more than the EAL domain. Varying concentrations achieved after purification resulted in protein exposures of various concentrations. However, 0.5 and 1 µM were tested for all three MAM constructs, and at 1 µM full-length MAM reduced IL-8 production with 60%, GGDEF 50%, and EAL 30% (Section 4.3). Each domain reduced IL-8 levels in Caco-2 cells but full-length MAM had highest effect. This may indicate that the combination of the two domains in full-length MAM gives a higher efficacy than the separated domains themselves. The NF-κB pathway assay shows a potential inhibition of full-length MAM at three concentrations (5.6, 1.8 and 0.8 nM) (Figure 4.4). Interestingly, the GGDEF and EAL domains separately did not inhibit the NF-κB signaling pathway. Despite this, the highest concentration of the GGDEF domain was below the threshold (Figure 4.4). Hence, higher concentrations of the proteins should also be included in further NF-κB assays, as this might reveal an effect not detectable in the current study.

Further experiments are required to understand the putative anti-inflammatory roles of the *M. capsulatus* Bath MAM homologue, but this study indicates an inhibitory role in the NF-κB pathway – which is also observed with the *F. prausnitzii* homologue. Of special interest is the investigation of peptides from *M. capsulatus* Bath MAM, perhaps the same peptides as from the *F. prausnitzii* MAM can elicit anti-inflammatory effects *in vitro* and *in vivo,* as seen in Quévrain et al. (2016b).

5.6 Endotoxin levels in the protein solutions

The NF-κB assay indicated presence of LPS in the protein solutions, as a color change indicating SEAP expression was observed in the wells with unspiked samples (Figure A-5) (Section 4.5). The LAL endotoxin detection assay revealed an average presence of 1.0 EU/mL LPS in the protein solutions (Table 4.5). The fact that the LPS contents are approximately the same in all solutions can indicate that the LPS was transferred to the protein solutions during the same step of protein extraction or purification. Sonicating the cells to disrupt the cell wall may disassociate LPS from the cells and release it into the supernatant used in further purification (Salek-Ardakani et al., 2002).

Despite LAL endotoxin detection assay being the standard for LPS detection and quantification (Wakelin et al., 2006), several limitations are related to the method (Harris et al., 1991). Most relevant in the current study is the fact that LPS may bind strongly to other proteins in the solution, hence not being detectable in the assay (Harris et al., 1991).

Generally, recombinant proteins expressed in *E. coli* are contaminated with endotoxin (Cardoso et al., 2007; Salek-Ardakani et al., 2002). Cardoso and colleagues (2007) measured LPS content, using the LAL assay, from production of three recombinant proteins using *E. coli*, whereas the concentrations ranged from 1.35-2.10 EU/mL, hence comparable with the LPS content in the current study. Salek-Ardakani et al. (2002) detected LPS contamination in the $1x10^4$ to $5x10^3$ EU/mL range after expressing proteins in *E. coli.* Endotoxin contamination is therefore a common challenge in production of proteins using *E. coli*.

The NF-κB pathway regulation assay may be affected by the LPS in the samples, as LPS interacts with TLR4 in the HEK-293 cells. Because the difference between unspiked and spiked samples are used to calculate the possible effect of the proteins, the effect of the LPS present in the samples is negligible.

Studies show that Caco-2 cells lack TLR4, hence the inflammatory response induced in Caco-2 cells is not through TLR4-LPS interaction (Naik et al., 2001). However, TLR2 with affinity for LPS is expressed in Caco-2 cells, but despite this, significant NF-κB activation by LPS in Caco-2 cells is only shown in TLR4-transformed Caco-2 cells (Naik et al., 2001). Additionally, Sonnier et al. (2010) conclude that Caco-2 cells are resistant to LPS, as LPS had no effect on TNF-α-induced release of IL-8. Hence, the Caco-2 cells used in the present study are unresponsive to LPS. Intestinal epithelial cells are constantly exposed to luminal LPS, thus it is advantageous of such cells not to respond to LPS if there is not a pathogenic infection for the cells to counteract. The fact that the Caco-2 assay in this study shows down-regulation of IL-8 after exposure of protein solutions, despite presence of LPS, supports the presented studies' conclusions.

Despite the studies indicating that LPS would not influence the assays of the present study, several approaches should be considered to remove the contaminant (Wakelin et al., 2006). Polymyxin B (PMB) is an antibiotic that specifically binds to the lipid A component of LPS, hence inactivating the endotoxin in solution without compromising the target protein (Cardoso et al., 2007; Cooperstock, 1974). However, PBM is reported to stimulate cytokine production in human cells, which would affect the assays of the present study (Damais et al., 1987; Jaber et al., 1998). MBP fusion proteins have affinity to amylose, hence may amylose resin columns be used to remove LPS from the solution (Salek-Ardakani et al., 2002). An amylose resin column may potentially replace the nickel-column used in the purification step of the present study, hence removing LPS from the solution already at the purification step. Methods using affinity columns to remove LPS are limited by the fact that LPS binds strongly to the protein, hence risking simultaneous removal of the target protein from the solution (Harris et al., 1991). A method that ensures disassociation of the LPS and protein is Triton-X114 phase separation, which have been used with high efficiency to remove LPS from a solution (Liu et al., 1997). If none of the presented methods are applicable, an alternative strategy could be to modify an *E. coli* strain to not express endotoxins toxic for human cells, without compromising its ability to over-express a recombinant protein (Mamat et al., 2015).

To verify that the LPS in the samples not affects the assays, a control solution prepared similarly as the protein solutions but instead with an empty vector should be tested, which would reveal the effect of solely the LPS. Although LPS is not considered to affect the *in vitro* cell assays of

the present study, caution is needed when investigating the effect of a solution containing LPS – the most ideal TLR4 agonist (Wakelin et al., 2006).

5.7 Concluding remarks and future perspectives

This study describes the successful production and purification of selected *M. capsulatus* Bath proteins, and a characterization of the proteins' putative effect on IL-8 expression in human intestinal epithelial cells (Caco-2 cells) and the NF-κB signaling pathway in a model using transformed HEK-293 cells.

M. capsulatus Bath is a non-commensal bacterium. Dunne et al. (2001) describes a requirement of microorganisms that confer beneficial health effects on mammalian hosts to have a common human – or animal origin. Since non-commensals have not been a subject of selection pressure in the mammalian gut during evolution, these microorganisms may not have lost their immunomodulatory properties (Christoffersen et al., 2015). This hypothesis can explain the ability of *M. capsulatus* Bath to modulate a mammalian immune response. For example, has the *M. capsulatus* Bath TIR-like protein has been kept throughout evolution despite no bacterial interaction partners.

The TIR-like protein significantly reduced IL-8 expression in Caco-2 cells, while its putative inhibitory role on NF-κB regulation was not clear. Further work on the TIR-like protein should focus on its potential effect on MAPK signaling, which might explain the NF-κB independent IL-8 regulation. The current study proposes that the *M. capsulatus* Bath TIR-like protein may modulate the host immune response, but further investigation is necessary to establish the exact mechanism.

MIF significantly reduced IL-8 expression in Caco-2 cells at lower concentrations and did not inhibit NF-κB signaling. As MIF homologues regulate TLR4 expression and interact with the MIF-receptor CD74, further experiments should involve TLR4 expression analysis and interaction assays with CD74.

Homologues of the *M. capsulatus* Bath SIMPL-like protein mediate TNF-α mediated NF-κB signaling. The present study shows a reduced IL-8 response in Caco-2 cells when exposed to the SIMPL-like protein and therefore *M. capsulatus* Bath SIMPL-like protein could serve other purposes than its homologues.

Full-length MAM both reduced IL-8 expression in Caco-2 cells and inhibited NF-κB signaling for some concentrations, which is in accordance to the hypothesized effects of MAM on

inflammation. Further analyses on peptides from MAM would be of great interest, as the *F. prausnitzii* MAM and five of its peptides have shown to reduce the inflammation parameters investigated in the present study (Quévrain et al., 2016b).

MAM, and the other proteins of interest, might be hydrolyzed to peptides during *in vivo* digestion. If *M. capsulatus* Bath, or proteins from the bacterium, would be given orally in treatment against intestinal inflammatory disorders in the future, one must consider the potential effects that digestion may have on structures and hence the functions of the proteins. There are established *in vitro* digestion experiments mimicking human digestion, which may be considered for further work on the project (Minekus et al., 2014).

Furthermore, to investigate the proteins' interaction with human cells is of interest. By targeting the His-tag of the different proteins with an immunofluorescent antibody, the protein and cell interaction can be visualized (Stadler et al., 2013). Such experiments could establish answers to whether the proteins are kept extracellularly or taken up by the cell, and can give indications on how the proteins might elicit their putative immunomodulatory functions. Studies have already investigated the interaction between *M. capsulatus* Bath and DCs (Indrelid, 2017), but additional experiments with a range of cell types are necessary.

The anti-inflammatory properties of *M. capsulatus* Bath are most likely multifactorial. It is not known whether it is proteins, or other components alone or in combination, from the bacterium that contribute to the anti-inflammatory properties. Despite this, this study indicates that *M. capsulatus* Bath derived proteins can modulate a host immune response. This study has provided good premises for further work on establishing an explanation for the bacterium's immunomodulatory properties. Additional experiments are required to characterize the exact mechanisms to which the proteins modulate a host immune response, both *in vitro* and *in vivo*.

REFERENCES

Askarian, F., Van Sorge, N. M., Sangvik, M., Beasley, F. C., Henriksen, J. R., Sollid, J. U., Van Strijp, J. A., Nizet, V. & Johannessen, M. (2014). A Staphylococcus aureus TIR domain protein virulence factor blocks TLR2-mediated NF-κB signaling. *Journal of innate immunity*, 6 (4): 485-498.

Augustijn, K. D., Kleemann, R., Thompson, J., Kooistra, T., Crawford, C. E., Reece, S. E., Pain, A., Siebum, A. H., Janse, C. J. & Waters, A. P. (2007). Functional characterization of the Plasmodium falciparum and P. berghei homologues of macrophage migration inhibitory factor. *Infection and immunity*, 75 (3): 1116-1128.

Awandare, G. A., Hittner, J. B., Kremsner, P. G., Ochiel, D. O., Keller, C. C., Weinberg, J. B., Clark, I. A. & Perkins, D. J. (2006). Decreased circulating macrophage migration inhibitory factor (MIF) protein and blood mononuclear cell MIF transcripts in children with Plasmodium falciparum malaria. *Clinical Immunology*, 119 (2): 219-225.

Awandare, G. A., Kremsner, P. G., Hittner, J. B., Keller, C. C., Clark, I. A., Weinberg, J. B. & Perkins, D. J. (2007). Higher production of peripheral blood macrophage migration inhibitory factor in healthy children with a history of mild malaria relative to children with a history of severe malaria. *The American journal of tropical medicine and hygiene*, 76 (6): 1033-1036.

Ayabe, T., Satchell, D. P., Wilson, C. L., Parks, W. C., Selsted, M. E. & Ouellette, A. J. (2000). Secretion of microbicidal α-defensins by intestinal Paneth cells in response to bacteria. *Nature immunology*, 1 (2): 113.

Belkaid, Y. & Hand, T. W. (2014). Role of the microbiota in immunity and inflammation. *Cell*, 157 (1): 121-141.

Benson, E. A., Goebl, M. G., Yang, F.-C., Kapur, R., McClintick, J., Sanghani, S., Clapp, D. W. & Harrington, M. A. (2010). Loss of SIMPL compromises TNF-α-dependent survival of hematopoietic progenitors. *Experimental hematology*, 38 (2): 71-81.

Beswick, E. J., Bland, D. A., Suarez, G., Barrera, C. A., Fan, X. & Reyes, V. E. (2005). Helicobacter pylori binds to CD74 on gastric epithelial cells and stimulates interleukin-8 production. *Infection and immunity*, 73 (5): 2736-2743.

Bolanos-Garcia, V. M. & Davies, O. R. (2006). Structural analysis and classification of native proteins from E. coli commonly co-purified by immobilised metal affinity chromatography. *Biochimica et Biophysica Acta (BBA)-General Subjects*, 1760 (9): 1304-1313.

Bondos, S. E. & Bicknell, A. (2003). Detection and prevention of protein aggregation before, during, and after purification. *Analytical biochemistry*, 316 (2): 223-231.

Bouskra, D., Brézillon, C., Bérard, M., Werts, C., Varona, R., Boneca, I. G. & Eberl, G. (2008). Lymphoid tissue genesis induced by commensals through NOD1 regulates intestinal homeostasis. *Nature*, 456 (7221): 507.

Bowman, J. (2006). The methanotrophs—the families Methylococcaceae and Methylocystaceae. *The Prokaryotes: Volume 5: Proteobacteria: Alpha and Beta Subclasses*: 266-289.

Bozza, M., Satoskar, A. R., Lin, G., Lu, B., Humbles, A. A., Gerard, C. & David, J. R. (1999). Targeted disruption of migration inhibitory factor gene reveals its critical role in sepsis. *Journal of Experimental Medicine*, 189 (2): 341-346.

Bozza, M. T., Martins, Y. C., Carneiro, L. A. & Paiva, C. N. (2012). Macrophage migration inhibitory factor in protozoan infections. *Journal of parasitology research*, 2012.

Breyner, N. M., Michon, C., De Sousa, C. S., Vilas Boas, P. B., Chain, F., Azevedo, V. A., Langella, P. & Chatel, J. M. (2017). Microbial anti-inflammatory molecule (MAM) from Faecalibacterium prausnitzii shows a protective effect on DNBS and DSS-induced colitis model in mice through inhibition of NF-κB pathway. *Frontiers in microbiology*, 8: 114.

Cai, Y., Moore, M., Goforth, R., Henry, R. & Beitle, R. (2004). Genomic data for alternate production strategies. I. Identification of major contaminating species for Cobalt+ 2 immobilized metal affinity chromatography. *Biotechnology and bioengineering*, 88 (1): 77-83.

Carding, S., Verbeke, K., Vipond, D. T., Corfe, B. M. & Owen, L. J. (2015). Dysbiosis of the gut microbiota in disease. *Microbial ecology in health and disease*, 26 (1): 26191.

Cardoso, L. S., Araujo, M. I., Góes, A. M., Pacífico, L. G., Oliveira, R. R. & Oliveira, S. C. (2007). Polymyxin B as inhibitor of LPS contamination of Schistosoma mansoni recombinant proteins in human cytokine analysis. *Microbial cell factories*, 6 (1): 1.

Casen, C., Vebø, H., Sekelja, M., Hegge, F., Karlsson, M., Ciemniejewska, E., Dzankovic, S., Frøyland, C., Nestestog, R. & Engstrand, L. (2015). Deviations in human gut microbiota: a novel diagnostic test for determining dysbiosis in patients with IBS or IBD. *Alimentary pharmacology & therapeutics*, 42 (1): 71-83.

Chan, S. L., Low, L. Y., Hsu, S., Li, S., Liu, T., Santelli, E., Le Negrate, G., Reed, J. C., Woods, V. L. & Pascual, J. (2009). Molecular mimicry in innate immunity crystal structure of a bacterial TIR domain. *Journal of Biological Chemistry*, 284 (32): 21386-21392.

Cho, I. & Blaser, M. J. (2012). The human microbiome: at the interface of health and disease. *Nature Reviews Genetics*, 13 (4): 260.

Christoffersen, T. E., Hult, L. T. O., Solberg, H., Bakke, A., Kuczkowska, K., Huseby, E., Jacobsen, M., Lea, T. & Kleiveland, C. R. (2015). Effects of the non-commensal Methylococcus capsulatus Bath on mammalian immune cells. *Molecular Immunology*, 66 (2): 107-116. doi: 10.1016/j.molimm.2015.02.019.

Cirl, C., Wieser, A., Yadav, M., Duerr, S., Schubert, S., Fischer, H., Stappert, D., Wantia, N., Rodriguez, N. & Wagner, H. (2008). Subversion of Toll-like receptor signaling by a unique family of bacterial Toll/interleukin-1 receptor domain–containing proteins. *Nature medicine*, 14 (4): 399.

Cooper, M. D. & Alder, M. N. (2006). The evolution of adaptive immune systems. *Cell*, 124 (4): 815-822.

Cooperstock, M. S. (1974). Inactivation of endotoxin by polymyxin B. *Antimicrobial Agents and Chemotherapy*, 6 (4): 422-425.

Cordery, D. V., Kishore, U., Kyes, S., Shafi, M. J., Watkins, K. R., Williams, T. N., Marsh, K. & Urban, B. C. (2007). Characterization of a Plasmodium falciparum macrophage-migration inhibitory factor homologue. *The Journal of infectious diseases*, 195 (6): 905-912.

Cormet-Boyaka, E., Jolivette, K., Bonnegarde-Bernard, A., Rennolds, J., Hassan, F., Mehta, P., Tridandapani, S., Webster-Marketon, J. & Boyaka, P. N. (2011). An NF-κB–independent and Erk1/2-dependent mechanism controls CXCL8/IL-8 responses of airway epithelial cells to cadmium. *Toxicological Sciences*, 125 (2): 418-429.

Cui, T., Cang, H., Yang, B. & He, Z.-G. (2019). Cyclic dimeric guanosine monophosphate: activation and inhibition of innate immune response. *Journal of innate immunity*, 11 (3): 246-252.

Damais, C., Jupin, C., Parant, M. & Chedid, L. (1987). Induction of human interleukin-1 production by polymyxin B. *Journal of immunological methods*, 101 (1): 51-56.

Dauletbaev, N., Eklove, D., Mawji, N., Iskandar, M., Di Marco, S., Gallouzi, I.-E. & Lands, L. C. (2011). Down-regulation of cytokine-induced interleukin-8 requires inhibition of p38 mitogen-activated protein kinase (MAPK) via MAPK phosphatase 1-dependent and-independent mechanisms. *Journal of Biological Chemistry*, 286 (18): 15998-16007.

Dinarello, C. A. & Thompson, R. C. (1991). Blocking IL-1: interleukin 1 receptor antagonist in vivo and in vitro. *Immunology today*, 12 (11): 404-410.

Dinarello, C. A. (1997). Interleukin-1. *Cytokine & growth factor reviews*, 8 (4): 253-265.

Dinarello, C. A. & van der Meer, J. W. (2013). *Treating inflammation by blocking interleukin-1 in humans*. Seminars in immunology: Elsevier.

Dobson, S. E., Augustijn, K. D., Brannigan, J. A., Schnick, C., Janse, C. J., Dodson, E. J., Waters, A. P. & Wilkinson, A. J. (2009). The crystal structures of macrophage migration inhibitory factor from Plasmodium falciparum and Plasmodium berghei. *Protein Science*, 18 (12): 2578-2591.

Dunne, C., O'Mahony, L., Murphy, L., Thornton, G., Morrissey, D., O'Halloran, S., Feeney, M., Flynn, S., Fitzgerald, G. & Daly, C. (2001). In vitro selection criteria for probiotic bacteria of human origin: correlation with in vivo findings. *The American journal of clinical nutrition*, 73 (2): 386s-392s.

Fingerle-Rowson, G., Koch, P., Bikoff, R., Lin, X., Metz, C. N., Dhabhar, F. S., Meinhardt, A. & Bucala, R. (2003). Regulation of macrophage migration inhibitory factor expression by glucocorticoids in vivo. *The American journal of pathology*, 162 (1): 47-56.

Fontes, M. R., Teh, T. & Kobe, B. (2000). Structural basis of recognition of monopartite and bipartite nuclear localization sequences by mammalian importin-α. *Journal of molecular biology*, 297 (5): 1183-1194.

Galperin, M. Y., Nikolskaya, A. N. & Koonin, E. V. (2001). Novel domains of the prokaryotic two-component signal transduction systems. *FEMS microbiology letters*, 203 (1): 11-21.

Gardner, M. J., Hall, N., Fung, E., White, O., Berriman, M., Hyman, R. W., Carlton, J. M., Pain, A., Nelson, K. E. & Bowman, S. (2002). Genome sequence of the human malaria parasite Plasmodium falciparum. *Nature*, 419 (6906): 498.

Gasteiger, E., Hoogland, C., Gattiker, A., Wilkins, M. R., Appel, R. D. & Bairoch, A. (2005). Protein identification and analysis tools on the ExPASy server. In *The proteomics protocols handbook*, pp. 571-607: Springer.

Godwin, P., Baird, A.-M., Heavey, S., Barr, M., O'Byrne, K. & Gately, K. A. (2013). Targeting nuclear factor-kappa B to overcome resistance to chemotherapy. *Frontiers in oncology*, 3: 120.

Gordon, S. (2002). Pattern recognition receptors: doubling up for the innate immune response. *Cell*, 111 (7): 927-930.

Gunawardene, A. R., Corfe, B. M. & Staton, C. A. (2011). Classification and functions of enteroendocrine cells of the lower gastrointestinal tract. *International journal of experimental pathology*, 92 (4): 219-231.

Harris, H., Eichbaum, E., Kane, J. & Rapp, J. (1991). Detection of endotoxin in triglyceride-rich lipoproteins in vitro. *The Journal of laboratory and clinical medicine*, 118 (2): 186-193.

He, X.-X., Yang, J., Ding, Y.-W., Liu, W., Shen, Q.-Y. & Xia, H. H. (2006). Increased epithelial and serum expression of macrophage migration inhibitory factor (MIF) in gastric cancer: potential role of MIF in gastric carcinogenesis. *Gut*, 55 (6): 797-802.

Headland, S. E. & Norling, L. V. (2015). *The resolution of inflammation: Principles and challenges*. Seminars in immunology: Elsevier.
Herias, M., Koninkx, J., Vos, J., In't Veld, J. H. & Van Dijk, J. (2005). Probiotic effects of Lactobacillus casei on DSS-induced ulcerative colitis in mice. *International journal of food microbiology*, 103 (2): 143-155.
Hoesel, B. & Schmid, J. A. (2013). The complexity of NF-κB signaling in inflammation and cancer. *Molecular cancer*, 12 (1): 86.
Hoffmann, E., Dittrich-Breiholz, O., Holtmann, H. & Kracht, M. (2002). Multiple control of interleukin-8 gene expression. *Journal of leukocyte biology*, 72 (5): 847-855.
Hooper, L. V. & Gordon, J. I. (2001). Commensal host-bacterial relationships in the gut. *Science*, 292 (5519): 1115-1118.
Indrelid, S., Mathiesen, G., Jacobsen, M., Lea, T. & Kleiveland, C. R. (2014). Computational and experimental analysis of the secretome of Methylococcus capsulatus (Bath). *PLoS ONE*, 9 (12): e114476. doi: 10.1371/journal.pone.0114476.
Indrelid, S. (2017). *The Soil Bacterium Methylococcus capsulatus Bath and its Interactions with Human Immune Cells in vitro*. Doctoral Thesis: Norwegian University of Life Sciences (NMBU).
Indrelid, S., Kleiveland, C., Holst, R., Jacobsen, M. & Lea, T. (2017). The Soil Bacterium Methylococcus capsulatus Bath Interacts with Human Dendritic Cells to Modulate Immune Function. *Frontiers in Microbiology*, 8 (320). doi: 10.3389/fmicb.2017.00320.
InvivoGen. (2019a). *HEK-Blue™ hTLR4*. Available at: https://www.invivogen.com/hek-blue-htlr4#contents (accessed: 04.18.2019).
InvivoGen. (2019b). *HEK-Blue™ Null1 Cells*. Available at: https://www.invivogen.com/hek-blue-null1 (accessed: 05.06.2019).
Iyer, L. M., Abhiman, S. & Aravind, L. (2008). MutL homologs in restriction-modification systems and the origin of eukaryotic MORC ATPases. *Biology direct*, 3 (1): 8.
Jaber, B., Sundaram, S., Neto, M. C., King, A. & Pereira, B. (1998). Polymyxin-B Stimulates Tumor Necrosis Factor-α Production by Human Peripheral Blood Mononuclear Cells. *The International journal of artificial organs*, 21 (5): 269-273.
Jain, A., Liu, R., Xiang, Y. K. & Ha, T. (2012). Single-molecule pull-down for studying protein interactions. *Nature protocols*, 7 (3): 445.
Kamada, N., Seo, S.-U., Chen, G. Y. & Núñez, G. (2013). Role of the gut microbiota in immunity and inflammatory disease. *Nature Reviews Immunology*, 13 (5): 321.
Kim, Y. & Pritts, T. A. (2017). The gastrointestinal tract. In *Geriatric Trauma and Critical Care*, pp. 35-43: Springer.
Kleiveland, C. R., Hult, L. T. O., Spetalen, S., Kaldhusdal, M., Christofferesen, T. E., Bengtsson, O., Romarheim, O. H., Jacobsen, M. & Lea, T. (2013). The Noncommensal Bacterium Methylococcus capsulatus (Bath) Ameliorates Dextran Sulfate (Sodium Salt)-Induced Ulcerative Colitis by Influencing Mechanisms Essential for Maintenance of the Colonic Barrier Function. *Applied and Environmental Microbiology*, 79 (1): 48-56. doi: 10.1128/aem.02464-12.
Kwon, H.-J., Breese, E. H., Vig-Varga, E., Luo, Y., Lee, Y., Goebl, M. G. & Harrington, M. A. (2004). Tumor necrosis factor alpha induction of NF-κB requires the novel coactivator SIMPL. *Molecular and cellular biology*, 24 (21): 9317-9326.
Leng, L., Metz, C. N., Fang, Y., Xu, J., Donnelly, S., Baugh, J., Delohery, T., Chen, Y., Mitchell, R. A. & Bucala, R. (2003). MIF signal transduction initiated by binding to CD74. *Journal of Experimental Medicine*, 197 (11): 1467-1476.

Liu, S., Tobias, R., McClure, S., Styba, G., Shi, Q. & Jackowski, G. (1997). Removal of endotoxin from recombinant protein preparations. *Clinical biochemistry*, 30 (6): 455-463.

Low, L. Y., Mukasa, T., Reed, J. C. & Pascual, J. (2007). Characterization of a TIR-like protein from Paracoccus denitrificans. *Biochemical and biophysical research communications*, 356 (2): 481-486.

Lu, H., Zhang, H., Wang, Q., Yuan, H., He, W., Zhao, Z. & Li, Y. (2001). Purification, refolding of hybrid hIFNγ-kringle 5 expressed in Escherichia coli. *Current microbiology*, 42 (3): 211-216.

Maharshak, N., Cohen, S., Lantner, F., Hart, G., Leng, L., Bucala, R. & Shachar, I. (2010). CD74 is a survival receptor on colon epithelial cells. *World journal of gastroenterology: WJG*, 16 (26): 3258.

Mamat, U., Wilke, K., Bramhill, D., Schromm, A. B., Lindner, B., Kohl, T. A., Corchero, J. L., Villaverde, A., Schaffer, L. & Head, S. R. (2015). Detoxifying Escherichia coli for endotoxin-free production of recombinant proteins. *Microbial cell factories*, 14 (1): 57.

Mankan, A. K., Müller, M., Witte, G. & Hornung, V. (2016). Cyclic Dinucleotides in the Scope of the Mammalian Immune System. In *Non-canonical Cyclic Nucleotides*, pp. 269-289: Springer.

Marcu, R., Choi, Y. J., Xue, J., Fortin, C. L., Wang, Y., Nagao, R. J., Xu, J., MacDonald, J. W., Bammler, T. K. & Murry, C. E. (2018). Human organ-specific endothelial cell heterogeneity. *iScience*, 4: 20-35.

Mariat, D., Firmesse, O., Levenez, F., Guimarães, V., Sokol, H., Doré, J., Corthier, G. & Furet, J. (2009). The Firmicutes/Bacteroidetes ratio of the human microbiota changes with age. *BMC microbiology*, 9 (1): 123.

Mateo, C., Fernandez-Lorente, G., Pessela, B. C., Vian, A., Carrascosa, A. V., Garcia, J. L., Fernandez-Lafuente, R. & Guisan, J. M. (2001). Affinity chromatography of polyhistidine tagged enzymes: New dextran-coated immobilized metal ion affinity chromatography matrices for prevention of undesired multipoint adsorptions. *Journal of Chromatography A*, 915 (1-2): 97-106.

Mayer, L. (2003). Mucosal immunity. *Pediatrics*, 111 (Supplement 3): 1595-1600.

McWhirter, S. M., Barbalat, R., Monroe, K. M., Fontana, M. F., Hyodo, M., Joncker, N. T., Ishii, K. J., Akira, S., Colonna, M. & Chen, Z. J. (2009). A host type I interferon response is induced by cytosolic sensing of the bacterial second messenger cyclic-di-GMP. *Journal of Experimental Medicine*, 206 (9): 1899-1911.

Miernyk, J. A. & Thelen, J. J. (2008). Biochemical approaches for discovering protein–protein interactions. *The Plant Journal*, 53 (4): 597-609.

Milanovic, M., Kracht, M. & Schmitz, M. L. (2014). The cytokine-induced conformational switch of nuclear factor κB p65 is mediated by p65 phosphorylation. *Biochemical Journal*, 457 (3): 401-413.

Minekus, M., Alminger, M., Alvito, P., Ballance, S., Bohn, T., Bourlieu, C., Carriere, F., Boutrou, R., Corredig, M. & Dupont, D. (2014). A standardised static in vitro digestion method suitable for food–an international consensus. *Food & function*, 5 (6): 1113-1124.

Naik, S., Kelly, E. J., Meijer, L., Pettersson, S. & Sanderson, I. R. (2001). Absence of Toll-like receptor 4 explains endotoxin hyporesponsiveness in human intestinal epithelium. *Journal of pediatric gastroenterology and nutrition*, 32 (4): 449-453.

Neagu, A., Neagu, M. & Dér, A. (2001). Fluctuations and the Hofmeister effect. *Biophysical journal*, 81 (3): 1285-1294.

Neutra, M. R., Mantis, N. J. & Kraehenbuhl, J.-P. (2001). Collaboration of epithelial cells with organized mucosal lymphoid tissues. *Nature Immunology*, 2: 1004. doi: 10.1038/ni1101-1004.
New England Biolabs Inc. (2019). *pMAL™ Protein Fusion and Purification System*. Available at: https://international.neb.com/products/e8200-pmal-protein-fusion-and-purification-system#Product%20Information (accessed: 05.05.2019).
Newman, R. M., Salunkhe, P., Godzik, A. & Reed, J. C. (2006). Identification and characterization of a novel bacterial virulence factor that shares homology with mammalian Toll/interleukin-1 receptor family proteins. *Infection and immunity*, 74 (1): 594-601.
Nigg, E. A. (1997). Nucleocytoplasmic transport: signals, mechanisms and regulation. *Nature*, 386 (6627): 779.
Nobre, C. C. G., de Araújo, J. M. G., de Medeiros Fernandes, T. A. A., Cobucci, R. N. O., Lanza, D. C. F., Andrade, V. S. & Fernandes, J. V. (2017). Macrophage migration inhibitory factor (MIF): Biological activities and relation with cancer. *Pathology & Oncology Research*, 23 (2): 235-244.
Norsk Helseinformatikk. (2017a). *Crohns sykdom*. Available at: https://nhi.no/sykdommer/magetarm/inflammatorisk-tarmsykdom/crohns-sykdom/?page=2 (accessed: 8 April).
Norsk Helseinformatikk. (2017b). *Ulcerøs kolitt*. Available at: https://nhi.no/sykdommer/magetarm/inflammatorisk-tarmsykdom/ulceros-kolitt/ (accessed: 8 April).
Novatchkova, M., Leibbrandt, A., Werzowa, J., Neubüser, A. & Eisenhaber, F. (2003). The STIR-domain superfamily in signal transduction, development and immunity. *Trends in biochemical sciences*, 28 (5): 226-229.
O'Neill, L. A. & Bowie, A. G. (2007). The family of five: TIR-domain-containing adaptors in Toll-like receptor signalling. *Nature Reviews Immunology*, 7 (5): 353.
Onishi, R. M., Park, S. J., Hanel, W., Ho, A. W., Maitra, A. & Gaffen, S. L. (2010). SEF/IL-17R (SEFIR) Is Not Enough AN EXTENDED SEFIR DOMAIN IS REQUIRED FOR IL-17RA-MEDIATED SIGNAL TRANSDUCTION. *Journal of Biological Chemistry*, 285 (43): 32751-32759.
Osawa, Y., Nagaki, M., Banno, Y., Brenner, D. A., Asano, T., Nozawa, Y., Moriwaki, H. & Nakashima, S. (2002). Tumor necrosis factor alpha-induced interleukin-8 production via NF-κB and phosphatidylinositol 3-kinase/Akt pathways inhibits cell apoptosis in human hepatocytes. *Infection and immunity*, 70 (11): 6294-6301.
Palm, N. W. & Medzhitov, R. (2009). Pattern recognition receptors and control of adaptive immunity. *Immunological reviews*, 227 (1): 221-233.
Pelaseyed, T., Bergström, J. H., Gustafsson, J. K., Ermund, A., Birchenough, G. M., Schütte, A., van der Post, S., Svensson, F., Rodríguez-Piñeiro, A. M. & Nyström, E. E. (2014). The mucus and mucins of the goblet cells and enterocytes provide the first defense line of the gastrointestinal tract and interact with the immune system. *Immunological reviews*, 260 (1): 8-20.
Pithadia, A. B. & Jain, S. (2011). Treatment of inflammatory bowel disease (IBD). *Pharmacological Reports*, 63 (3): 629-642.
Quévrain, E., Maubert, M.-A., Sokol, H., Devreese, B. & Seksik, P. (2016a). The presence of the anti-inflammatory protein MAM, from Faecalibacterium prausnitzii, in the intestinal ecosystem. *Gut*, 65 (5): 882-882.
Quévrain, E., Maubert, M., Michon, C., Chain, F., Marquant, R., Tailhades, J., Miquel, S., Carlier, L., Bermúdez-Humarán, L. & Pigneur, B. (2016b). Identification of an anti-

inflammatory protein from Faecalibacterium prausnitzii, a commensal bacterium deficient in Crohn's disease. *Gut*, 65 (3): 415-425.
Radhakrishnan, G. K. & Splitter, G. A. (2010). Biochemical and functional analysis of TIR domain containing protein from Brucella melitensis. *Biochemical and biophysical research communications*, 397 (1): 59-63.
Rana, R. R., Zhang, M., Spear, A. M., Atkins, H. S. & Byrne, B. (2013). Bacterial TIR-containing proteins and host innate immune system evasion. *Medical microbiology and immunology*, 202 (1): 1-10.
Reboldi, A. & Cyster, J. G. (2016). Peyer's patches: organizing B-cell responses at the intestinal frontier. *Immunological reviews*, 271 (1): 230-245.
Risso, C., Choudhary, S., Johannessen, A. & Silverman, J. (2018). Methanotrophy Goes Commercial: Challenges, Opportunities, and Brief History. In Kalyuzhnaya, M. G. & Xing, X.-H. (eds) *Methane Biocatalysis: Paving the Way to Sustainability*, pp. 293-298. Cham: Springer International Publishing.
Rockland Immunochemicals Inc. (2016). *AccuSignal ELISA Kits* Available at: https://rockland-inc.com/ELISA-Kits.aspx (accessed: 05.06.2019).
Roger, T., Froidevaux, C., Martin, C. & Calandra, T. (2003). Macrophage migration inhibitory factor (MIF) regulates host responses to endotoxin through modulation of Toll-like receptor 4 (TLR4). *Journal of endotoxin research*, 9 (2): 119-123.
Roger, T., Delaloye, J., Chanson, A.-L., Giddey, M., Le Roy, D. & Calandra, T. (2012). Macrophage migration inhibitory factor deficiency is associated with impaired killing of gram-negative bacteria by macrophages and increased susceptibility to Klebsiella pneumoniae sepsis. *The Journal of infectious diseases*, 207 (2): 331-339.
Romarheim, O. H., Øverland, M., Mydland, L. T., Skrede, A. & Landsverk, T. (2010). Bacteria grown on natural gas prevent soybean meal-induced enteritis in Atlantic salmon. *The Journal of nutrition*, 141 (1): 124-130.
Romarheim, O. H., Landsverk, T., Mydland, L. T., Skrede, A. & Øverland, M. (2013). Cell wall fractions from Methylococcus capsulatus prevent soybean meal-induced enteritis in Atlantic salmon (Salmo salar). *Aquaculture*, 402: 13-18.
Rossem, V. & Vos, D. (1998). Polarized secretion of IL-6 and IL-8 by human retinal pigment epithelial cells. *Clinical & Experimental Immunology*, 112 (1): 34-43.
Salek-Ardakani, S., Stuart, A. D., Arrand, J. E., Lyons, S., Arrand, J. R. & Mackett, M. (2002). High level expression and purification of the Epstein-Barr virus encoded cytokine viral interleukin 10: efficient removal of endotoxin. *Cytokine*, 17 (1): 1-13.
Sender, R., Fuchs, S. & Milo, R. (2016). Revised estimates for the number of human and bacteria cells in the body. *PLoS biology*, 14 (8): e1002533.
Shaul, Y. & Seger, R. (2006). The detection of MAPK signaling. *Current protocols in molecular biology*, 73 (1): 18.12. 1-18.12. 35.
Singh, A., Upadhyay, V., Upadhyay, A. K., Singh, S. M. & Panda, A. K. (2015). Protein recovery from inclusion bodies of Escherichia coli using mild solubilization process. *Microbial cell factories*, 14 (1): 41.
Sonnier, D. I., Bailey, S. R., Schuster, R. M., Lentsch, A. B. & Pritts, T. A. (2010). TNF-α induces vectorial secretion of IL-8 in Caco-2 cells. *Journal of Gastrointestinal Surgery*, 14 (10): 1592-1599.
Sparkes, A., De Baetselier, P., Roelants, K., De Trez, C., Magez, S., Van Ginderachter, J. A., Raes, G., Bucala, R. & Stijlemans, B. (2017). The non-mammalian MIF superfamily. *Immunobiology*, 222 (3): 473-482.
Spear, A. M., Loman, N. J., Atkins, H. S. & Pallen, M. J. (2009). Microbial TIR domains: not necessarily agents of subversion? *Trends in microbiology*, 17 (9): 393-398.

Spear, A. M., Rana, R. R., Jenner, D. C., Flick-Smith, H. C., Oyston, P. C., Simpson, P., Matthews, S. J., Byrne, B. & Atkins, H. S. (2012). A Toll/interleukin (IL)-1 receptor domain protein from Yersinia pestis interacts with mammalian IL-1/Toll-like receptor pathways but does not play a central role in the virulence of Y. pestis in a mouse model of bubonic plague. *Microbiology*, 158 (6): 1593-1606.

Stadler, C., Rexhepaj, E., Singan, V. R., Murphy, R. F., Pepperkok, R., Uhlén, M., Simpson, J. C. & Lundberg, E. (2013). Immunofluorescence and fluorescent-protein tagging show high correlation for protein localization in mammalian cells. *Nature methods*, 10 (4): 315.

Sugimoto, M. A., Sousa, L. P., Pinho, V., Perretti, M. & Teixeira, M. M. (2016). Resolution of inflammation: what controls its onset? *Frontiers in immunology*, 7: 160.

Sveen, A. (2016). *Studies on proteins from Methylococcus capsulatus Bath: Expression in Lactobacillus plantarum WCFS1, purification and large-scale fermentation*. https://nmbu.brage.unit.no/nmbu-xmlui/?locale=no: Norwegian University of Life Sciences.

Takeda, K. & Akira, S. (2004). *TLR signaling pathways*. Seminars in immunology: Elsevier.

Takeuchi, O. & Akira, S. (2010). Pattern recognition receptors and inflammation. *Cell*, 140 (6): 805-820.

Tlaskalová-Hogenová, H., Štěpánková, R., Hudcovic, T., Tučková, L., Cukrowska, B., Lodinová-Žádnıková, R., Kozáková, H., Rossmann, P., Bártová, J. & Sokol, D. (2004). Commensal bacteria (normal microflora), mucosal immunity and chronic inflammatory and autoimmune diseases. *Immunology letters*, 93 (2-3): 97-108.

UniProt. (2019). *UniProtKB - Q6SZW1 (SARM1_HUMAN)*. Available at: https://www.uniprot.org/uniprot/Q6SZW1 (accessed: 04.29.2019).

Vig, E., Green, M., Liu, Y., Yu, K.-Y., Kwon, H.-J., Tian, J., Goebl, M. G. & Harrington, M. A. (2001). SIMPL is a tumor necrosis factor-specific regulator of nuclear factor-κB activity. *Journal of Biological Chemistry*, 276 (11): 7859-7866.

Villaverde, A. & Carrió, M. M. (2003). Protein aggregation in recombinant bacteria: biological role of inclusion bodies. *Biotechnology letters*, 25 (17): 1385-1395.

Wakelin, S. J., Sabroe, I., Gregory, C. D., Poxton, I. R., Forsythe, J. L., Garden, O. J. & Howie, S. E. (2006). "Dirty little secrets"—endotoxin contamination of recombinant proteins. *Immunology letters*, 106 (1): 1-7.

Wang, S., Liu, Z., Wang, L. & Zhang, X. (2009). NF-κB signaling pathway, inflammation and colorectal cancer. *Cellular & molecular immunology*, 6 (5): 327.

Ward, N., Larsen, Ø., Sakwa, J., Bruseth, L., Khouri, H., Durkin, A. S., Dimitrov, G., Jiang, L., Scanlan, D. & Kang, K. H. (2004). Genomic insights into methanotrophy: the complete genome sequence of Methylococcus capsulatus (Bath). *PLoS biology*, 2 (10): e303.

Wasiel, A. A., Rozeboom, H. J., Hauke, D., Baas, B.-J., Zandvoort, E., Quax, W. J., Thunnissen, A.-M. W. & Poelarends, G. J. (2010). Structural and functional characterization of a macrophage migration inhibitory factor homologue from the marine cyanobacterium Prochlorococcus marinus. *Biochemistry*, 49 (35): 7572-7581.

Westra, D. F., Welling, G. W., Koedijk, D. G., Scheffer, A. J., The, T. H. & Welling-Wester, S. (2001). Immobilised metal-ion affinity chromatography purification of histidine-tagged recombinant proteins: a wash step with a low concentration of EDTA. *Journal of Chromatography B: Biomedical Sciences and Applications*, 760 (1): 129-136.

Wong, M. L. & Medrano, J. F. (2005). Real-time PCR for mRNA quantitation. *Biotechniques*, 39 (1): 75-85.

Wu, B., Gong, J., Liu, L., Li, T., Wei, T. & Bai, Z. (2012). Evolution of prokaryotic homologues of the eukaryotic SEFIR protein domain. *Gene*, 492 (1): 160-166.
Wu, R.-Q., Zhang, D.-F., Tu, E., Chen, Q.-M. & Chen, W. (2014). The mucosal immune system in the oral cavity—an orchestra of T cell diversity. *International journal of oral science*, 6 (3): 125.
Yadav, M., Zhang, J., Fischer, H., Huang, W., Lutay, N., Cirl, C., Lum, J., Miethke, T. & Svanborg, C. (2010). Inhibition of TIR domain signaling by TcpC: MyD88-dependent and independent effects on Escherichia coli virulence. *PLoS pathogens*, 6 (9): e1001120.
Yen, T.-H. & Wright, N. A. (2006). The gastrointestinal tract stem cell niche. *Stem cell reviews*, 2 (3): 203-212.
Yu, L.-L., Yu, H.-G., Yu, J.-P., Luo, H.-S., Xu, X.-M. & Li, J.-H. (2004). Nuclear factor-kB p65 (RelA) transcription factor is constitutively activated in human colorectal carcinoma tissue. *World journal of gastroenterology: WJG*, 10 (22): 3255.
Yuan, Q. & Walker, W. A. (2004). Innate immunity of the gut: mucosal defense in health and disease. *Journal of pediatric gastroenterology and nutrition*, 38 (5): 463-473.
Zaylaa, M., Al Kassaa, I., Alard, J., Peucelle, V., Boutillier, D., Desramaut, J., Dabboussi, F., Pot, B. & Grangette, C. (2018). Probiotics in IBD: Combining in vitro and in vivo models for selecting strains with both anti-inflammatory potential as well as a capacity to restore the gut epithelial barrier. *Journal of functional foods*, 47: 304-315.
Zhang, J.-M. & An, J. (2007). Cytokines, inflammation and pain. *International anesthesiology clinics*, 45 (2): 27.
Zhang, M., Qiu, X., Zhang, H., Yang, X., Hong, N., Yang, Y., Chen, H. & Yu, C. (2014). Faecalibacterium prausnitzii inhibits interleukin-17 to ameliorate colorectal colitis in rats. *PloS one*, 9 (10): e109146.
Zhang, Q., Zmasek, C. M., Cai, X. & Godzik, A. (2011). TIR domain-containing adaptor SARM is a late addition to the ongoing microbe–host dialog. *Developmental & Comparative Immunology*, 35 (4): 461-468.
Øverland, M., Tauson, A.-H., Shearer, K. & Skrede, A. (2010). Evaluation of methane-utilising bacteria products as feed ingredients for monogastric animals. *Archives of animal nutrition*, 64 (3): 171-189.

APPENDIX

Figure A-1. Precipitation of TIR during buffer exchange. Use of the pNIC-CH_TIR construct from 2016 (Sveen (2016)) resulted in heavy precipitation during buffer exchange after the IMAC purification of the protein. Both the solutions above and below the column showed heavy precipitation with opaque/gel like features (indicated by the arrows). The observed precipitation was solvedby constructing a new plasmid (pMAL-c5X_TIR) with a MPB, a common approach to increase the solubility of recombinant proteins.

A

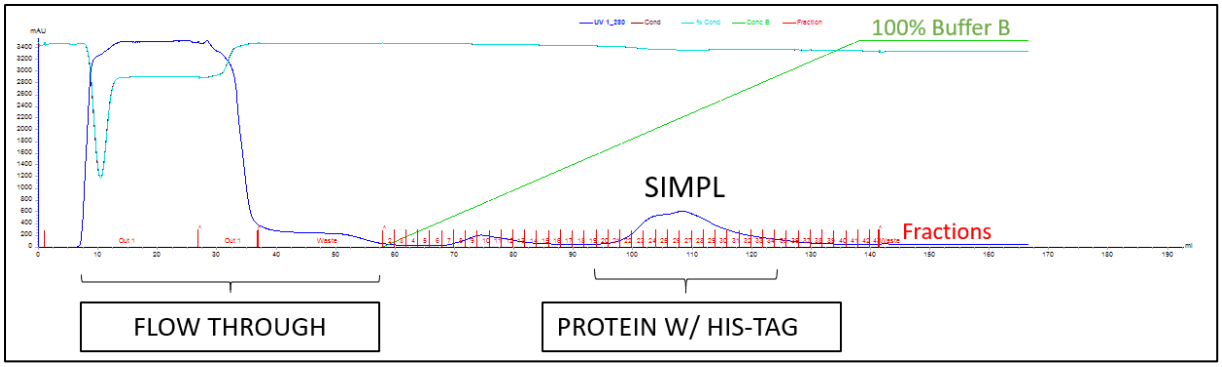

B

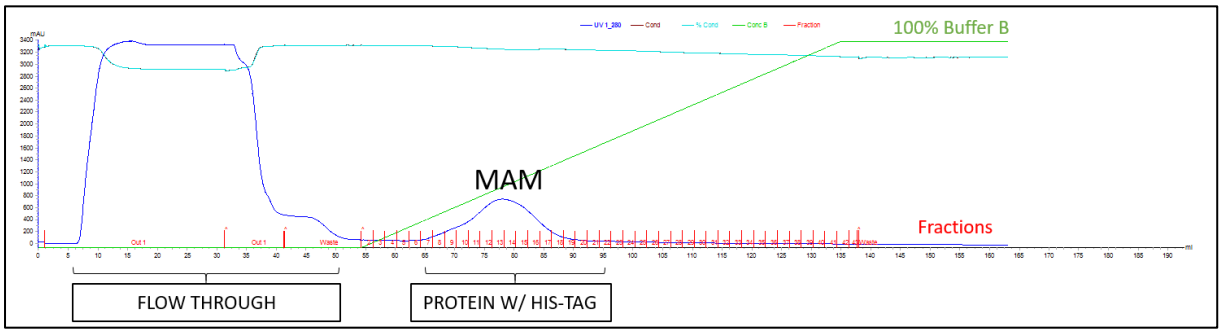

C

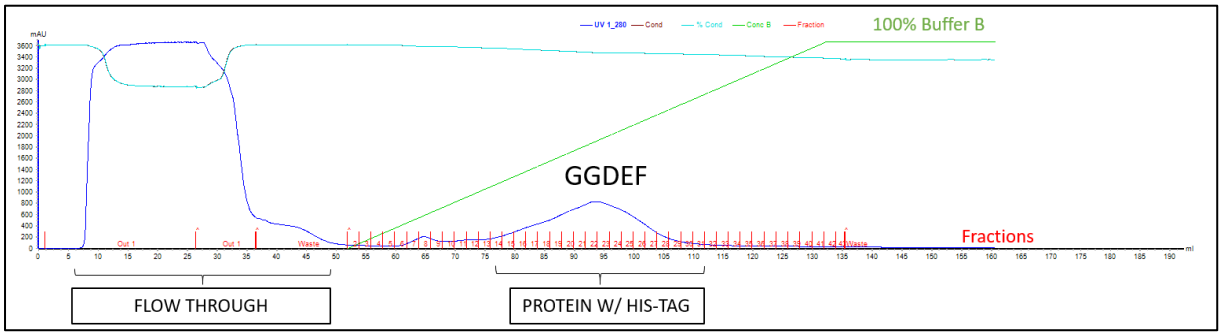

D

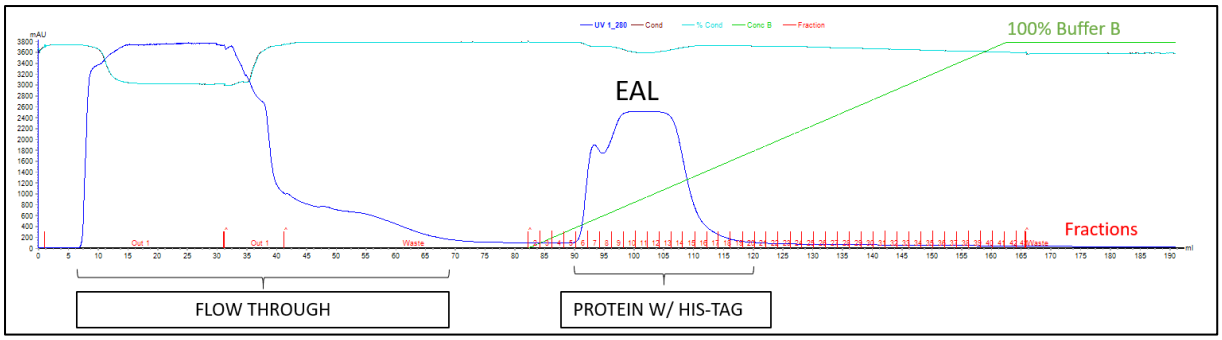

Figure A-2. See figure legend on the next page.

Figure A-2. Chromatograms from IMAC purifications of SIMPL, full-length MAM, GGDEF domain and EAL domain. Protein elution from the column was monitored by detecting A_{280} (dark blue line) of the column flow through. The green line shows the imidazole gradient applied to the system via buffer B to elute the protein bound to the HisTrap™ column. The brown and light blue lines show the conductivity of the solutions in the column. Fraction numbers are shown in red along the x-axis. The first peak represents the non-bound protein (flow through) and the second peak represents the His-tagged protein. The chromatograms were generated using the UniCorn™ 64 Software. **A)** Purification of SIMPL. A small peak can be seen at fractions 9-10. Fractions 9, 10, 22-31 were further analyzed. **B)** Purification of full-length MAM. Fractions 6-21 were further analyzed. **C)** Purification of the GGDEF domain. Fractions 8, 15-27 were further analyzed. **D)** Purification of the EAL domain**.** Fractions 5-18 were further analyzed.

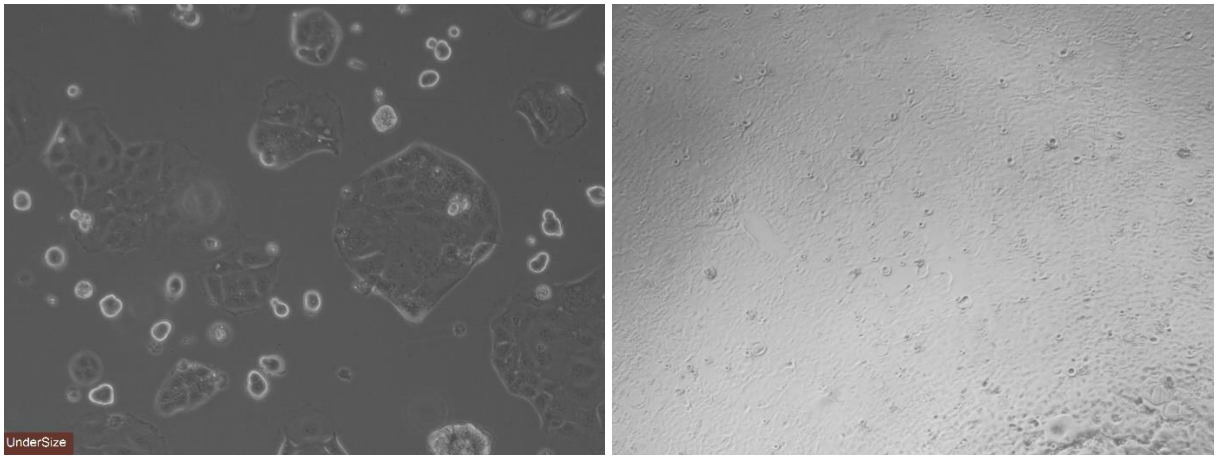

Figure A-3. Light microscopy of Caco-2 cells grown in culture. The cells were monitored during maintenance, and before/under/after assays by bright field light microscopy. **Left:** Caco-2 cells grown in culture flask. The large sized cells have adhered and grown, while the smaller cells have not yet adhered to the flask. Image taken at 10X magnitude. **Right:** Caco-2 cells grown to confluency in 12-well plates in preparation for the inflammation assay. Image taken at 4X magnitude.

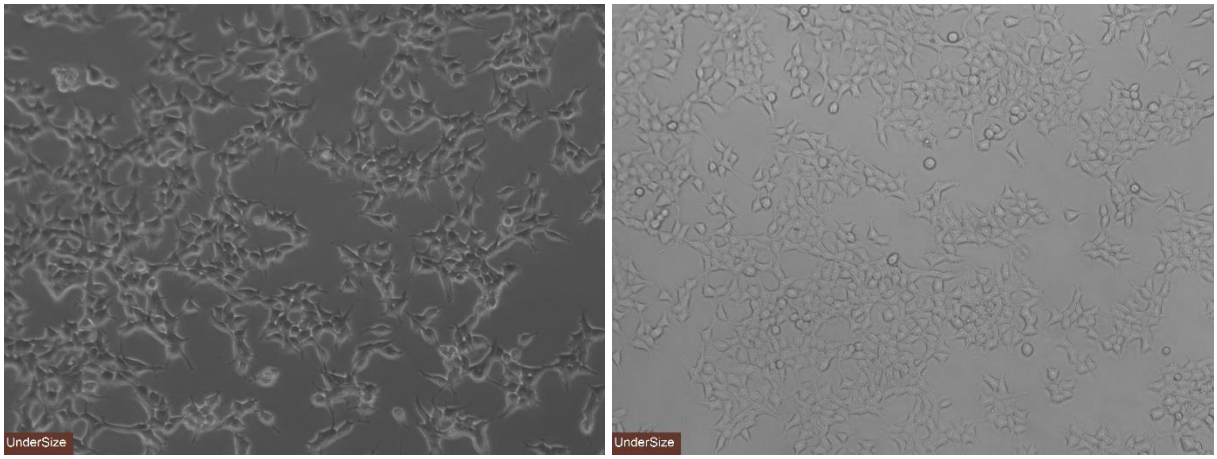

Figure A-4. Light microscopy of HEK-293 cells grown in culture. The cells were monitored during maintenance, and before/under/after assays by bright field light microscopy. **Left:** HEK-TLR4 cells at 50% confluency in a culture flask. Image taken at 10X magnitude. **Right:** HEK-Null cells grown to 50% confluency in a culture flask. Image taken at 10X magnitude.

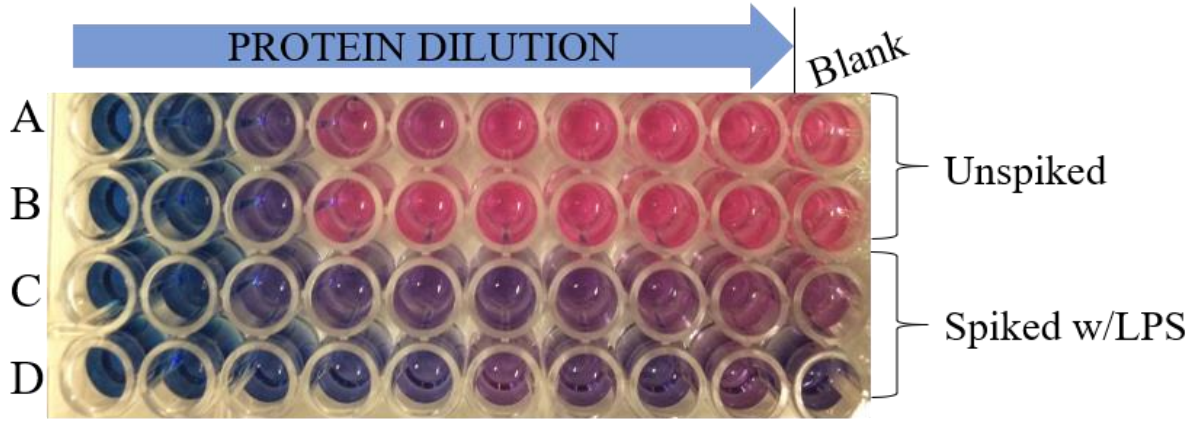

Figure A-5. Example of plate setup for the HEK-293 cell NF-*κ*B pathway assay. HEK-293 cells were grown in a 96-well plate and stimulated the following day. A protein gradient was added to the plates horizontally, starting at highest to lowest concentration. Well 10 was added the corresponding volume of endotoxin-free water (blank). Rows A+B were unspiked (supplemented with endotoxin-free water, no LPS added), while rows C+D were spiked with 0.1 EU/mL O55:B5 *E. coli* LPS. To quantify expression of the reporter gene SEAP, absorbance of the plates was read at 620 nm 1-6 hours after exposure. The proteins' effect on the NF-κB pathway was calculated as the percentage difference in absorbance between unspiked and spiked wells for a sample compared to the unspiked and spiked blank wells. An effect higher than 25% on the activation of the NF-κB pathway was considered inhibitory on the pathway, hence was the threshold set to 75% when calculating the percentage differences. The color development in wells 1-3 in rows A+B indicates a potential LPS content in the protein solutions.

Norges miljø- og biovitenskapelige universitet
Noregs miljø- og biovitskapelege universitet
Norwegian University of Life Sciences

Postboks 5003
NO-1432 Ås
Norway